STUDY OF POSITION CONTROL IN TWO CLASSES OF HYDRAULICALLY-ACTUATED MANIPULATORS

by

Abdo Al-Zaher

A thesis
presented to the University of Manitoba
in fulfilment of the
thesis requirement for the degree of
Master of Science
in
Mechanical & Industrial Engineering

Winnipeg, Manitoba, Canada 1994

©Abdo Al-Zaher 1994

National Library of Canada

Bibliothèque nationale du Canada

Acquisitions and Bibliographic Services Branch

Direction des acquisitions et des services bibliographiques

395 Wellington Street
Ottawa, Ontario
K1A 0N4

395, rue Wellington
Ottawa (Ontario)
K1A 0N4

Your file Votre référence

Our file Notre référence

The author has granted an irrevocable non-exclusive licence allowing the National Library of Canada to reproduce, loan, distribute or sell copies of his/her thesis by any means and in any form or format, making this thesis available to interested persons.

L'auteur a accordé une licence irrévocable et non exclusive permettant à la Bibliothèque nationale du Canada de reproduire, prêter, distribuer ou vendre des copies de sa thèse de quelque manière et sous quelque forme que ce soit pour mettre des exemplaires de cette thèse à la disposition des personnes intéressées.

The author retains ownership of the copyright in his/her thesis. Neither the thesis nor substantial extracts from it may be printed or otherwise reproduced without his/her permission.

L'auteur conserve la propriété du droit d'auteur qui protège sa thèse. Ni la thèse ni des extraits substantiels de celle-ci ne doivent être imprimés ou autrement reproduits sans son autorisation.

ISBN 0-315-92314-8

Canada

Name Abdo Al-Zaher

Dissertation Abstracts International is arranged by broad, general subject categories. Please select the one subject which most nearly describes the content of your dissertation. Enter the corresponding four-digit code in the spaces provided.

Study of Position Control in two classes of Hydraulically-Actuated manipulators

SUBJECT TERM

0546

SUBJECT CODE

UMI

Subject Categories

THE HUMANITIES AND SOCIAL SCIENCES

COMMUNICATIONS AND THE ARTS

Architecture 0729
Art History 0377
Cinema 0900
Dance 0378
Fine Arts 0357
Information Science 0723
Journalism 0391
Library Science 0399
Mass Communications 0708
Music 0413
Speech Communication 0459
Theater 0465

EDUCATION

General 0515
Administration 0514
Adult and Continuing 0516
Agricultural 0517
Art 0273
Bilingual and Multicultural 0282
Business 0688
Community College 0275
Curriculum and Instruction 0727
Early Childhood 0518
Elementary 0524
Finance 0277
Guidance and Counseling 0519
Health 0680
Higher 0745
History of 0520
Home Economics 0278
Industrial 0521
Language and Literature 0279
Mathematics 0280
Music 0522
Philosophy of 0998
Physical 0523
Psychology 0525
Reading 0535
Religious 0527
Sciences 0714
Secondary 0533
Social Sciences 0534
Sociology of 0340
Special 0529
Teacher Training 0530
Technology 0710
Tests and Measurements 0288
Vocational 0747

LANGUAGE, LITERATURE AND LINGUISTICS

Language
- General 0679
- Ancient 0289
- Linguistics 0290
- Modern 0291

Literature
- General 0401
- Classical 0294
- Comparative 0295
- Medieval 0297
- Modern 0298
- African 0316
- American 0591
- Asian 0305
- Canadian (English) 0352
- Canadian (French) 0355
- English 0593
- Germanic 0311
- Latin American 0312
- Middle Eastern 0315
- Romance 0313
- Slavic and East European 0314

PHILOSOPHY, RELIGION AND THEOLOGY

Philosophy 0422
Religion
- General 0318
- Biblical Studies 0321
- Clergy 0319
- History of 0320
- Philosophy of 0322

Theology 0469

SOCIAL SCIENCES

American Studies 0323
Anthropology
- Archaeology 0324
- Cultural 0326
- Physical 0327

Business Administration
- General 0310
- Accounting 0272
- Banking 0770
- Management 0454
- Marketing 0338

Canadian Studies 0385
Economics
- General 0501
- Agricultural 0503
- Commerce-Business 0505
- Finance 0508
- History 0509
- Labor 0510
- Theory 0511

Folklore 0358
Geography 0366
Gerontology 0351
History
- General 0578
- Ancient 0579
- Medieval 0581
- Modern 0582
- Black 0328
- African 0331
- Asia, Australia and Oceania 0332
- Canadian 0334
- European 0335
- Latin American 0336
- Middle Eastern 0333
- United States 0337

History of Science 0585
Law 0398
Political Science
- General 0615
- International Law and Relations 0616
- Public Administration 0617

Recreation 0814
Social Work 0452
Sociology
- General 0626
- Criminology and Penology 0627
- Demography 0938
- Ethnic and Racial Studies 0631
- Individual and Family Studies 0628
- Industrial and Labor Relations 0629
- Public and Social Welfare 0630
- Social Structure and Development 0700
- Theory and Methods 0344

Transportation 0709
Urban and Regional Planning 0999
Women's Studies 0453

THE SCIENCES AND ENGINEERING

BIOLOGICAL SCIENCES

Agriculture
- General 0473
- Agronomy 0285
- Animal Culture and Nutrition 0475
- Animal Pathology 0476
- Food Science and Technology 0359
- Forestry and Wildlife 0478
- Plant Culture 0479
- Plant Pathology 0480
- Plant Physiology 0817
- Range Management 0777
- Wood Technology 0746

Biology
- General 0306
- Anatomy 0287
- Biostatistics 0308
- Botany 0309
- Cell 0379
- Ecology 0329
- Entomology 0353
- Genetics 0369
- Limnology 0793
- Microbiology 0410
- Molecular 0307
- Neuroscience 0317
- Oceanography 0416
- Physiology 0433
- Radiation 0821
- Veterinary Science 0778
- Zoology 0472

Biophysics
- General 0786
- Medical 0760

EARTH SCIENCES

Biogeochemistry 0425
Geochemistry 0996
Geodesy 0370
Geology 0372
Geophysics 0373
Hydrology 0388
Mineralogy 0411
Paleobotany 0345
Paleoecology 0426
Paleontology 0418
Paleozoology 0985
Palynology 0427
Physical Geography 0368
Physical Oceanography 0415

HEALTH AND ENVIRONMENTAL SCIENCES

Environmental Sciences 0768
Health Sciences
- General 0566
- Audiology 0300
- Chemotherapy 0992
- Dentistry 0567
- Education 0350
- Hospital Management 0769
- Human Development 0758
- Immunology 0982
- Medicine and Surgery 0564
- Mental Health 0347
- Nursing 0569
- Nutrition 0570
- Obstetrics and Gynecology .. 0380
- Occupational Health and Therapy 0354
- Ophthalmology 0381
- Pathology 0571
- Pharmacology 0419
- Pharmacy 0572
- Physical Therapy 0382
- Public Health 0573
- Radiology 0574
- Recreation 0575
- Speech Pathology 0460
- Toxicology 0383

Home Economics 0386

PHYSICAL SCIENCES

Pure Sciences

Chemistry
- General 0485
- Agricultural 0749
- Analytical 0486
- Biochemistry 0487
- Inorganic 0488
- Nuclear 0738
- Organic 0490
- Pharmaceutical 0491
- Physical 0494
- Polymer 0495
- Radiation 0754

Mathematics 0405
Physics
- General 0605
- Acoustics 0986
- Astronomy and Astrophysics 0606
- Atmospheric Science 0608
- Atomic 0748
- Electronics and Electricity 0607
- Elementary Particles and High Energy 0798
- Fluid and Plasma 0759
- Molecular 0609
- Nuclear 0610
- Optics 0752
- Radiation 0756
- Solid State 0611

Statistics 0463

Applied Sciences

Applied Mechanics 0346
Computer Science 0984
Engineering
- General 0537
- Aerospace 0538
- Agricultural 0539
- Automotive 0540
- Biomedical 0541
- Chemical 0542
- Civil 0543
- Electronics and Electrical 0544
- Heat and Thermodynamics 0348
- Hydraulic 0545
- Industrial 0546
- Marine 0547
- Materials Science 0794
- Mechanical 0548
- Metallurgy 0743
- Mining 0551
- Nuclear 0552
- Packaging 0549
- Petroleum 0765
- Sanitary and Municipal 0554
- System Science 0790

Geotechnology 0428
Operations Research 0796
Plastics Technology 0795
Textile Technology 0994

PSYCHOLOGY

General 0621
Behavioral 0384
Clinical 0622
Developmental 0620
Experimental 0623
Industrial 0624
Personality 0625
Physiological 0989
Psychobiology 0349
Psychometrics 0632
Social 0451

Nom ______________________________

Dissertation Abstracts International est organisé en catégories de sujets. Veuillez s.v.p. choisir le sujet qui décrit le mieux votre thèse et inscrivez le code numérique approprié dans l'espace réservé ci-dessous.

______________________________ SUJET

☐☐☐☐ CODE DE SUJET

U·M·I

Catégories par sujets

HUMANITÉS ET SCIENCES SOCIALES

COMMUNICATIONS ET LES ARTS
Architecture 0729
Beaux-arts 0357
Bibliothéconomie 0399
Cinéma 0900
Communication verbale 0459
Communications 0708
Danse 0378
Histoire de l'art 0377
Journalisme 0391
Musique 0413
Sciences de l'information 0723
Théâtre 0465

ÉDUCATION
Généralités 515
Administration 0514
Art 0273
Collèges communautaires 0275
Commerce 0688
Économie domestique 0278
Éducation permanente 0516
Éducation préscolaire 0518
Éducation sanitaire 0680
Enseignement agricole 0517
Enseignement bilingue et multiculturel 0282
Enseignement industriel 0521
Enseignement primaire. 0524
Enseignement professionnel 0747
Enseignement religieux 0527
Enseignement secondaire 0533
Enseignement spécial 0529
Enseignement supérieur 0745
Évaluation 0288
Finances 0277
Formation des enseignants 0530
Histoire de l'éducation 0520
Langues et littérature 0279
Lecture 0535
Mathématiques 0280
Musique 0522
Orientation et consultation 0519
Philosophie de l'éducation 0998
Physique 0523
Programmes d'études et enseignement 0727
Psychologie 0525
Sciences 0714
Sciences sociales 0534
Sociologie de l'éducation 0340
Technologie 0710

LANGUE, LITTÉRATURE ET LINGUISTIQUE
Langues
- Généralités 0679
- Anciennes 0289
- Linguistique 0290
- Modernes 0291

Littérature
- Généralités 0401
- Anciennes 0294
- Comparée 0295
- Mediévale 0297
- Moderne 0298
- Africaine 0316
- Américaine 0591
- Anglaise 0593
- Asiatique 0305
- Canadienne (Anglaise) 0352
- Canadienne (Française) 0355
- Germanique 0311
- Latino-américaine 0312
- Moyen-orientale 0315
- Romane 0313
- Slave et est-européenne 0314

PHILOSOPHIE, RELIGION ET THÉOLOGIE
Philosophie 0422
Religion
- Généralités 0318
- Clergé 0319
- Études bibliques 0321
- Histoire des religions 0320
- Philosophie de la religion 0322

Théologie 0469

SCIENCES SOCIALES
Anthropologie
- Archéologie 0324
- Culturelle 0326
- Physique 0327

Droit 0398
Économie
- Généralités 0501
- Commerce-Affaires 0505
- Économie agricole 0503
- Économie du travail 0510
- Finances 0508
- Histoire 0509
- Théorie 0511

Études américaines 0323
Études canadiennes 0385
Études féministes 0453
Folklore 0358
Géographie 0366
Gérontologie 0351
Gestion des affaires
- Généralités 0310
- Administration 0454
- Banques 0770
- Comptabilité 0272
- Marketing 0338

Histoire
- Histoire générale 0578
- Ancienne 0579
- Médiévale 0581
- Moderne 0582
- Histoire des noirs 0328
- Africaine 0331
- Canadienne 0334
- États-Unis 0337
- Européenne 0335
- Moyen-orientale 0333
- Latino-américaine 0336
- Asie, Australie et Océanie 0332

Histoire des sciences 0585
Loisirs 0814
Planification urbaine et régionale 0999
Science politique
- Généralités 0615
- Administration publique 0617
- Droit et relations internationales 0616

Sociologie
- Généralités 0626
- Aide et bien-àtre social 0630
- Criminologie et établissements pénitentiaires 0627
- Démographie 0938
- Études de l' individu et de la famille 0628
- Études des relations interethniques et des relations raciales 0631
- Structure et développement social 0700
- Théorie et méthodes. 0344
- Travail et relations industrielles 0629

Transports 0709
Travail social 0452

SCIENCES ET INGÉNIERIE

SCIENCES BIOLOGIQUES
Agriculture
- Généralités 0473
- Agronomie. 0285
- Alimentation et technologie alimentaire 0359
- Culture 0479
- Élevage et alimentation 0475
- Exploitation des péturages 0777
- Pathologie animale 0476
- Pathologie végétale 0480
- Physiologie végétale 0817
- Sylviculture et faune 0478
- Technologie du bois 0746

Biologie
- Généralités 0306
- Anatomie 0287
- Biologie (Statistiques) 0308
- Biologie moléculaire 0307
- Botanique 0309
- Cellule 0379
- Écologie 0329
- Entomologie 0353
- Génétique 0369
- Limnologie 0793
- Microbiologie 0410
- Neurologie 0317
- Océanographie 0416
- Physiologie 0433
- Radiation 0821
- Science vétérinaire 0778
- Zoologie 0472

Biophysique
- Généralités 0786
- Medicale 0760

SCIENCES DE LA TERRE
Biogéochimie 0425
Géochimie 0996
Géodésie 0370
Géographie physique 0368
Géologie 0372
Géophysique 0373
Hydrologie 0388
Minéralogie 0411
Océanographie physique 0415
Paléobotanique 0345
Paléoécologie 0426
Paléontologie 0418
Paléozoologie 0985
Palynologie 0427

SCIENCES DE LA SANTÉ ET DE L'ENVIRONNEMENT
Économie domestique 0386
Sciences de l'environnement 0768
Sciences de la santé
- Généralités 0566
- Administration des hipitaux 0769
- Alimentation et nutrition 0570
- Audiologie 0300
- Chimiothérapie 0992
- Dentisterie 0567
- Développement humain 0758
- Enseignement 0350
- Immunologie 0982
- Loisirs 0575
- Médecine du travail et thérapie 0354
- Médecine et chirurgie 0564
- Obstétrique et gynécologie 0380
- Ophtalmologie 0381
- Orthophonie 0460
- Pathologie 0571
- Pharmacie 0572
- Pharmacologie 0419
- Physiothérapie 0382
- Radiologie 0574
- Santé mentale 0347
- Santé publique 0573
- Soins infirmiers 0569
- Toxicologie 0383

SCIENCES PHYSIQUES
Sciences Pures
Chimie
- Genéralités 0485
- Biochimie 487
- Chimie agricole 0749
- Chimie analytique 0486
- Chimie minérale 0488
- Chimie nucléaire 0738
- Chimie organique 0490
- Chimie pharmaceutique 0491
- Physique 0494
- PolymÇres 0495
- Radiation 0754

Mathématiques 0405
Physique
- Généralités 0605
- Acoustique 0986
- Astronomie et astrophysique 0606
- Electronique et électricité 0607
- Fluides et plasma 0759
- Météorologie 0608
- Optique 0752
- Particules (Physique nucléaire) 0798
- Physique atomique 0748
- Physique de l'état solide 0611
- Physique moléculaire 0609
- Physique nucléoire 0610
- Radiation 0756

Statistiques 0463

Sciences Appliqués Et Technologie
Informatique 0984
Ingénierie
- Généralités 0537
- Agricole 0539
- Automobile 0540
- Biomédicale 0541
- Chaleur et ther modynamique 0348
- Conditionnement (Emballage) 0549
- Génie aérospatial 0538
- Génie chimique 0542
- Génie civil 0543
- Génie électronique et électrique 0544
- Génie industriel 0546
- Génie mécanique 0548
- Génie nucléaire 0552
- Ingénierie des systömes 0790
- Mécanique navale 0547
- Métallurgie 0743
- Science des matériaux 0794
- Technique du pétrole 0765
- Technique minière 0551
- Techniques sanitaires et municipales 0554
- Technologie hydraulique 0545

Mécanique appliquée 0346
Géotechnologie 0428
Matières plastiques (Technologie) 0795
Recherche opérationnelle 0796
Textiles et tissus (Technologie) 0794

PSYCHOLOGIE
Généralités 0621
Personnalité 0625
Psychobiologie 0349
Psychologie clinique 0622
Psychologie du comportement 0384
Psychologie du développement 0620
Psychologie expérimentale 0623
Psychologie industrielle 0624
Psychologie physiologique 0989
Psychologie sociale 0451
Psychométrie 0632

STUDY OF POSITION CONTROL IN TWO CLASSES OF

HYDRAULICALLY-ACTUATED MANIPULATORS

BY

ABDO AL-ZAHER

A Thesis submitted to the Faculty of Graduate Studies of the University of Manitoba in partial fulfillment of the requirements of the degree of

MASTER OF SCIENCE

© 1994

Permission has been granted to the LIBRARY OF THE UNIVERSITY OF MANITOBA to lend or sell copies of this thesis, to the NATIONAL LIBRARY OF CANADA to microfilm this thesis and to lend or sell copies of the film, and LIBRARY MICROFILMS to publish an abstract of this thesis.

The author reserves other publication rights, and neither the thesis nor extensive extracts from it may be printed or other-wise reproduced without the author's written permission.

I hereby declare that I am the sole author of this thesis.
I authorize the University of Manitoba to lend this thesis to other institutions or individuals for the purpose of scholarly research.

Abdo Al-Zaher

I further authorize the University of Manitoba to reproduce this thesis by photocopying or by other means, in total or in part, at the request of other institutions or individuals for the purpose of scholarly research.

Abdo Al-Zaher

Abstract

This thesis investigates some relevant aspects of position control in hydraulically-actuated manipulators. Poor rigidity, load dependent and nonlinear characteristic of actuation are common problems in these systems. The choice of the control method depends on the structure of the manipulator (light-duty or heavy-duty), the type of the pump supply (constant pressure or constant flow), the type of the valving system (closed-center or open-center) and the valve's lap conditions (zero-lapped or over-lapped).

Two classes of manipulators are studied. The first class of manipulators operate from a constant pump pressure and are controlled by closed-center valves. These manipulators are used for indoor environments where high pressure oil is readily available. The second class of manipulators are operated by a constant flow pump and are controlled by open-center valves. They are designed for heavy-duty tasks in unstructured outdoor environments.

Reliable models are first developed to accurately simulate the nonlinear performance of both classes of manipulators. The accuracy of the models are verified with experimental data of available literature. The application of different control techniques are then studied. Basic performance measures such as stability, acceptable steady-state accuracy and transient response are evaluated. The requirements and conditions, in which velocity or acceleration feedback can improve the response, are discussed using both parameter plane and root locus methods.

For the case of pressure compensated manipulators, the application of two different strategies, namely "non-interactive" and "load-insensitive" controllers are investigated. It is shown that the non-interactive controller, although capable of reducing the effect of interaction in multi-link motions, cannot compensate for the load. The load-insensitive controller performed relatively better than the non-interactive controller in both canceling the effect of load and reducing the interaction effects.

For the case of constant flow manipulators, the effects of dead-bands and delay in the valve response are studied. Suggestions for improving the response are made. It is shown that the effect of delay in the valving system can be removed by the appropriate choice of velocity feedback.

In this work the analysis and the selection of control gains are performed in a frequency-domain that requires a linearization of nonlinear equations describing the dynamics of hydraulics and linkages. It is shown that this linearization, although effective, may lead to an unwanted response if the parameters are not updated with the change of operating points.

The significance of this thesis is firstly, reliable simulation programs were developed which can be used to examine various control algorithms. Effect of variation of several parameters of the system can be examined before an actual implementation is carried out. Secondly, a number of control algorithms were examined on two different classes of manipulators. The performance of the algorithms was compared with each other. This comparison revealed some fundamental insights into the important issues of control of hydraulic manipulators.

Acknowledgments

I would like to express my deep and sincere appreciation to the following people:

Dr. N. Sepehri, my academic advisor for his guidance, effort, time, and his patience during my research.

Members of the examining committee, Dr. A.B. Thornton-Trump (Department of Mechanical and Industrial Engineering) and Dr. Bahman S. Kermanshahi an adjunct professor at the Department of Electrical and Computer Engineering (from Tokyo Metropolitan University, Japan) for their remarks, comments and support of this thesis.

Dr. Douglas Ruth head of the Mechanical and Industrial Engineering Department for his support.

Dr. A. ATA, (CAD/CAM , Ford Co., Detroit, MI, U.S.A.) for his support.

All friends among them B. Awadh, Hassen Zghal, A. Lohse, P. Tataryn, P, S-tumph, T. Corbet, and I. Zeghpi.

And finally my Parents, brothers and sisters for their unlimited support and love.

TABLE OF CONTENTS

LIST OF FIGURES

FIGURE PAGE

FIGURE PAGE

FIGURE PAGE

Nomenclature

i	index (joint number)
α	adjusted parameter
β	adjusted parameter
σ	real root
ω_n	natural frequency
$\acute{\sigma}$	normalized real root
$\acute{\omega_n}$	normalized natural frequency
A_{Ii},A_{Oi}	piston effective areas
C_i	hydraulic compliance
d_i	viscous damping of the ith cylinder
F_{ai}	actuating force of the ith cylinder
$\mathcal{F}_a$	actuating torque vector
F_{ci}	Coulomb friction of the ith cylinder
F_{ei}	effective force of the ith cylinder
k_a	acceleration feedback gain
k_v	velocity feedback gain
k_p	proportional gain
K_{pfi}	actuating force feedback gain
K_{ui}	flow-gain coefficient
K_{pi}	flow-pressure coefficient
P_{Ii}	pressure of supply line
P_{Oi}	pressure of return line
P_l	load pressure

P_s	supply pressure
q_i	joint angles
Q_{Ii}	flow rate to in ith cylinder (valve port)
Q_{Oi}	flow rate from the ith cylinder (valve port)
T_i	torque generated by hydraulic cylinders
T_f	time constant of high-pass filter
x_i	piston displacement
$\dot{x}_i$	piston velocity
X_i	spool displacement
U_i	control input to the servo-valve

CHAPTER 1

INTRODUCTION

1.1 Preliminary Remarks

The science and technology of robotics have developed to a great extent in recent years. Many robots have been built and put into use in a wide variety of tasks including welding, machine loading/unloading and recently, assembly. Each of these applications impose different demands on the robot. Robot designers try to meet these demands by applying flexible, reliable and accurate control systems.

Three types of actuators that are commonly used to power a robotic arm are electric, pneumatic and hydraulic. Each type has its own advantages and disadvantages. The choice of actuator type which should be used is dependent on the application and the condition in which the robot arm is directed to work.

Electric actuators are known to be accurate, quiet, simple to use and clean devices. They are capable of being included in sophisticated control systems. On the other hand, electric actuators suffer from power limitations; they can produce peak force/torque for only a small part of the cycle because they have limited ability to dissipate heat. Pneumatic devices are cheap, clean and safe. However, they are inaccurate, noisy and very load-sensitive.

Hydraulic power systems are the best choice for indoor factories where oil pressure sources are readily available and for most outdoor application and environments (Davies 81). Hydraulic devices consist of components that are standard, safe and easy to maintain. In hazardous environments, such as explosive atmospheres or wet environments, where electric device would not survive, the utilization of hydraulic actuators become inevitable. There are a number of other reasons which makes hydraulic power systems attractive to robot designers. Hydraulic fluid acts as a lubricant. Heat can be conducted by the the hydraulic fluid and dissipated through lines and reservoirs. Hydraulic actuators have the ability to generate high forces for a long period of time.

In spite of the above advantages, hydraulic devices are relatively more expensive than comparable electrical power systems and are noisy and messy. Hydraulic systems are complex, nonlinear and difficult to analyze for control purposes. Some common problems in controlling hydraulic systems are listed in the following.

The first problem is the poor dynamic performance of the individual hydraulic actuator. This problem is due to the high inertia and high compliance caused by the flexible connecting hoses, large volume of fluid under compression and trapped air in the hydraulic fluid. The analysis performed for the UNIMATE 2000B showed that 98% of the deflection of the horizontal arm, under a concentrated force, is due to the hydraulic factors (Rivin 85). The high inertia and high compliance reduce the natural frequency and the damping effect of the joint mechanism.

The second problem is the interaction during a multi-link motion. The interaction effect is intensified by the hydraulic compliance and may lead to serious control problems.

The third problem is the nonlinear characteristics of the robot structure, as well as the actuation mechanism. The performance of hydraulic valves is very load dependent. The load experienced due to inertia, gravity and interaction, either among the linkages or with the surrounding, is seen as a disturbing load that affects the valve performance.

There have been some investigations that addressed the above issues and different approaches were suggested. The valuable study by Hanafusa *et al.* (1980) examined acceleration (actuating force) feedback in order to improve the dynamic performance of the individual hydraulic actuator. They further elaborated on the application of pressure feedback control towards developing non-interactive and load-insensitive control systems (Hanafusa and Wang, 1983). The objective of their work was to eliminate or at least reduce the effect of interaction among the links as well as between the manipulator and the environment. Limited experimental studies on a small-scale articulated robot were performed.

Kulkarni *et al.* (1984) studied an adaptive control for an electrohydraulic position servo-mechanism. Halme *et al.* (1985) designed a multivariable control technique for controlling hydraulic manipulators. The importance of including hydraulic dynamics in the control of manipulators has also been investigated (Sepehri *et al.*, 1990).

Today's conventional hydraulic robots in the manufacturing industry work on a constant pressure supply system. Therefore, most control studies, including those mentioned above, were intended for such robots. Each link in these robots is activated independently, with high-performance, closed-center hydraulic valves. However, there exists a class of hydraulic manipulators that do not exhibit characteristics of the conventional hydraulic robots. These manipulators are heavy-duty and are extensively used in the forest, mining and construction industries. Excavators and feller-bunchers are the examples. In these machines the hydraulic actuation contains many forms of imperfections which cannot be prevented inexpensively. Excavators for example, use open-center, asymmetric valves with dead-bands operating from a constant flow pump system. Excavators constantly interact with the environment and are subjected to a variety of load conditions. These manipulators are presently controlled by skilled operators and do not benefit from computer-assisted controls; however, they have the potential to be automated (Sepehri and Lawrence, 1992). The application of a model-based control technique to these machines has recently been investigated. The method which heavily relies on the exact model and model parameters of the system, allows the control of the velocity of the implement. No report was found in relation to accurate position control of the end-effector.

1.2 General Objective and Scope of Thesis

In this thesis, a step-by-step study is conducted comprising theoretical, mathematical, simulation and experimental components. The objectives are firstly, to develop reliable simulation tools in order to facilitate future studies in the area of control of hydraulically-actuated manipulators. The second objective is to offer some fundamental insights into the task of accurate positioning in such hydraulically actuated robots.

Two different valving systems are studied; a constant pressure system with closed-center valves commonly used for indoor industrial robots and a constant flow system with open-center valves used in outdoor heavy-duty manipulators . Simulation models based on the exact nonlinear equations are developed for both hydraulic configurations. Careful attention, at the component level, is paid and systematic cycle of simulation, experimentation, fine-tuning and iteration of the cycle is performed to bring the simulations close to reality. The theoretical analysis is performed in a frequency domain.

Different control techniques are examined through their application to a typical indoor robot arm. The emphasis has been put on the load-insensitivity and non-interactiveness of the controllers of these manipulators. Many issues, including the effects of poor rigidity are addressed. For the case of heavy-duty manipulators, the focus is on the effect of delay in valve responses, dead-bands, lap conditions, saturation of the flow through the valves and lack of supply pressure. The purpose is to investigate the degree to which these nonlinearities affect the performance of such manipulator within a simple closed-loop control system.

The remainder of this thesis is organized as follows:

Chapter 2 presents the derivation of mathematical models of two degree-of-freedom articulated robots driven by electrohydrulic servo-valves, the representation of transfer function of light-duty and heavy-duty robot arms and two different methods of system analysis. The first method is the parameter plane method used for a third-order system analysis. The second method is the root locus method used for a fourth-order system analysis.

Chapter 3 discusses the application of various control actions (actuating force feedback compensation, non-interactive control and load-insensitive system) to the class of manipulators operating from a constant pressure supply.

Chapter 4 discusses the effect of velocity and acceleration feedback on the performance of fourth-order systems (for the second class of manipulators). Delay in the spool displacement, dead-band on the servo-valve input and over-lapped conditions are examined with a simple, closed-loop control.

Chapter 5 demonstrates some experimental results considering joint motion for the main axes of a five degree-of-freedom hydraulic robot (UNIMATE MK II 2000). Conclusions of this thesis are outlined in Chapter 6.

CHAPTER 2

SYSTEM MODELING AND ANALYSIS

In order to analyze and design a control system, a mathematical model that describes the dynamics of the system accurately or at least fairly well, must be derived. A mathematical model is not unique to a given system; it can be represented in many different ways. Once a mathematical model of a system is obtained, various analytical and computer tools can be used for the purpose of analysis and synthesis. The representation of the transfer function is convenient for the transient response analysis of single-input and single-output systems. The state-space representation is the best method in dealing with multi-input and multi-output systems. In this chapter, the mathematical models for two classes of hydraulic manipulators are derived. Two different methods of system analysis are introduced; *parameter plane method* and *root locus method* which are used to describe the performance of the first class and second class of manipulators, respectively.

2.1 Mathematical Model

Figures 2.1-a and 2.2-a are schematics of two typical robot arms; light-duty and heavy-duty robots, respectively. Each robot is composed of two links which are driven by hydraulic cylinders. Each cylinder is connected with a servo-valve through flexible hoses. The valves monitor the flow to and from the cylinders. Depending on the type of valves and pump that have been used, the pump type could be either a constant pressure or a constant displacement. Electrical signals are utilized to direct the flow of the hydraulic oil to and from the cylinder.

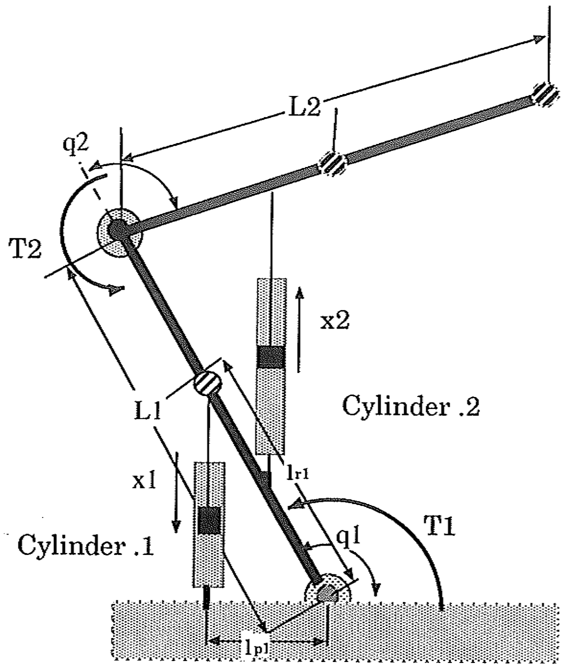

(a) Link Mechanism.

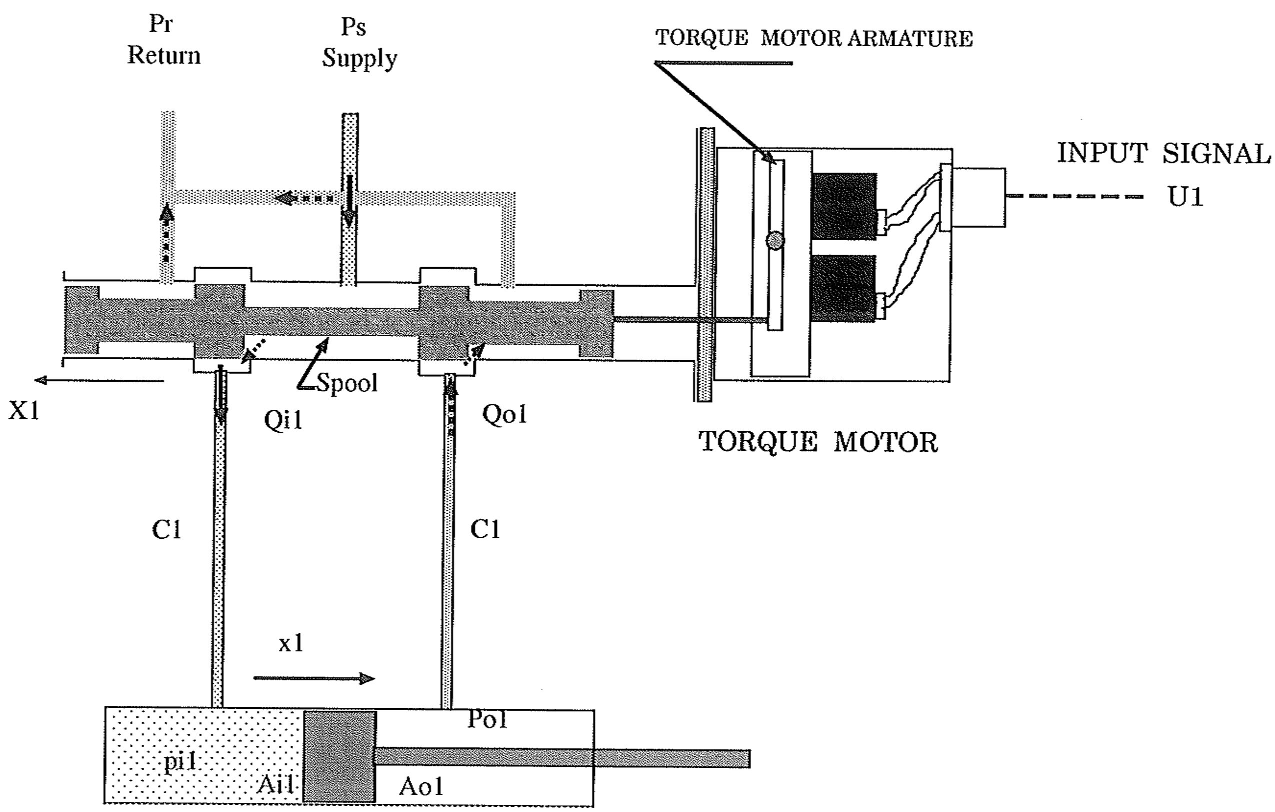

(b) Hydraulic driving unit (closed center valve)

Figure 2.1: Light-duty mechanism and hydraulic driving unit (closed-center valve)

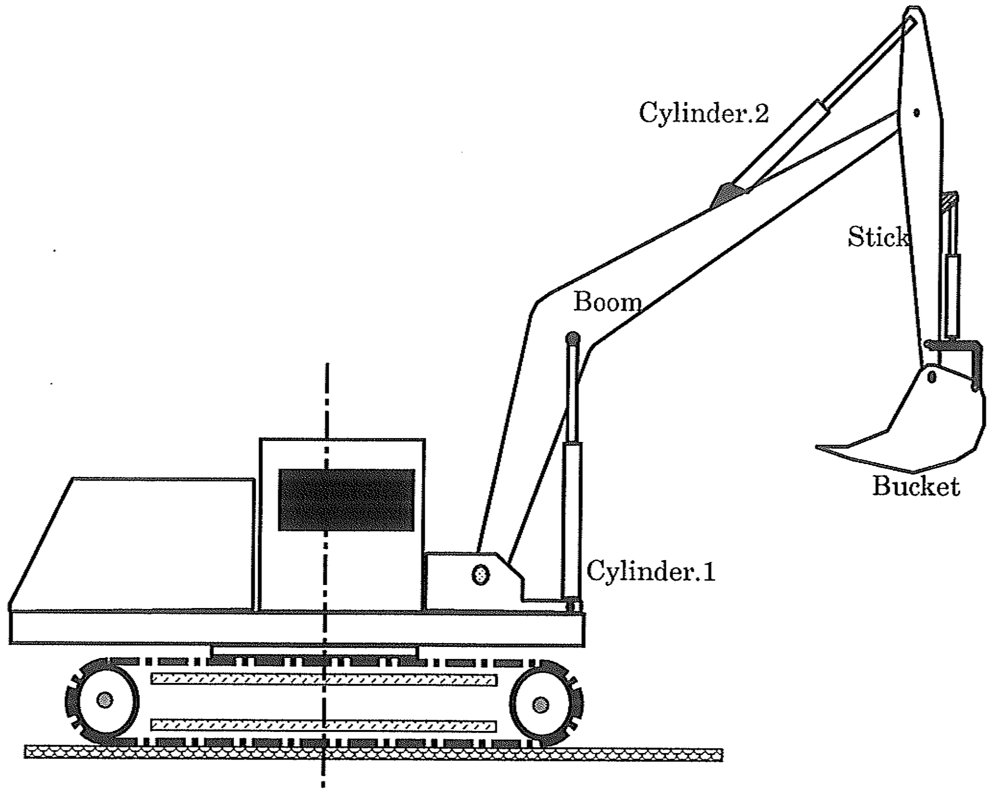

a - Heavy-duty excavator

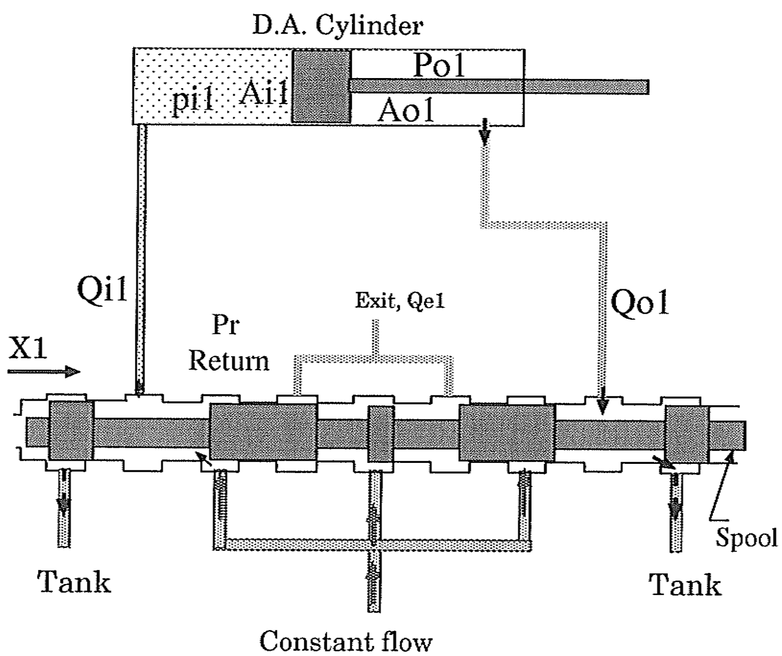

b- Hydraulic driving unit (open center valve)

Figure 2.2: Heavy-duty mechanism and hydraulic driving unit (open-center valve)

2.1.1 Equations of Motion

Equations of motion are derived through the Lagrange algorithm (Schilling, 1990).

$$\sum_{j=1}^{n} D_{ij}(q)\ddot{q}_j + \sum_{k=1}^{n}\sum_{j=1}^{n} C^i_{kj}(q)\dot{q}_k\dot{q}_j + h_i(q) + b_i(\dot{q}) = T_i$$

where T_i is the torque generated by the hydraulic cylinder and q_i denote joint angles. The first term $\sum_{j=1}^{n} D_{ij}(q)\ddot{q}_j$ is an *acceleration term* that represents the inertia forces and torques generated by the motion of links. The second term $\sum_{k=1}^{n}\sum_{j=1}^{n} C^i_{kj}(q)\dot{q}_k\dot{q}_j$ is a *product velocity term* associated with Coriolis and centrifugal forces. The third term $h_i(q)$ is a *position term* representing gravity loading. The fourth term $b_i(\dot{q})$ is a *velocity term* representing the viscous friction.

For the case of a two-link manipulator, similar to the one shown in Figure 2.1-a, the above equation can be presented as follows:

$$\begin{aligned}
T_1 &= [a_1 + 2a_3 cosq_2]\ddot{q}_1 + [a_2 + a_3 cosq_2]\ddot{q}_2 - a_3(2\dot{q}_1 + \dot{q}_2)\dot{q}_2 sinq_2 + a_4 cosq_1 \\
&\quad + a_5 cosq_1 + a_6 cos(q_1 + q_2) \\
T_2 &= [a_2 + a_3 cosq_2]\ddot{q}_1 + [a_2]\ddot{q}_2 + a_3\dot{q}_1{}^2 sinq_2 + a_6 cos(q_1 + q_2) \qquad (2.1)
\end{aligned}$$

where $a_{i(i=1,2\ldots,6)}$ are functions of the dimensions and mass of the links evaluated as following:

$$\begin{aligned}
a_1 &= I_1 + I_2 + m_1 l_{g1}^2 + m_2 l_{g2}^2 + m_2 L_1^2 = \frac{m_1 L_1^2}{3} + \frac{m_2 L_2^2}{3} + m_2 L_1^2 \\
a_2 &= I_2 + m_2.L_1 l_{g2}^2 = \frac{m_2 L_2^2}{3} \\
a_3 &= m_2.L_1 l_{g2} = \frac{m_2 L_1 L_2}{2} \\
a_4 &= m_1.l_{g1} g_0 = \frac{g_0 m_1 L_1}{2} \\
a_5 &= m_2.L_1 g_0 = g_0 m_2 L_1 \\
a_6 &= m_2.l_{g2} g_0 = \frac{g_0 m_2 L_2}{2}
\end{aligned}$$

where

L_1, L_2, m_1 and m_2 represent length and mass of link one and link two, respectively, I_1 and I_2 represent the mass moments of inertia around the center of gravity of link one and link two, respectively, and l_{g1} and l_{g2} represent the distance of the center of gravity of link one and link two with respect to the rotation axis, respectively (we have assumed that the center of gravity for each link is located at the middle of the link).

Equation (2.1) is a nonlinear equation, and must be linearized about a reference point for the purpose of further analysis. Using Taylor's series about an operating point and neglecting the higher order terms. The operating points are $(\hat{q}_1, \hat{\dot{q}}_1, \hat{\ddot{q}}_1)$, $(\hat{q}_2, \hat{\dot{q}}_2, \hat{\ddot{q}}_2)$, for links one and two, respectively.

For small variation about the corresponding reference point and neglecting small terms, the final linearized model becomes:

$$\begin{aligned}\Delta T_1 &= T_1 - \hat{T}_1 = [a_1 + 2a_3 cos\hat{q}_2]\Delta\ddot{q}_1 + [a_2 + a_3 cos\hat{q}_2]\Delta\ddot{q}_2 \\ \Delta T_2 &= T_2 - \hat{T}_2 = [a_2 + a_3 cos\hat{q}_2]\Delta\ddot{q}_1 + [a_2]\Delta\ddot{q}_2\end{aligned}$$

Writing the linearized equations in matrix form:

$$\begin{vmatrix}\Delta T_1 \\ \Delta T_2\end{vmatrix} = \begin{vmatrix}H_{11} & H_{12} \\ H_{21} & H_{22}\end{vmatrix}\begin{vmatrix}\Delta\ddot{q}_1 \\ \Delta\ddot{q}_2\end{vmatrix} \tag{2.2}$$

where

$$\begin{aligned}H_{11} &= a_1 + 2a_3 cos\hat{q}_2, \\ H_{12} &= a_2 + a_3 cos\hat{q}_2, \\ H_{21} &= a_2 + a_3 cos\hat{q}_2, \\ H_{22} &= a_2.\end{aligned}$$

The details of the linearization are shown in Appendix A.

2.1.2 Hydraulic Driving Unit

Each link has its own hydraulic driving unit. The main components of hydraulic driving units are directional valves, connecting hoses, and cylinders (or motors). Directional control valves are usually located between the pump and actuators of a hydraulic circuit. The primary function of a directional control valve is to control the direction of the flow to the actuator (i.e. in order to determine which actuator port will be the inlet port). In other words, it is the directional control valve that is used to cause the hydraulic cylinder to extend, retract, and stop.

The most widely used valves are the sliding valves (Johnson, 1973). They are classified by the number of ways "flow" can enter and leave the valve, the number of lands (number of lands on a spool vary from one, two, three, four and special valves have as many as six lands), or the lap conditions. Lap conditions is the physical relationship between spool metering lands and port openings. In this study sliding valves are classified as:

- **An open-center valve** refers to an under-lapped conditions in which the lands are slightly narrower than the porting area of the body or sleeve. When the valve is centered, this arrangement allows for a constant flow of oil from the pressure side of the pump to flow across the ports to the tank.
- **A closed-center valve** refers to zero-lapped or over-lapped conditions. The over-lapped valve construction is not common in servo-valves because it create a dead-zone and makes the valve unresponsive to small signals.

In some applications, the open-center valves are necessary to be used such as where the valve is at the null position in a high temperature environment for extended periods of time and a continuous flow is required to maintain reasonable fluid temperature. Open-center valves are required in a constant flow system (Merritt, 1967). The spool can be shifted manually, pneumatically, hydraulically, mechanically or electrically.

One important method of actuating the spool is by means of an electrical solenoid or torque motor.

Figure 2.1-b shows the schematic of the hydraulic driving unit using a closed-center four-way valve operating from a constant pressure pump system. Figure 2.2-b shows the schematic of the hydraulic driving unit using an open-center five-way valve operating from a constant flow pump system.

Valve Dynamics

The nonlinear algebraic equations which describe the pressure-flow curves can be represented as follows:

- for positive spool displacement $X_i > 0$

$$\begin{aligned} Q_{Ii} &= KwX_i\sqrt{P_s - P_{Ii}} \\ Q_{Oi} &= KwX_i\sqrt{P_{Oi} - P_r} \end{aligned}$$

- for negative spool displacement $Xi < 0$

$$\begin{aligned} Q_{Ii} &= KwX_i\sqrt{P_{Ii} - P_r} \\ Q_{Oi} &= KwX_i\sqrt{P_s - P_{Oi}} \end{aligned}$$

where $K = c_d\sqrt{\frac{2}{\rho}}$ is the metering coefficient, w is the spool area gradient, X_i is the spool displacement (proportional to the servo-valve input, U_i), Q_{Ii} and Q_{Oi} are the flow rates of the ith unit, P_{Ii} and P_{Oi} are the pressures of supply line and return line, respectively and P_s is the pump pressure.

Using a Taylor's series expansion about the operating "zero spool displacement" and neglecting the higher order terms, we obtain the following linearized model (Merritt, 1967):

$$\begin{aligned} Q_{Ii} &= K_{ui}U_i - K_{pi}P_{Ii} \\ Q_{Oi} &= K_{ui}U_i + K_{pi}P_{Oi} \end{aligned} \tag{2.3}$$

where K_{ui} and K_{pi} are the flow gain and flow-pressure coefficients, respectively, The numerical values of the coefficients K_{ui} and K_{pi} can be determined as follows:

$$\begin{aligned} K_{ui} &= Kw\sqrt{\frac{P_s - P_l}{2}} \\ K_{pi} &= \frac{KwX_i}{2\sqrt{2(P_s - P_l)}} \\ P_l &= \Delta P = P_{Ii} - P_{Oi} \end{aligned}$$

where $P_l = P_{Ii} - P_{Oi}$ is the load pressure.

Pipe Dynamics

The continuity equations for the ith servo-valve output ports are represented as:

$$\begin{aligned} C_{i1}\dot{P}_{Ii} = Q_{Ii} - A_{Ii}\dot{x}_i \;&\Rightarrow\; Q_{Ii} = C_{i1}\dot{P}_{Ii} + A_{Ii}\dot{x}_i \\ C_{i2}\dot{P}_{Oi} = A_{Oi}\dot{x}_i - Q_{Oi} \;&\Rightarrow\; Q_{Oi} = -C_{i2}\dot{P}_{Oi} + A_{Oi}\dot{x}_i \end{aligned} \tag{2.4}$$

where A_{Ii} and A_{Oi} are the piston effective areas, $\dot{x}_i$ is the piston velocity, C_i is the hydraulic compliance of the system. The numerical values of C_i can be determined as follows:

$$C_i = \frac{V}{\beta_e} = \frac{Volume\ of\ one\ champer\ including\ lines}{Effective\ bulk\ modulus}$$

Note that in the absence of entrapped air the effective bulk modulus is $210,000\ psi$. Thus, a small percentage of air in the hydraulic fluid can decrease the effective bulk modulus substantially (for a 1000 psi pressure level, β_e would be $84,000\,psi$) (Merritt, 1967).

The joint displacement, q_i, and piston displacement, x_i, are related by geometrical configuration. By considering small changes at certain angle $\hat{q}_i$, the following relation holds:

$$dx_i = J_i(\hat{q}_i)dq_i \tag{2.5}$$

The numerical value of J_i can be evaluated as follows (see Figure 2.1-a):

$$l_i^2 = l_{pi}^2 + l_{ri}^2 + 2l_{pi}l_{ri}cosq_i$$

$$
\begin{aligned}
2l_i\frac{dl_i}{dt} &= -2l_{pi}l_{ri}sinq_i\frac{dq_i}{dt} \\
\frac{dl_i}{dt} &= \dot{x} = \frac{-l_{pi}l_{ri}sinq_i}{\sqrt{l_pi^2 + l_ri^2 + 2l_{pi}l_{ri}cosq_i}}\dot{q}_i
\end{aligned}
$$

Comparing this equation with Equation (2.5) we can obtain $J_i\hat{q}_i$:

$$
J_i(\hat{q_i}) = \frac{-l_{pi}l_{ri}sin\hat{q}_i}{\sqrt{l_pi^2 + l_ri^2 + 2l_{pi}l_{ri}cos\hat{q}_i}}
$$

2.1.3 The Effective Actuating Force, F_ei, and the Joint Torque, T_i

The relationship between the effective actuating force of the ith joint ,F_{ei}, and the ith joint torque ,T_i, is obtained by applying the principle of virtual work.

$$
T_i\delta q_i = F_{ei}\delta x_i \tag{2.6}
$$

F_{ei} is related to the actuating force F_{ai} of the ith cylinder as follows:

$$
\begin{aligned}
F_{ei} &= F_{ai} - d_i\dot{x}_i - F_{ci} \\
F_{ai} &= P_{Ii}A_{Ii} - P_{Oi}A_{Oi}
\end{aligned} \tag{2.7}
$$

By substituting Equations (2.5) and (2.7) into Equation (2.6), the joint torque at $\hat{q}_i$ is obtained as follows:

$$
T_i = [F_{ai} - d_i\dot{x}_i - F_{ci}]J_i(\hat{q_i}) \tag{2.8}
$$

where d_i is the viscous damping of the ith cylinder and F_{ci} is Coulomb friction of the ith cylinder.

2.1.4 Transfer Function Representation

The transfer is defined as the ratio of the Laplace transform of the output variable to the Laplace transform of the input variable. The transfer function from the servo-valve input, U_i (voltage or current), to the joint angle, q_i, is obtained from Equations (2.2) through (2.8). In the remaining text, all variables such as q_i and T_i are used to represent a small change near the corresponding reference point without the gradient, Δ. Also, note that $\hat{J}_i$ is used instead of $J_i(\hat{q_i})$.

The following relationship of Laplace transformation is obtained from combining Equations (2.2), (2.5) and (2.8).

Recalling Equation (2.2)

$$\begin{vmatrix} T_1(s) \\ T_2(s) \end{vmatrix} = \begin{vmatrix} H_{11}s^2 & H_{12}s^2 \\ H_{21}s^2 & H_{22}s^2 \end{vmatrix} \begin{vmatrix} q_1(s) \\ q_2(s) \end{vmatrix} = \begin{vmatrix} \hat{J}_1(F_{a1} - d_1 s x_1 - F_{c1}) \\ \hat{J}_2(F_{a2} - d_2 s x_2 - F_{c2}) \end{vmatrix}$$

and rearranging these equations by moving terms from the left side to the right side we obtain:

$$\begin{vmatrix} H_{11}s^2 + \hat{J}_1^{\,2} d_1 s & H_{12}s^2 \\ H_{21}s^2 & H_{22}s^2 + \hat{J}_2^{\,2} d_2 s \end{vmatrix} \begin{vmatrix} q_1(s) \\ q_2(s) \end{vmatrix} = \begin{vmatrix} \hat{J}_1 F_{a1}(s) \\ \hat{J}_2 F_{a2}(s) \end{vmatrix}$$

The above equation can be represented as follows:

$$H(s)q(s) = \mathcal{F}_a(s) \tag{2.9}$$

where

$$H(s) = \begin{vmatrix} H_{11}s^2 + \hat{J}_1^{\,2} d_1 s & H_{12}s^2 \\ H_{21}s^2 & H_{22}s^2 + \hat{J}_2^{\,2} d_2 s \end{vmatrix} \qquad q(s) = \begin{vmatrix} q_1(s) \\ q_2(s) \end{vmatrix} \qquad \mathcal{F}_a(s) = \begin{vmatrix} \hat{J}_1 F_{a1}(s) \\ \hat{J}_2 F_{a2}(s) \end{vmatrix}$$

The actuating force, $F_a(s)$, can be derived from the characteristics of the hydraulic driving system by combining Equations (2.3), (2.4) and (2.7) (assuming that $C_{i1} = C_{i2} = C_i$):

(a): By equating (2.3) and (2.4) then, P_{Ii} and P_{Oi} can be obtained

$$\begin{aligned} K_{ui}U_i - K_{pi}P_{Ii} &= C_i\dot{P}_{Ii} + A_{Ii}\dot{x}_i \\ K_{ui}U_i + K_{pi}P_{Oi} &= -C_i\dot{P}_{Oi} + A_{Oi}\dot{x}_i \end{aligned}$$

Solving for P_{Ii} and P_{Oi},

$$P_{Ii} = \frac{K_{ui}U_i - A_{Ii}sx_i}{C_i s + K_{pi}} = \frac{K_{ui}U_i - A_{Ii}s\hat{J}_i q_i(s)}{C_i s + K_{pi}}$$

$$P_{Oi} = \frac{-K_{ui}U_i + A_{Oi}sx_i}{C_is + K_{pi}} = \frac{-K_{ui}U_i + A_{Oi}s\hat{J}_iq_i(s)}{C_is + K_{pi}}$$

(b): Substituting P_{Ii} and P_{Oi} into Equations (2.7) yields

$$F_{ai}(s) = \frac{1}{C_is + K_{pi}}[K_{ui}U_i(s)(A_{Ii} + A_{Oi}) - (A_{Ii}{}^2 + A_{Oi}{}^2)s\hat{J}_iq_i(s)] \quad (2.10)$$

Writing Equation (2.10) in a matrix form (after multiplying both sides by $\hat{J}_i$),

$$\mathcal{F}_a(s) = \begin{vmatrix} \frac{K_{u1}(A_{I1}+A_{O1})\hat{J}_1}{C_1s+K_{p1}} & 0 \\ 0 & \frac{K_{u2}(A_{I2}+A_{O2})\hat{J}_2}{C_2s+K_{p2}} \end{vmatrix} \begin{vmatrix} U_1(s) \\ U_2(s) \end{vmatrix} - \begin{vmatrix} \frac{K_{u1}(A_{I1}^2+A_{O1}^2)\hat{J}_1{}^2s}{C_1s+K_{p1}} & 0 \\ 0 & \frac{K_{u2}(A_{I2}^2+A_{O2}^2)\hat{J}_2{}^2s}{C_2s+K_{p2}} \end{vmatrix} \begin{vmatrix} q_1(s) \\ q_2(s) \end{vmatrix}$$

Equation (2.10) then becomes:

$$\mathcal{F}_a(s) = A(s)U(s) - B(s)q(s) \quad (2.11)$$

where

$$A(s) = \begin{vmatrix} \frac{K_{u1}(A_{I1}+A_{O1})\hat{J}_1}{C_1s+K_{p1}} & 0 \\ 0 & \frac{K_{u2}(A_{I2}+A_{O2})\hat{J}_2}{C_2s+K_{p2}} \end{vmatrix}$$

$$U(s) = \begin{vmatrix} U_1(s) \\ U_2(s) \end{vmatrix}$$

$$B(s) = \begin{vmatrix} \frac{(A_{I1}^2+A_{O1}^2)\hat{J}_1{}^2s}{C_1s+K_{p1}} & 0 \\ 0 & \frac{(A_{I2}^2+A_{O2}^2)\hat{J}_2{}^2s}{C_2s+K_{p2}} \end{vmatrix}$$

$$q(s) = \begin{vmatrix} q_1(s) \\ q_2(s) \end{vmatrix}$$

Substituting Equation (2.9) into Equation (2.11) gives

$$H(s)q(s) = A(s)U(s) - B(s)q(s)$$

or,

$$q(s) = [H(s) + B(s)]^{-1}A(s)U(s) \quad (2.12)$$

By adding the two matrices $H(s)$ and $B(s)$ and multiplying them by $A(s)U(s)$ gives

$$\begin{vmatrix} q_1(s) \\ q_2(s) \end{vmatrix} = \begin{vmatrix} H_{11}s^2 + \hat{J_1}^2 d_1 s + \frac{(A_{I1}^2 + A_{O1}^2)\hat{J_1}^2 s}{C_1 s + K_{p1}} & H_{12}s^2 \\ H_{21}s^2 & H_{22}s^2 + \hat{J_2}^2 d_2 s + \frac{(A_{I2}^2 + A_{O2}^2)\hat{J_2}^2 s}{C_2 s + K_{p2}} \end{vmatrix}^{-1}$$

$$\begin{vmatrix} \frac{K_{u1}(A_{I1} + A_{O1})\hat{J}_1}{C_1 s + K_{p1}} & 0 \\ 0 & \frac{K_{u2}(A_{I2} + A_{O2})\hat{J}_2}{C_2 s + K_{p2}} \end{vmatrix} \begin{vmatrix} U_1(s) \\ U_2(s) \end{vmatrix}$$

The transfer function of a single link mechanism is given by the diagonal components of Equation (2.12) as follows (this means that one joint is fixed which implies $q_1 = 0$ or $q_2 = 0$):

$$q_i(s) = [H_{ii}s^2 + \hat{J}_1^2 d_i s + \frac{(A_{Ii}^2 + A_{Oi}^2)\hat{J}_i^2 s}{C_i s + K_{pi}}]^{-1} \frac{K_{ui}(A_{Ii} + A_{Oi})\hat{J}_i}{C_i s + K_{pi}} U_i(s)$$

$$\begin{aligned} \frac{q_i(s)}{U_i(s)} &= \frac{K_{ui}(A_{Ii} + A_{Oi})\hat{J}_i}{(C_i s + K_{pi})[H_{ii}s^2 + \hat{J}_i^2 d_i s + \frac{(A_{Ii}^2 + A_{Oi}^2)\hat{J}_i^2 s}{C_i s + K_{pi}}]} \\ &= \frac{K_{ui}(A_{Ii} + A_{Oi})\hat{J}_i}{(C_i s + K_{pi})[H_{ii}s^2 + \hat{J}_i^2 d_i s] + (A_{Ii}^2 + A_{Oi}^2)\hat{J}_i^2 s} \end{aligned}$$

Then, the final form of the transfer function, $G_i(s)$, for a single link mechanism driven by electrohydraulic servo-valve is:

$$G_i(s) = \frac{q_i(s)}{U_i(s)} = \frac{K_{ui}(A_{Ii} + A_{Oi})\hat{J}_i}{H_{ii}C_i s^3 + (\hat{J}_i^2 d_i C_i + K_{pi}H_{ii})s^2 + \hat{J}_i^2(d_i K_{pi} + A_{Ii}^2 + A_{Oi}^2)s} \tag{2.13}$$

Equation (2.13) is a third-order transfer function which may be used to describe the dynamics performance of a single link servo-mechanism arm (closed-center valve with constant pressure pump). It should be noted that in the above analysis the servo-valve dynamic response was assumed to be fast enough so that it's delay effect can be neglected. Previous study showed that the inclusion of servo-valve dynamics has only a filtering effect on the pressure response and makes no different to the velocity response (Watton, 1987).

However, for the case of heavy-duty manipulators (open-center valve with constant flow pump), the effect of the servo-valve cannot be ignored. Previous experimental study by Sepehri (1990), showed a first-order relationship between the servo-valve input and the corresponding spool displacement. This relation (transfer function) can be represented by a first-order time lag as follows:

$$\frac{X_i}{U_i} = \frac{k}{\tau s + 1}$$

where k is the gain and τ is the time constant. Then, the final form of the transfer function for a single link heavy-duty arm including the valve dynamic is:

$$G_i(s) = \frac{k}{(1+\tau s)} \frac{K_{ui}(A_{Ii} + A_{Oi})\hat{J}_i}{H_{ii}C_i s^3 + (\hat{J}_i^2 d_i C_i + K_{pi}H_{ii})s^2 + \hat{J}_i^2(d_i K_{pi} + A_{Ii}^2 + A_{Oi}^2)s} \tag{2.14}$$

Equation (2.14) is a fourth-order transfer function which can be used to describe the dynamics performance of a single link servo-mechanism of a heavy-duty manipulators.

Inspecting Equations (2.13) and (2.14) shows that the valve coefficients K_{ui} and K_{pi} are extremely important in determining stability, frequency response, and other dynamic characteristics:

- The flow gain coefficient, K_{ui}, directly affects the open-loop gain constant of the system, thus, it has a direct influence on the system stability.
- The flow-pressure coefficient, K_{pi}, directly affects the damping ratio thus, can be used to determine the response shape of the system.

2.2 System Analysis

In the design of a control system, one must be able to predict the dynamic behavior of the system, whose components are known. The relative stability and the transient response of a closed-loop system are directly related to the location of the roots of the characteristic equation. It is necessary to adjust one or more system parameters in order to obtain suitable root locations. Therefore, it is worthwhile to determine how the roots of the characteristic equation of a given system migrate about the $\alpha - \beta$ plane or the $s-$ plane, as the parameters are varied. The parameter plane method will be used for the third-order system analysis, and root locus method will be used for the fourth-order system analysis.

2.2.1 Parameter Plane Analysis of Third-order Systems

The transfer function of the third-order system under consideration is represented by the following general form (see Figure 2.3)

$$G(s) = \frac{a_3}{s(s^2 + a_1 s + a_2)} \tag{2.15}$$

Writing Equation (2.13) in the form of Equation (2.15) gives

$$G(s) = \frac{\frac{K_{ui}(A_{Ii}+A_{Oi})\hat{J}_i}{H_{ii}C_i}}{s[s^2 + \frac{(\hat{J}_i^2 d_i C_i + K_{pi} H_{ii})}{H_{ii}C_i} s + \frac{\hat{J}_i^2(d_i K_{pi} + A_{Ii}^2 + A_{Oi}^2)}{H_{ii}C_i}]} \tag{2.16}$$

Equating Equations (2.16) and (2.15) we obtain the following parameters.

$$\begin{aligned}
a_1 &= \frac{(\hat{J}_i^2 d_i C_i + K_{pi} H_{ii})}{H_{ii} C_i} \\
a_2 &= \frac{\hat{J}_i^2 (d_i K_{pi} + A_{Ii}^2 + A_{Oi}^2)}{H_{ii} C_i} \\
a_3 &= \frac{K_{ui}(A_{Ii} + A_{Oi})\hat{J}_i}{H_{ii} C_i}
\end{aligned}$$

Normalizing Equation (2.15) gives Equation (2.17)

$$G(s) = 1/s_1(s_1^2 + \alpha s_1 + \beta) \tag{2.17}$$

where

$s_1 = s/a_3^{1/3}$	is the new operator of Laplace transformation
$\alpha = a_1/a_3^{1/3}$	is an adjusted parameter
$\beta = a_2/a_3^{2/3}$	is an adjusted parameter
$a_3^{1/3}t$	is the normalized time.

a_3 is the time scale of the response of Equation (2.17), while α and β are parameters that determine the shape of response.

The unity closed-loop transfer function of Equation (2.16) is

$$G(s) = \frac{a_3}{s(s^2 + a_1 s + a_2) + a_3} = \frac{\sigma\omega_n^2}{(s+\sigma)(s^2 + 2\zeta\omega_n s + \omega_n^2)} \tag{2.18}$$

where σ and ω_n are the real root and natural frequency, respectively ($\sigma\omega_n^2 = a_3$). They are normalized as follows:

$$\acute{\sigma} = \frac{\sigma}{a_3^{1/3}} \qquad \acute{\omega_n} = \frac{\omega_n}{a_3^{1/3}}$$

Then, α and β are related to ζ and $\acute{\omega_n}$ by the following equations (Hanafusa and Asada, 1980):

$$\begin{aligned} \alpha &= \frac{1}{\acute{\omega}_n^2}(2\acute{\omega}_n^3\zeta + 1). \\ \beta &= \frac{1}{\acute{\omega_n}}(\acute{\omega}_n^3 + 2\zeta). \end{aligned} \tag{2.19}$$

Siljak (1969) described a design procedure of a third-order system by using the $\alpha - \beta$ diagram (Parameter plane method). This method implies such a mapping for the characteristic curves of the system (constant ζ, $\acute{\omega_n}$ and $\acute{\sigma}$) on the $\alpha - \beta$ plane. Figure 2.4 represents the characteristic curves of the system under consideration. By observing the step responses for the specified values of α and β which are related to σ, ω_n and ζ as seen in Equation (2.19), the roots of the characteristic equation can be determined at any desired response. The unit-step response, $c(t)$, of Equation (2.18) can be calculated from the following Equation:

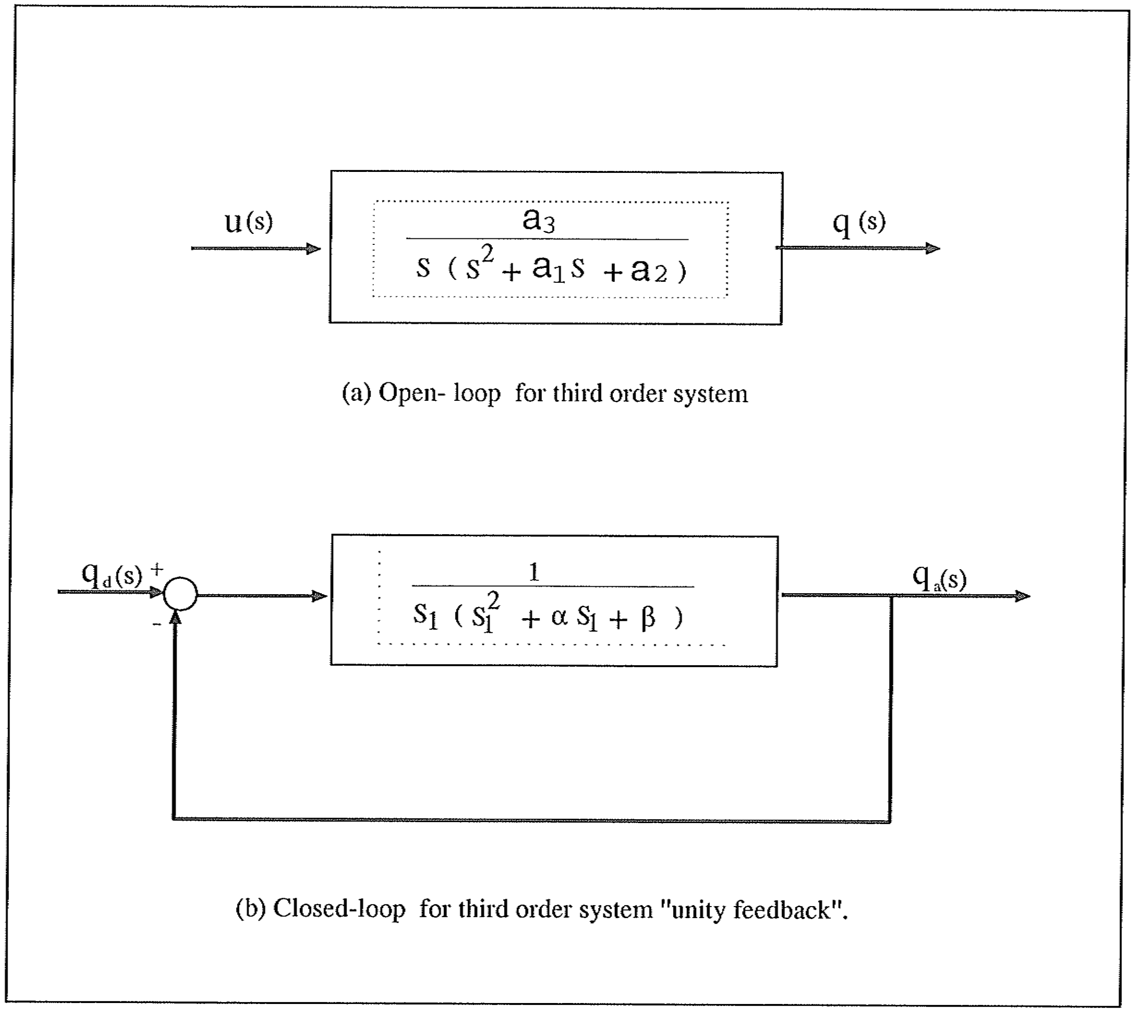

Figure 2.3: Open and closed-loop of third-order system

$$c(t) = 1 - A_1 e^{\sigma t} + A_2 e^{-\omega_n \zeta t} \sin[(\omega_n \sqrt{1 - \zeta^2})t + \phi]$$

where the constants A_1, A_2 and ϕ are dependent on α and β. It is clear that, the nature of the response depends inherently upon the values of ζ, ω_n and σ. The philosophy of system design is to establish a simple correlation between the system parameters and the characteristic roots so that the roots may be set at desired locations by adjusting the system parameters. The parameter plane method is also useful in guiding the computer simulation in finding the system elements and parameters that will result in the desired system performance characteristic. Now, we can

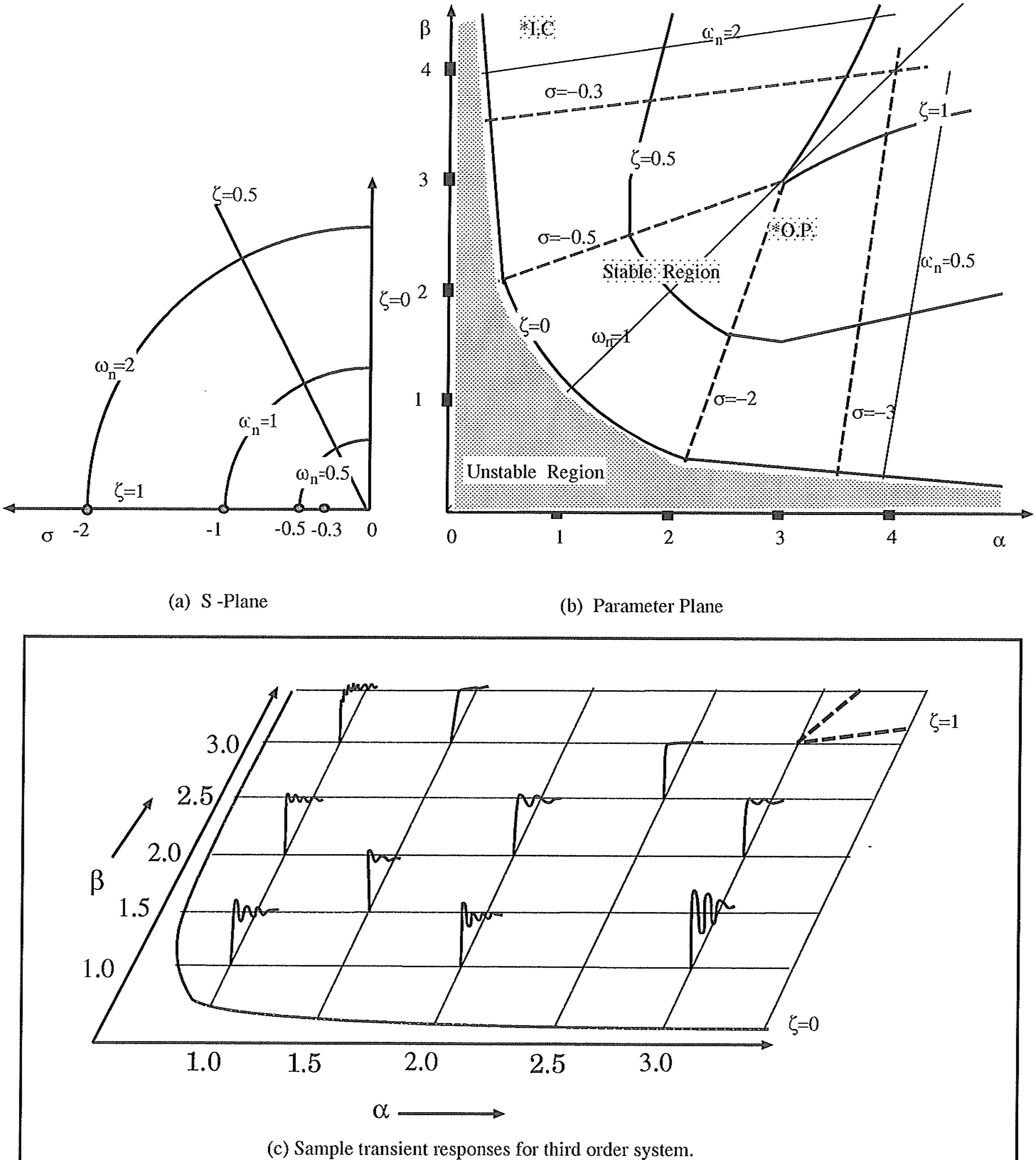

(a) S -Plane

(b) Parameter Plane

(c) Sample transient responses for third order system.

Figure 2.4: Parameter plane curves of third-order system

conclude that, the parameter plane techniques provide information about the effects on the system overall behavior of changing the operating conditions and parameters. Therefore, it can be used not only for system stability analysis but also as a design tool in cases where the specifications of the system performance are given in either the time or the frequency domain. For the robot arm shown in Figure 2.1, whose parameters are listed in Appendix B, the corresponding α and β were found to be $\alpha = 0.45$ and $\beta = 5.0$.

2.2.2 Root Locus Analysis of Fourth-order Systems

The root locus technique is another graphical method of determining the location of the roots of the characteristic equation as function of a parameter. The root locus, therefore, provides information not only for the absolute stability of the system but also for its degree of stability. If the system is unstable or has an unacceptable transient response, the root locus method indicates a possible way to improve the response. The root locus technique is recommended for analyzing high order systems.

The open-loop transfer function for the system shown in Figure 2.5-b, is represented as follows:

$$K\frac{Z(s)}{P(s)} = \frac{K}{s(s+\frac{1}{\tau})(s^2+a_1 s+a_2)}$$

where $K = ka_3/\tau$. There are four poles; two real and two complex:

$$\begin{aligned} s_{1,2} &= -\frac{a_1}{2} \pm j\sqrt{a_2 - \frac{{a_1}^2}{4}} = -\zeta\omega_n \pm j\omega_n\sqrt{1-\zeta^2} \\ s_3 &= 0 \\ s_4 &= -\frac{1}{\tau} \end{aligned}$$

where

$\omega_n = \sqrt{a_2}$

$\zeta = \frac{a_1}{2\sqrt{a_2}}$

The root locus plot is shown in Figure 2.6.

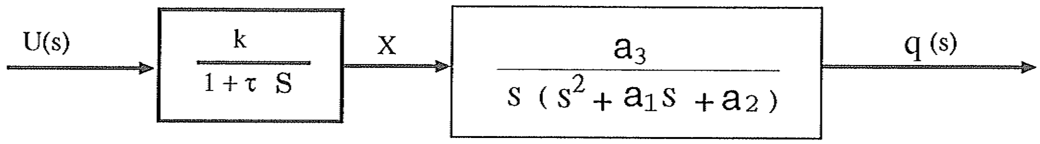

(a) Open- loop for fourth-order system

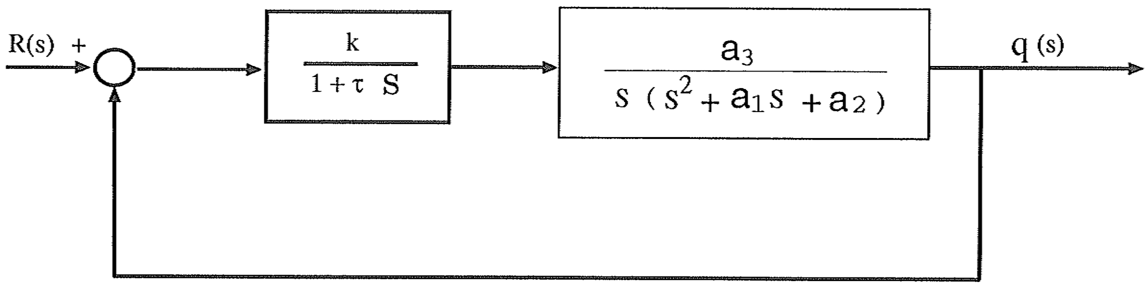

(b) Closed- loop (unity feedback) for fourth-order system

Figure 2.5: Open and closed loop of fourth-order system

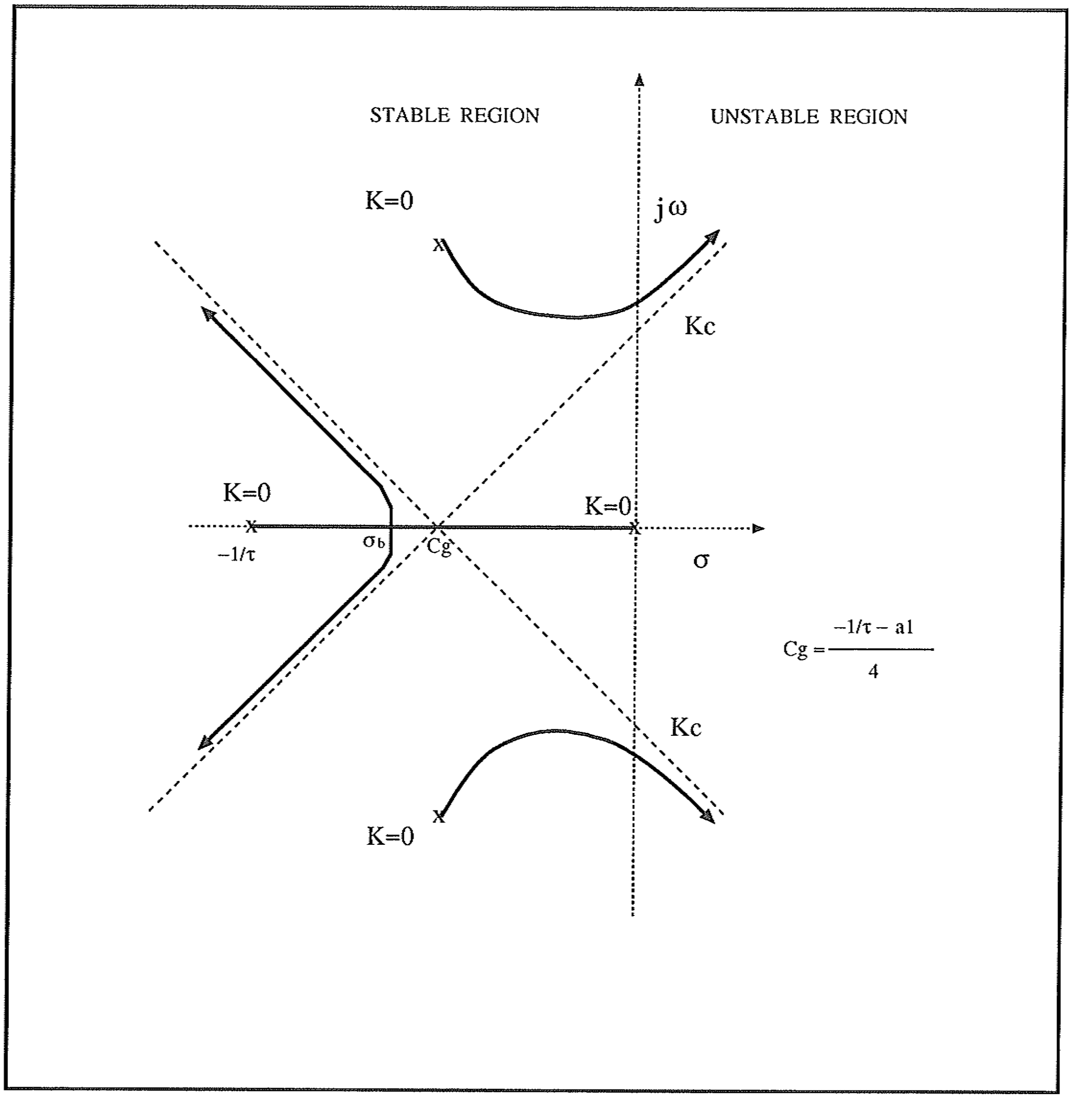

Figure 2.6: Root locus for the fourth-order system system (without compensation)

CHAPTER 3

HYDRAULIC ROBOT OPERATING FROM A CONSTANT PRESSURE

In this chapter, we will study the performance of the two degree-of-freedom robot which is shown in Figure 2.1. The mathematical model of this robot was developed in the previous chapter. We consider the robot as a light-duty robot arm using closed-center valves (zero-lapped conditions) operating from a constant supply pressure. The physical parameters of the robot have been chosen to resemble the hydraulic robot which is used in Kyoto University (Hanafusa and Asada, 1983) and they are listed in Appendix B. Three different control strategies will be discussed as applied to this model; actuating force feedback control, non-interaction control and load-insensitive control. The objective is to control the joint angles with faster response and less oscillation. Also the effect of the interaction between the linkage and loading will be considered

3.1 Feedback Compensation of Third-order Systems

The dynamic performance of the robot arm (under consideration) is described by a third-order and first type system. In general, velocity and acceleration feedback compensation are employed to control a third order system (Ogata, 1990). Whether to use velocity, acceleration or both as a feedback signal depends on the structure of the system. The system shown in Figure 3.1 is a third order system, in addition to proportional control, velocity and acceleration are used as feedback signals. The inclusion of velocity and acceleration feedback allows the parameters of the system to be adjusted from $\{a_1, a_2, a_3, \alpha,$ and $\beta\}$ to $\{a_1^*, a_2^*, a_3^*, \alpha^*$ and $\beta^*\}$, which will be examined in the following sections.

3.1.1 Velocity Feedback Compensation

When velocity feedback $G_f = k_v s$ is applied, the set of system parameters change as follows:

$$a_1^* = a_1, \qquad a_2^* = a_2 + a_3 k_v, \qquad a_3^* = a_3,$$
$$\alpha^* = \alpha, \qquad \beta^* = a_2/a_3^{2/3} + (a_3 k_v)/a_3^{2/3}.$$

Therefore, β increases while α does not change.

$$\beta^* = \beta + (a_3 k_v)/a_3^{2/3} \tag{3.1}$$

3.1.2 Acceleration Feedback Compensation

When acceleration feedback $G_f = k_a s^2$ is applied, the set of system parameters change as follows:

$$a_1^* = a_1 + a_3 k_a, \qquad a_2^* = a_2, \qquad a_3^* = a_3,$$
$$\alpha^* = a_1/a_3^{1/3} + (a_3 k_a)/a_3^{1/3}, \qquad \beta^* = \beta.$$

Therefore, α increases while β does not change.

$$\alpha^* = \alpha + (a_3 k_a)/a_3^{1/3} \tag{3.2}$$

3.1.3 Velocity & Acceleration Feedback Compensation

When both velocity and acceleration feedback ,$G_f = k_v s + k_a s^2$, are applied, the set of system parameters change as follows:

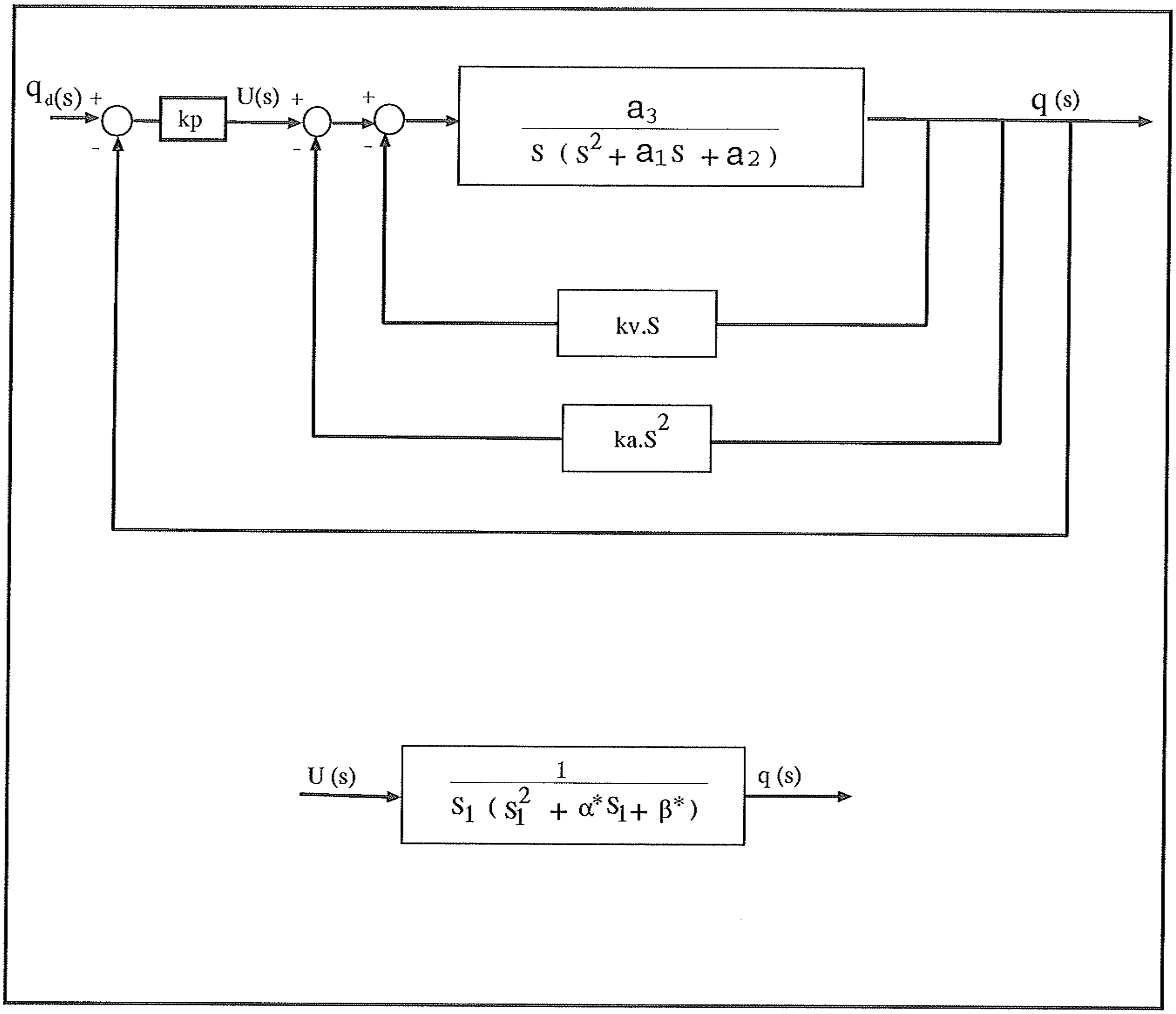

Figure 3.1: Velocity and acceleration feedback compensation

$$a_1^* = a_1 + a_3 k_a, \qquad a_2^* = a_2 + a_3 k_v,, \qquad a_3^* = a_3,$$
$$\alpha^* = \alpha + (a_3 k_a)/a_3^{1/3}, \qquad \beta^* = \beta + (a_3 k_v)/a_3^{2/3}.$$

Therefore, α and β have increased.

$$\begin{aligned} \alpha^* &= \alpha + (a_3 k_a)/a_3^{1/3} \\ \beta^* &= \beta + (a_3 k_v)/a_3^{2/3} \end{aligned} \tag{3.3}$$

The effects of velocity and acceleration feedback compensation are shown in Figure 3.2-a. Two different cases are considered as:

- When β is much larger than α, ($\beta \gg \alpha$) in the original system (as represented by point A in Figure 3.2), the effect of acceleration feedback increases ζ. Therefore, stability and damping are improved. The velocity feedback has no effects on the improvement in this case.

- When α is much larger than β, ($\alpha \gg \beta$), for different system parameters as represented by point B in Figure 3.2, the effects of the feedback compensation are opposite to the previous case.

The response time can be determined by adjusting the gain constant a_3. Increasing a_3 further, decrease α and β simultaneously and the system approaches unstable region. Knowing the parameters of the system, the nature of the feedback signal can be determined for a desired system response. In regards to the robot arm under consideration at which $\alpha = 0.45$ and $\beta = 5.0$ ($\beta \gg \alpha$) acceleration will be used as feedback signal.

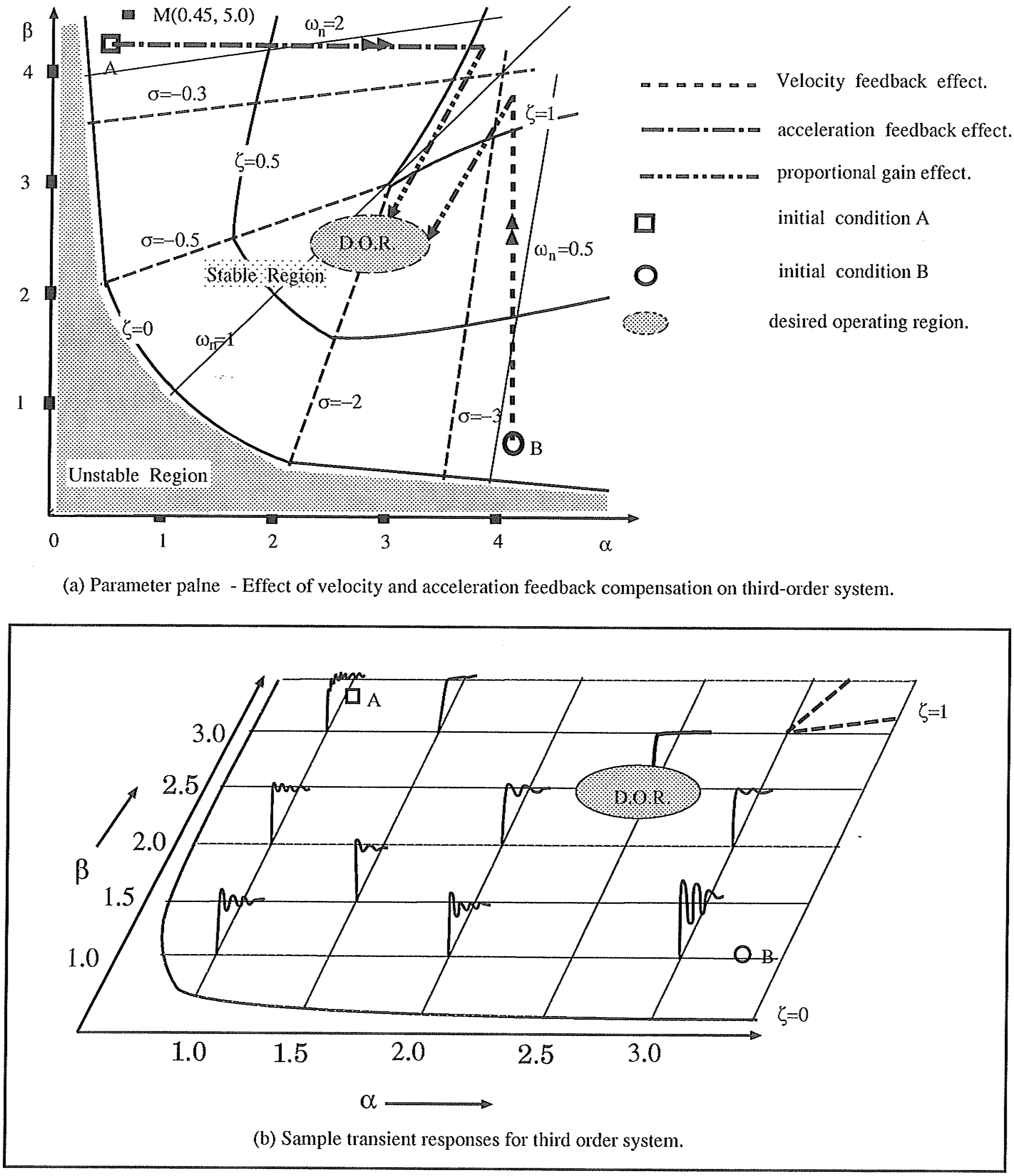

(a) Parameter palne - Effect of velocity and acceleration feedback compensation on third-order system.

(b) Sample transient responses for third order system.

Figure 3.2: Parameter plane and effect of velocity and acceleration feedback

3.2 Single-link Position Control

3.2.1 Closed-loop System with Actuating Force Feedback

In practical applications, actuating force feedback is used for electrohydraulic servomechanisms instead of acceleration feedback. The actuating force is determined by measuring the pressures on both sides of the piston. However, the pressure feedback causes static control error due to a static disturbance force. It is thus necessary to insert a high pass filter in the feedback loop in order to eliminate the feedback of steady state force differences (Welch, 1962). Referring to Figure 3.3-c, the actuating force F_{ai} of Equation (2.7) is used as a feedback signal. The input to the servo-valve changes from U_i to U_i^*:

$$U_i^* = U_i - \frac{K_{pfi}T_{fi}s}{1+T_{fi}s}F_{ai} \tag{3.4}$$

where K_{pfi} is the gain constant of actuating force feedback loop, and T_{fi} is the time constant of the high pass filter. By recalling Equation (2.10) and replacing U_i by U_i^*, the driving force of the piston is obtained as follows

$$F_{ai}(s) = \frac{1}{C_i s + K_{pi}}[K_{ui}U_i^*(A_{Ii} + A_{Oi}) - (A_{Ii}^2 + A_{Oi}^2)s\hat{J}_i q_i(s)]$$

$$\begin{aligned} F_{ai}(s) = \frac{1}{C_i s + K_{pi}}[K_{ui}U_i(A_{Ii} + A_{Oi}) \quad & -K_{ui}(A_{Ii} + A_{Oi})\tfrac{K_{pfi}T_{fi}s}{1+T_{fi}s}F_{ai} \\ & -(A_{Ii}^2 + A_{Oi}^2)s\hat{J}_i q_i(s)] \end{aligned}$$

Solving for $F_{ai}(s)$

$$F_{ai}(s) = \frac{1}{C_i s + K_{pi} + K_{ui}(A_{Ii} + A_{Oi})\frac{K_{pfi}T_{fi}s}{1+T_{fi}s}}[K_{ui}(A_{Ii} + A_{Oi})U_i - (A_{Ii}^2 + A_{Oi}^2)s\hat{J}_i q_i(s)]$$

$$F_{ai}(s) = \frac{1}{C_i s + K_{pi}^*}[K_{ui}U_i(A_{Ii} + A_{Oi}) - (A_{Ii}^2 + A_{Oi}^2)s\hat{J}_i q_i(s)] \tag{3.5}$$

This result shows that the effect of the actuating force feedback is represented by replacing K_{pi} by K^*_{pi}.

where

$$K^*_{pi} = K_{pi} + K_{pfi}\frac{K_{ui}(A_{Ii} + A_{Oi})T_{fi}s}{1 + T_{fi}s} \tag{3.6}$$

The control input becomes as follows:

$$U^*_i = U_i - K_{pfi}F^*_{ai} \tag{3.7}$$

$$U^*_i = k_p(q_{i.des} - q_{i.act}) - K_{pfi}F^*_{ai} \tag{3.8}$$

where F^*_{ai} is the output of high pass filter (H.P.F.).

3.2.2 Simulation Results

A unit-step input is used as a test signal for the simulation program which simulates the joints motion of the robot shown in Figure 2.1. Link "one" is commanded to move from the reference position $q_1 = 90°$ to the desired position $q_1 = 99°$ while, q_2 is fixed at $q_2 = -45°$.

- Results of using only proportional control (without actuating force feedback) Figures 3.4 through 3.9 show the simulation results using proportional control. Figure 3.4, represents the step responses of q_1 for different values of gain. Clearly, the proportional control affects the response time of the system, in the manner of high gain reduces response time. However, as a result of increasing the gain constant of the system, the system response becomes more oscillatory and requires more settling time. From this figure the desired response time can be determined by selecting appropriate proportional gain. Figure 3.5 shows the control input of the system for the desired gain, ($k_{p1} = 0.02$), and the signal of actuating force feedback. From this figure (only using proportional control), the gain of the actuating force is adjusted in order to be used for improving the response. Figures 3.6 and 3.7 represent the actuating force of the hydraulic actuator and the pressures in both lines, respectively. Effect of loading and compliance of the hydraulic system on the system response are shown in Figures 3.8 and 3.9, respectively. In both figures, the unit-step response of q_1 becomes oscillatory and requires more settling time ($k_{p1} = 0.02$).

- Results of using proportional control and actuating force feedback

  Figures 3.10 through 3.15 show the simulation results using proportional control and actuating force feedback. Figure 3.10 shows the improvement of step response of q_1 previously shown in Figure 3.4 ($k_{p1} = 0.02$). The effect of the actuating force changes with the actuating frequency, thus, the actuating force feedback gain, K_{pf1} is determined by observing the step responses at which the response of Figure 3.4 becomes without overshoots and without oscillations. When the inertia load is increased, the result shows overshoots and increased settling time. Therefore, it is necessary to compensate for the disturbance due to the expected load increase with an adjusted K_{pf1} as shown in Figure 3.14. In this experiment $K_{pf1} = 0.6 \times 10^{-7}$ and $T_{f1} = 1.0$. Referring to Figure 3.12, the actuating force required to hold the robot in this configuration is very small ($57.75\ N$).

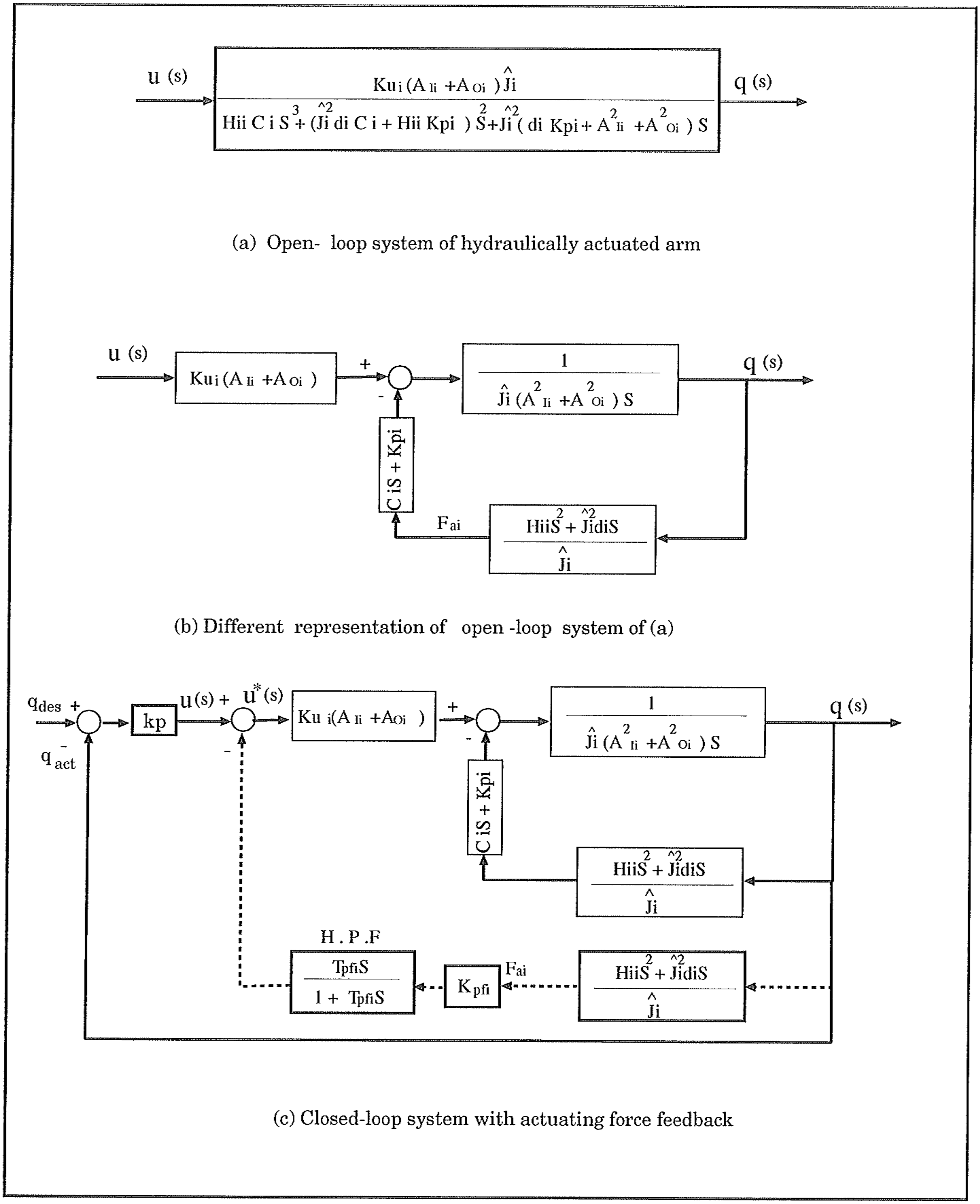

(a) Open- loop system of hydraulically actuated arm

(b) Different representation of open -loop system of (a)

(c) Closed-loop system with actuating force feedback

Figure 3.3: Closed-loop system with actuating force feedback

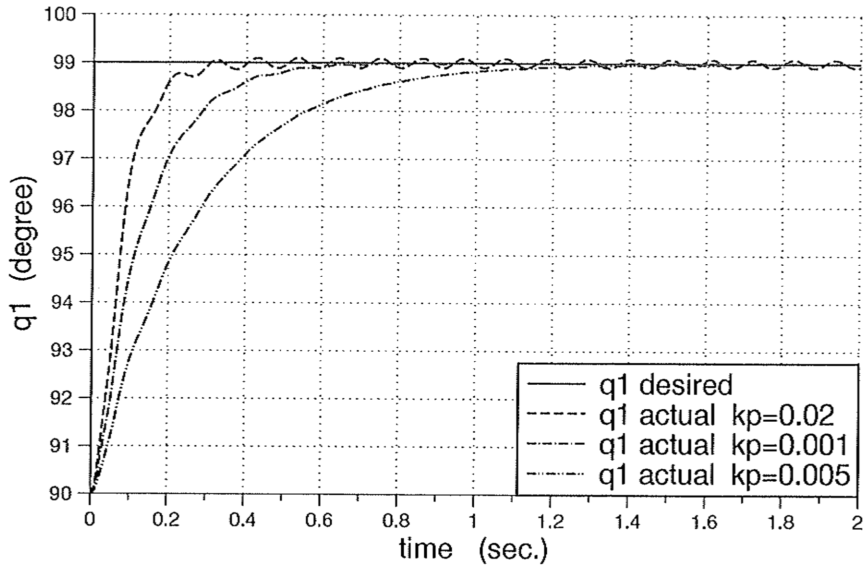

Figure 3.4: Step response of q_1; proportional control

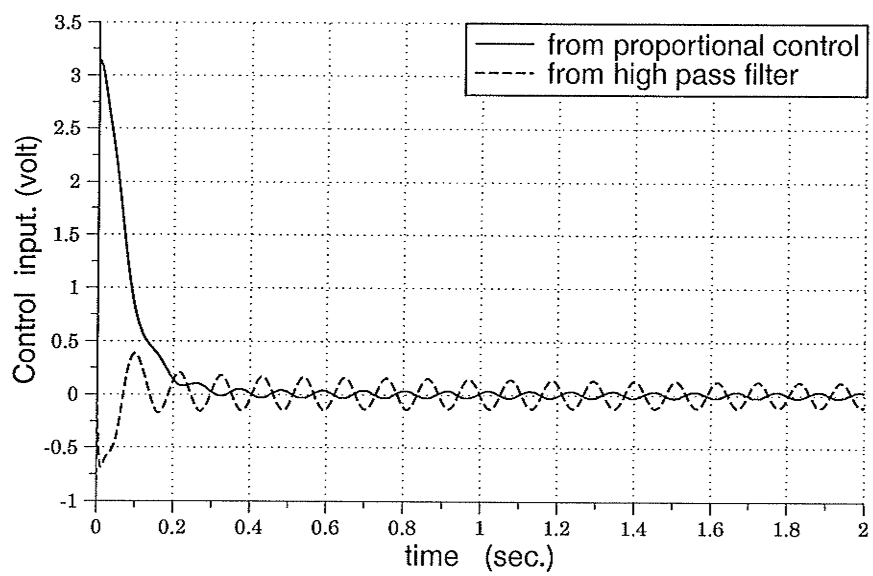

Figure 3.5: Control input

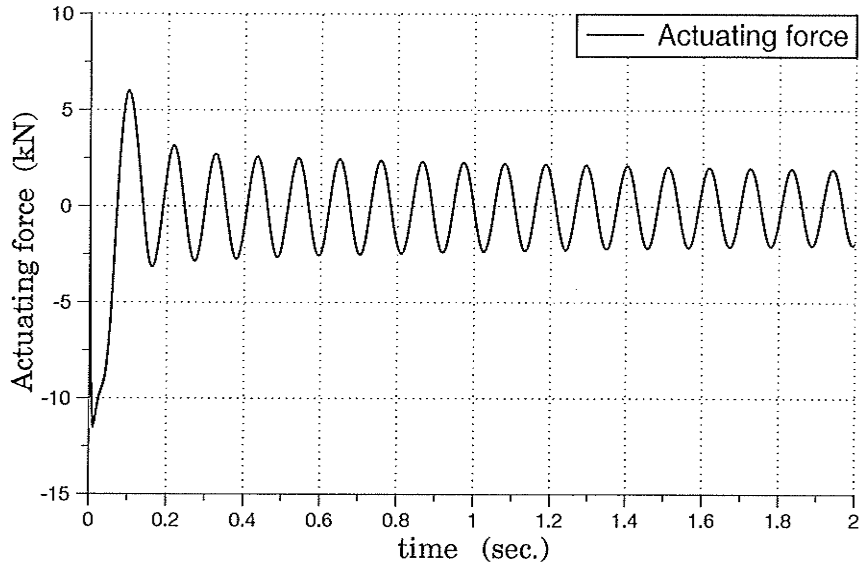

Figure 3.6: Actuating force

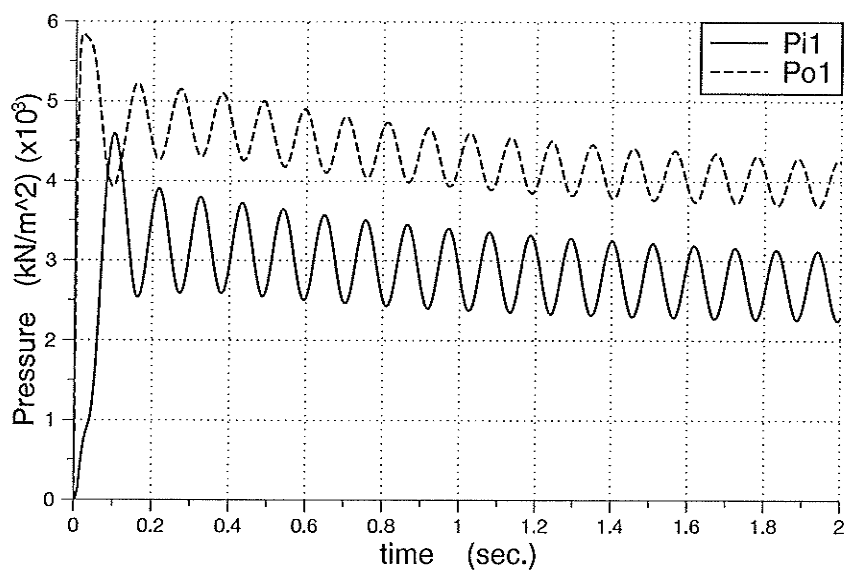

Figure 3.7: Pressures P_{i1} and P_{o1}

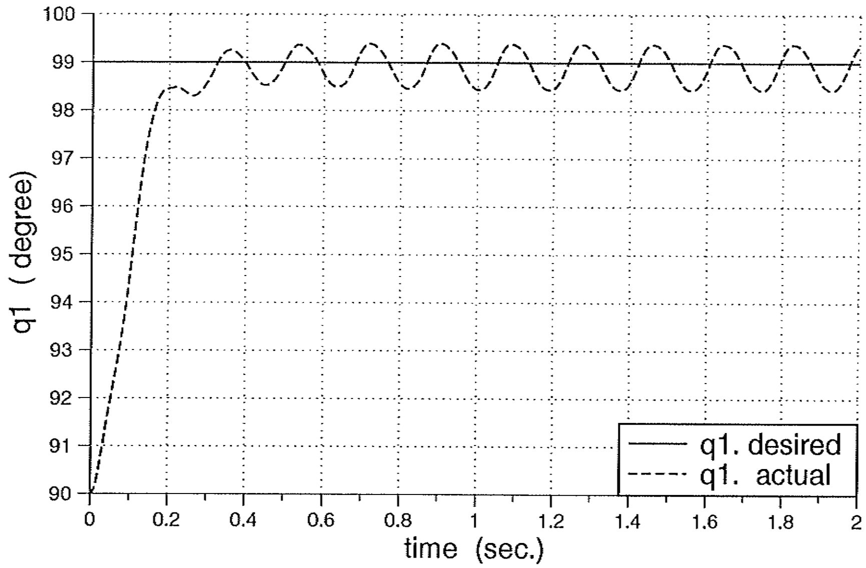

Figure 3.8: Step response of q_1; loaded (three times inertia)

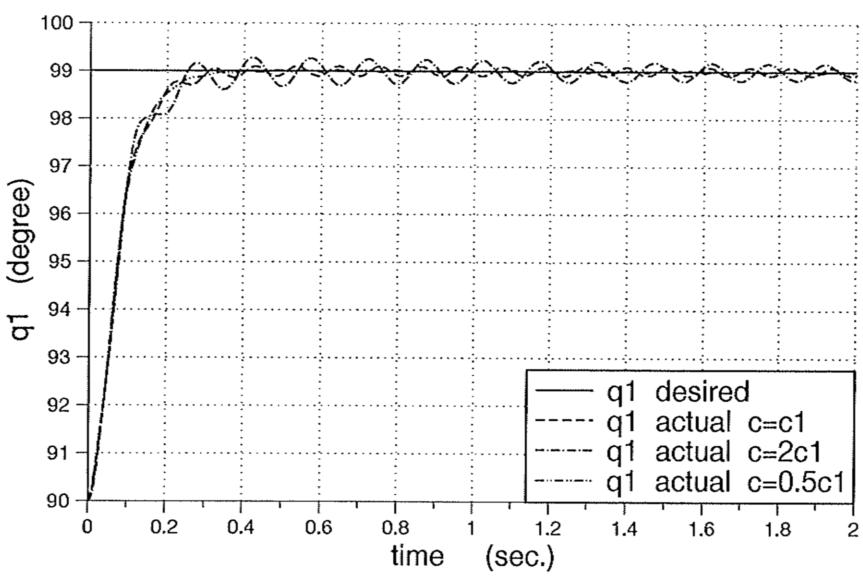

Figure 3.9: Effect of changing C

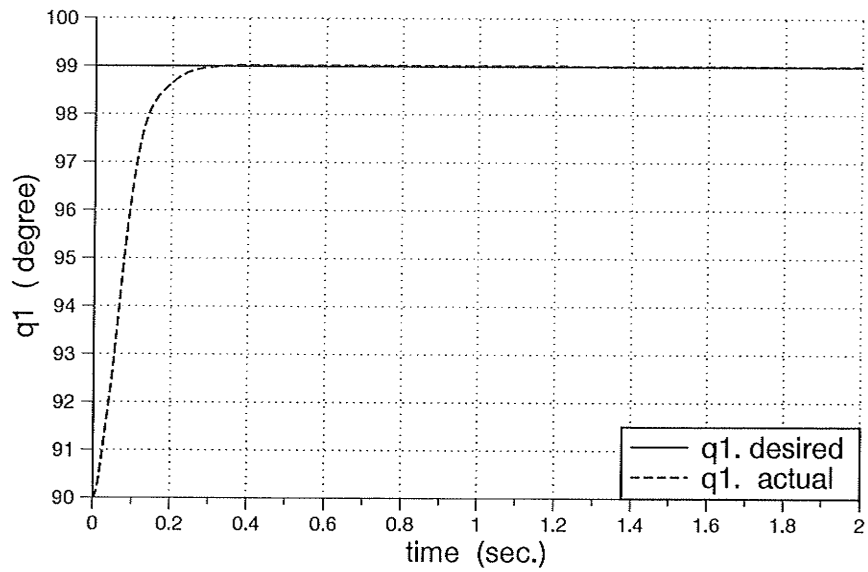

Figure 3.10: Step response of q_1; actuating force feedback

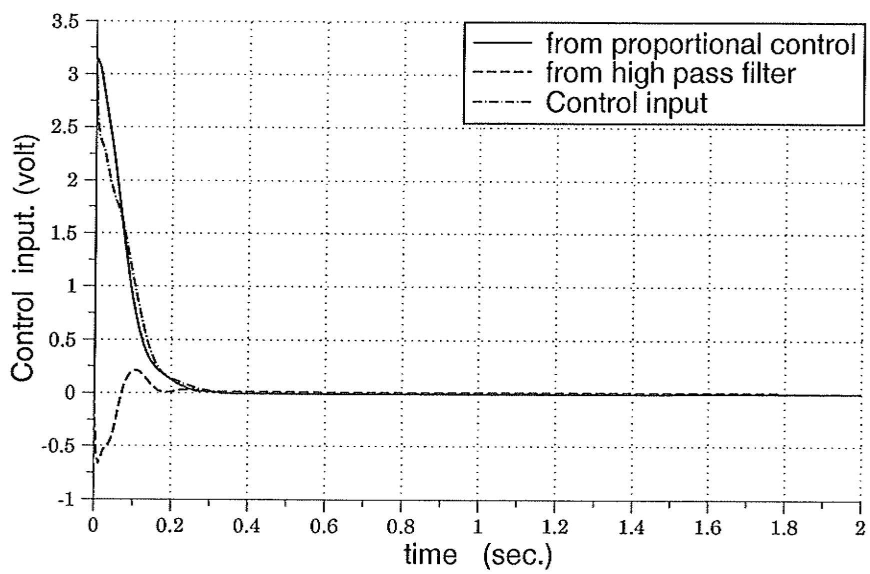

Figure 3.11: Control input

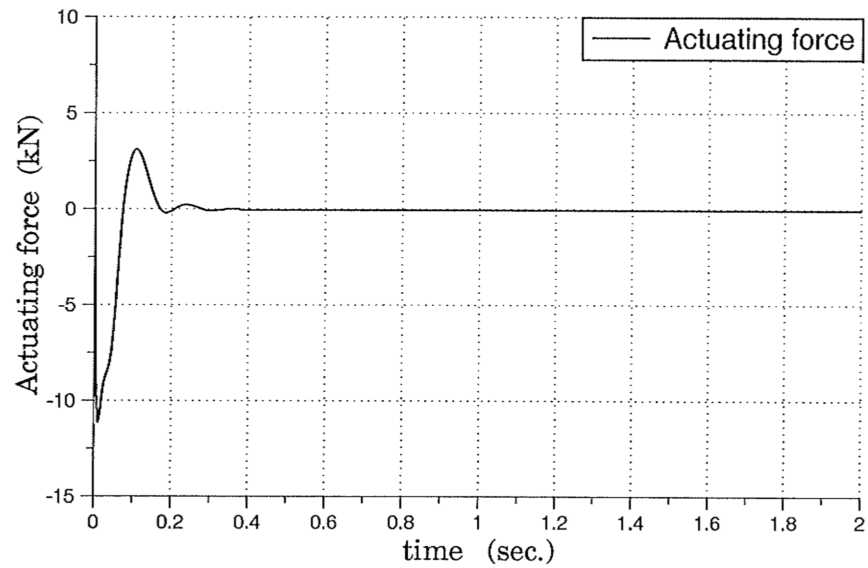

Figure 3.12: Actuating force

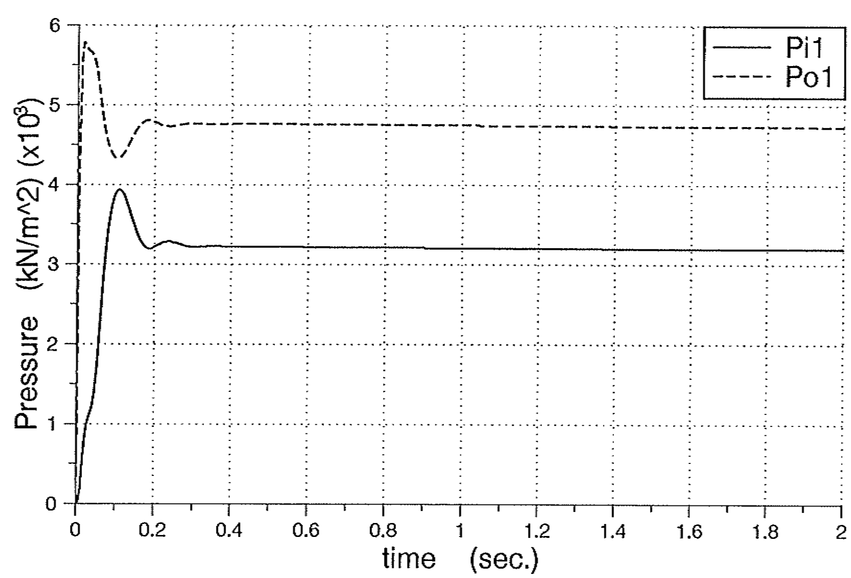

Figure 3.13: Pressures P_{i1} and P_{o1}

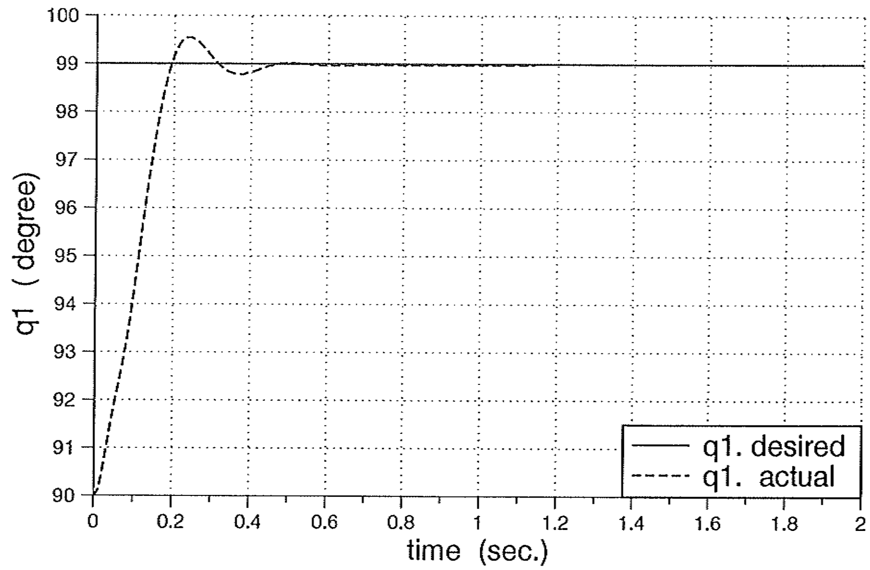

Figure 3.14: Step response of q_1; loaded

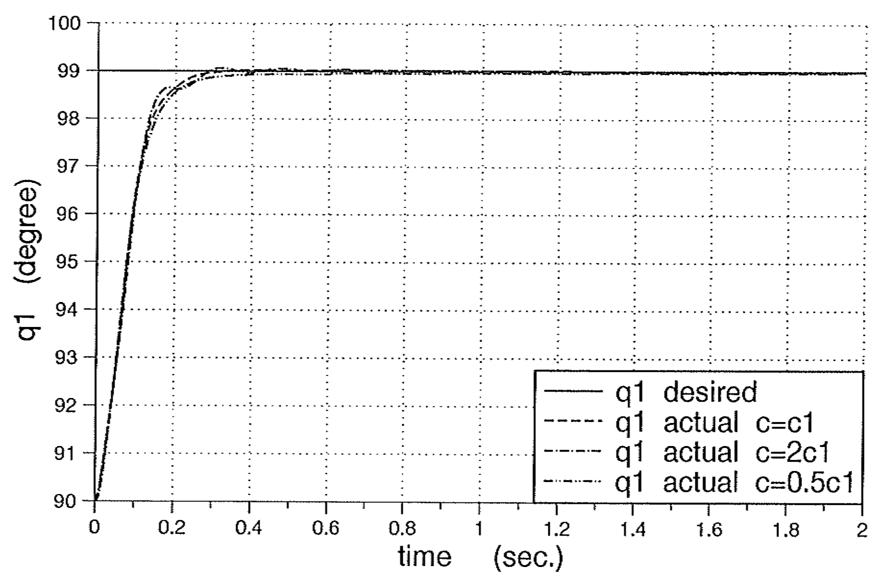

Figure 3.15: Effect of changing C

3.3 Multi-link Position Control

3.3.1 Compensation For Interaction Between Two Link Motions

Many control systems have multiple inputs and multiple outputs. It is often desired that changes in one reference input affect only one output. If such non-interaction or uncoupling can be achieved, then there is no interaction between the outputs. The closed-loop transfer matrix must be a diagonal one for non-interaction control as seen in Equation (3.9).

$$\begin{vmatrix} q_1(s) \\ q_2(s) \end{vmatrix} = G(s) \begin{vmatrix} U_1(s) \\ U_2(s) \end{vmatrix}$$

$$G(s) = \begin{vmatrix} G_{11}(s) & 0 \\ 0 & G_{22}(s) \end{vmatrix} \tag{3.9}$$

The compensation for interaction of multi-link motions (two link motions in our simulation) is applied after the individual servo system is improved as a single-link mechanism. Recall Equation (2.11) where the actuating force is represented,

$$\mathcal{F}_a(s) = A(s)U(s) - B(s)q(s)$$

where

$$\begin{aligned} A(s) &= \begin{vmatrix} \frac{K_{u1}(A_{I1}+A_{O1})\hat{J}_1}{C_1 s+K_{p1}} & 0 \\ 0 & \frac{K_{u2}(A_{I2}+A_{O2})\hat{J}_2}{C_2 s+K_{p2}} \end{vmatrix} \\ U(s) &= \begin{vmatrix} U_1(s) \\ U_2(s) \end{vmatrix} \\ B(s) &= \begin{vmatrix} \frac{(A_{I1}^2+A_{O1}^2)\hat{J}_1{}^2 s}{C_1 s+K_{p1}} & 0 \\ 0 & \frac{(A_{I2}^2+A_{O2}^2)\hat{J}_2{}^2 s}{C_2 s+K_{p2}} \end{vmatrix} \\ q(s) &= \begin{vmatrix} q_1(s) \\ q_2(s) \end{vmatrix} \end{aligned}$$

It was previously shown that using the filtered actuated force, F^*_{ai}, as a feedback signal improved the individual joint response, which means the flow-pressure coefficient has changed from K_{pi} to K^*_{pi} defined as:

$$K^*_{pi} = K_{pi} + K_{pfi}\frac{K_{ui}(A_{Ii} + A_{Oi})T_{fi}s}{1 + T_{fi}s}$$

Now, the actuating force is represented as follows instead of Equation (2.11).

$$\mathcal{F}_a(s) = A^*(s)U(s) - B^*(s)q(s) \tag{3.10}$$

By applying the actuating force for non-interaction control, the input to the servo valve is changed from U_i to $\hat{U}_i$ defined as:

$$\hat{U}(s) = U(s) - K_f(s)\mathcal{F}_a(s) \tag{3.11}$$

where

$K_f(s)$ is the transfer matrix of the actuating force feedback loop. By substituting $\hat{U}(s)$ instead of $U(s)$ in Equation (3.10) the actuating force becomes as follow

$$\mathcal{F}_{ai}(s) = A^*(s)U(s) - A^*(s)K_f(s)\mathcal{F}_a(s) - B^*(s)q(s)$$

$$\mathcal{F}_{ai}(s) = [I + A^*(s)K_f(s)]^{-1}[A^*(s)U(s) - B^*(s)q(s)] \tag{3.12}$$

Substitution in Equation (2.9) gives

$$[I + A^*(s)K_f(s)]H(s)q(s) = [A^*(s)U(s) - B^*(s)q(s)]$$

With these changes the equation of motion becomes as:

$$q(s) \;=\; [H(s) + A^*(s)K_f(s)H(s) + B^*(s)]^{-1}A^*(s)U(s) \tag{3.13}$$

The non-interaction of the equation of motion can be achieved by making the coefficient matrix of Equation (3.13) a diagonal one by determining right elements for $K_f(s)$

$$q(s) \;=\; [H_d(s) + B^*(s)]^{-1}A^*(s)U(s) \tag{3.14}$$

where $H_d(s)$ is the desired diagonal matrix which has the same elements as $H(s)$. Equating Equations (3.13) and (3.14) yields

$$K_f(s) = A^{*-1}(s)[H_d(s) - H(s)]H^{-1}(s). \tag{3.15}$$

where

$$A^{*-1}(s) = \begin{vmatrix} \frac{C_1 s + K_{p1}^*}{K_{u1}(A_{I1}+A_{O1})\hat{J}_1} & 0 \\ 0 & \frac{C_2 s + K_{p2}^*}{K_{u2}(A_{I2}+A_{O2})\hat{J}_2} \end{vmatrix}$$

$$H_d(s) - H(s) = \begin{vmatrix} 0 & H_{12}s^2 \\ H_{21}s^2 & 0 \end{vmatrix}$$

$$H^{-1}(s) = \begin{vmatrix} \frac{H_{22}s^2 + \hat{J}_2^{\,2} d_2 s}{\Delta} & \frac{-H_{12}s^2}{\Delta} \\ \frac{-H_{21}s^2}{\Delta} & \frac{H_{11}s^2 + \hat{J}_1^{\,2} d_1 s}{\Delta} \end{vmatrix}$$

Δ is the determinant of matrix H(s)

$$\Delta = (H_{11}H_{22} - H_{12}^2)s^4 + (H_{11}\hat{J}_2^{\,2} d_2 + H_{22}\hat{J}_1^{\,2} d_1)s^3 + (\hat{J}_1^{\,2} d_1 . \hat{J}_2^{\,2} d_2)s^2$$

$$K_f(s) = \begin{vmatrix} \frac{C_1 s + K_{p1}^*}{K_{u1}(A_{I1}+A_{O1})\hat{J}_1} & 0 \\ 0 & \frac{C_2 s + K_{p2}^*}{K_{u2}(A_{I2}+A_{O2})\hat{J}_2} \end{vmatrix} \begin{vmatrix} 0 & H_{12}s^2 \\ H_{21}s^2 & 0 \end{vmatrix} \begin{vmatrix} \frac{H_{22}s^2 + \hat{J}_2^{\,2} d_2 s}{\Delta} & \frac{-H_{12}s^2}{\Delta} \\ \frac{-H_{21}s^2}{\Delta} & \frac{H_{11}s^2 + \hat{J}_1^{\,2} d_1 s}{\Delta} \end{vmatrix}$$

$$K_f(s) = \begin{vmatrix} \frac{C_1 s + K_{p1}^*}{K_{u1}(A_{I1}+A_{O1})\hat{J}_1} & 0 \\ 0 & \frac{C_2 s + K_{p2}^*}{K_{u2}(A_{I2}+A_{O2})\hat{J}_2} \end{vmatrix} \begin{vmatrix} \frac{-H_{12}^2 s^4}{\Delta} & \frac{H_{12}s^2(H_{11}s^2 + \hat{J}_1^{\,2} d_1 s)}{\Delta} \\ \frac{H_{12}s^2(H_{22}s^2 + \hat{J}_2^{\,2} d_2 s)}{\Delta} & \frac{-H_{12}^2 s^4}{\Delta} \end{vmatrix}$$

$$K_f(s) = \begin{vmatrix} -\frac{C_1 s + K_{p1}^*}{K_{u1}(A_{I1}+A_{O1})\hat{J}_1}\frac{H_{12}^2 s^4}{\Delta} & \frac{C_1 s + K_{p1}^*}{K_{u1}(A_{I1}+A_{O1})\hat{J}_1}\frac{H_{12}s^2(H_{11}s^2 + \hat{J}_1^{\,2} d_1 s)}{\Delta} \\ \frac{C_2 s + K_{p2}^*}{K_{u2}(A_{I2}+A_{O2})\hat{J}_2}\frac{H_{12}s^2(H_{22}s^2 + \hat{J}_2^{\,2} d_2 s)}{\Delta} & -\frac{C_2 s + K_{p2}^*}{K_{u2}(A_{I2}+A_{O2})\hat{J}_2}\frac{H_{12}^2 s^4}{\Delta} \end{vmatrix}$$

The exact numerical value of each element of $K_f(s)$ can be found from the above equation. As a first approximation (Hanafusa, 1980), one must consider the first two terms of each element. Therefore, each element of $K_f(s)$ is represented as follows:

$$K_{f11} = c_{11f_0}s + c_{11f_1}$$

$$K_{f12} = c_{12f_0}s + c_{12f_1}$$

$$\begin{aligned} K_{f21} &= c_{21f_0}s + c_{21f_1} \\ K_{f22} &= c_{21f_0}s + c_{22f_1} \end{aligned}$$

Finally, the control input to the servovalves are:

$$\left\{ \begin{array}{c} \hat{U}_1 \\ \\ \hat{U}_2 \end{array} \right\} = \left| \begin{array}{c} k_{p1}(q_{1.des} - q_{1.act}) - K_{pf1}F_{a1}^* \\ \\ k_{p2}(q_{2.des} - q_{2.act}) - K_{pf2}F_{a2}^* \end{array} \right| - \left| \begin{array}{cc} -K_{f11} & K_{f12} \\ \\ K_{f21} & -K_{f22} \end{array} \right| \left\{ \begin{array}{c} \hat{J}_2 F_{a1} \\ \\ \hat{J}_2 F_{a1} \end{array} \right\} \tag{3.16}$$

3.3.2 Simulation Results

A unit-step input is used as a test signal for the simulation program which simulates the joints motion of the robot in Figure 2.1. Joint one, q_1, was commanded to move from the reference position $q_1 = 90°$ to the desired position $q_1 = 99°$ and joint two, q_2, was commanded to move from the reference position $q_2 = -45°$ to the desired position $q_2 = -35°$. Non-interactive control was implemented after having the response of each link improved as a single link servo-mechanism by using actuating force feedback. In this section we study the performance of moving both joint at the same time.

- Results of without non-interactive control

  Figures 3.16 and 3.17, represent the unit-step response of q_1 of and q_2, respectively. Clearly, link one was less influenced by the interaction forces than was link two.

- Results of with non-interactive control

  Figures 3.18 and 3.19, represent the step response of q_1 and q_2, respectively. Response of joint one has improved and is more stable than the response of joint two. The reason for this behavior is believed to be due to the fact that similar servo-valve configurations are used for both links. Therefore, for the interaction forces it is important to know the exact system parameters. Loading the system with three times the inertia for the same gains (non-interaction control) not only intensifies the interaction forces but also creates a steady state force disturbance as shown in Figures 3.20 and 3.21.

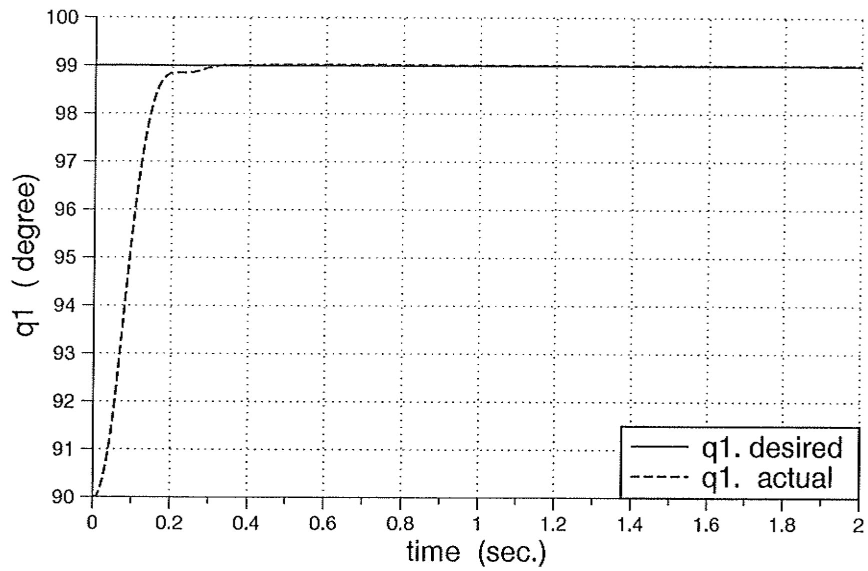

Figure 3.16: Step response; q_1 without non-interactive control

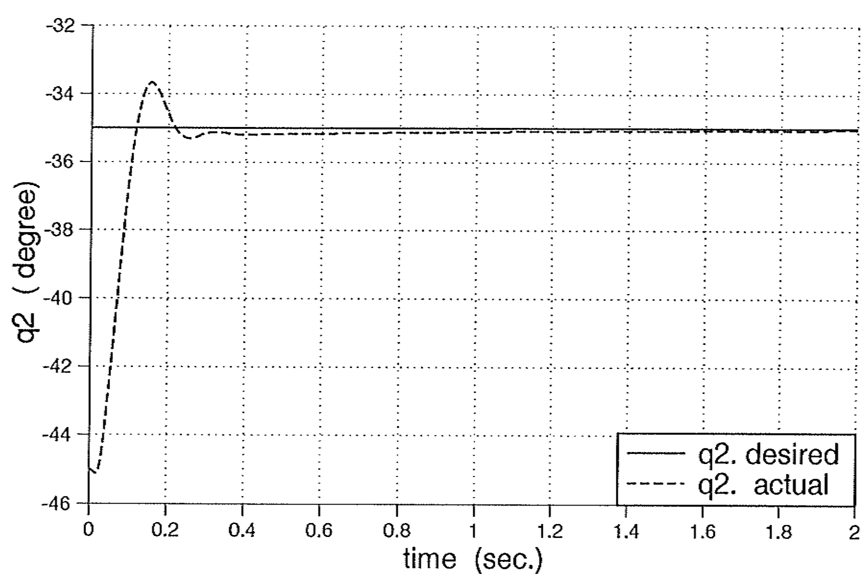

Figure 3.17: Step response; q_2 without non-interactive control

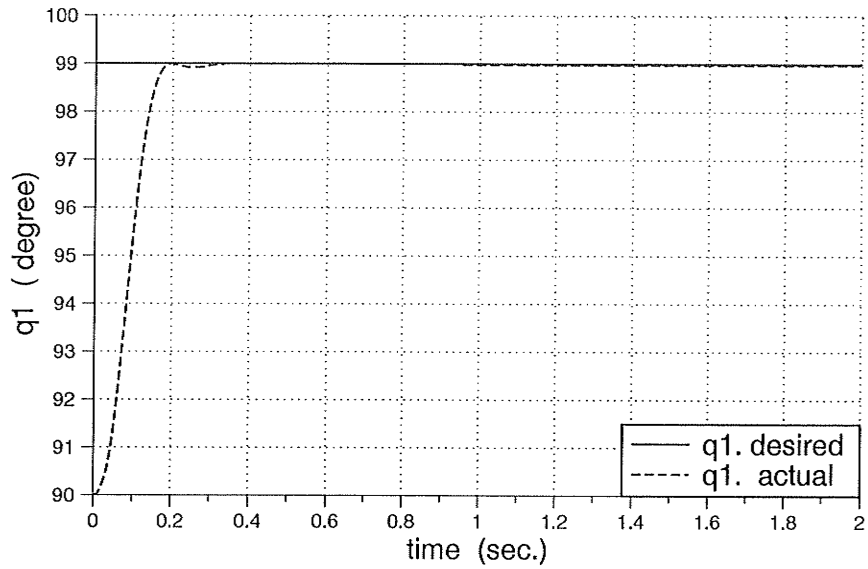

Figure 3.18: Step response; q_1 with non-interactive control

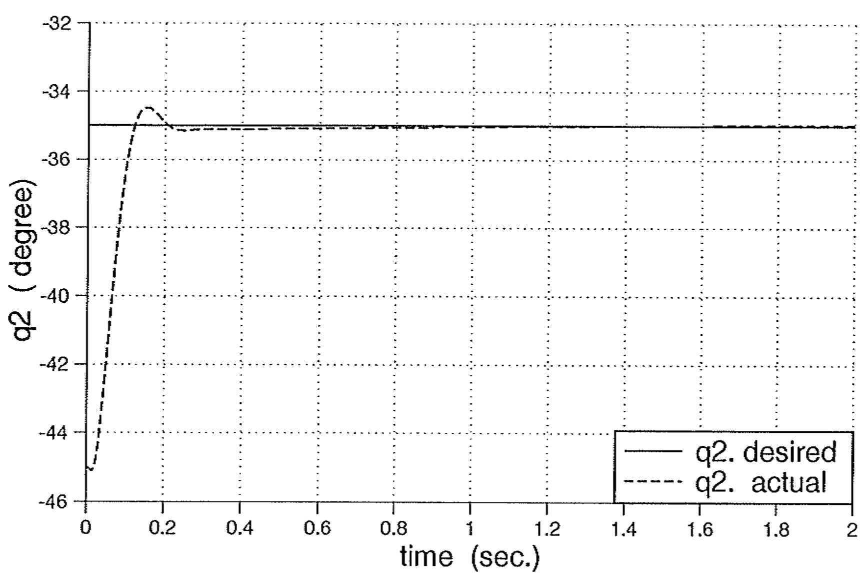

Figure 3.19: Step response; q_2 with non-interactive control

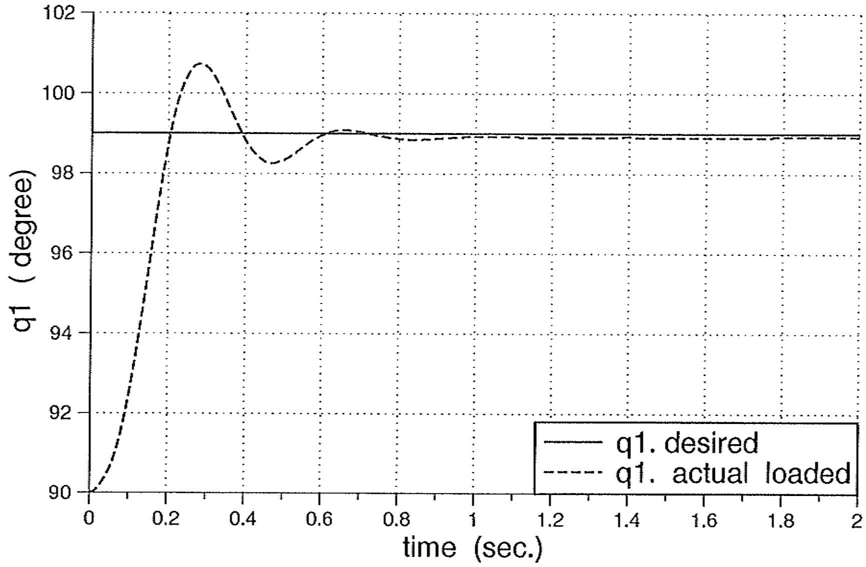

Figure 3.20: Step response; q_1 with non-interactive control (loaded three times inertia)

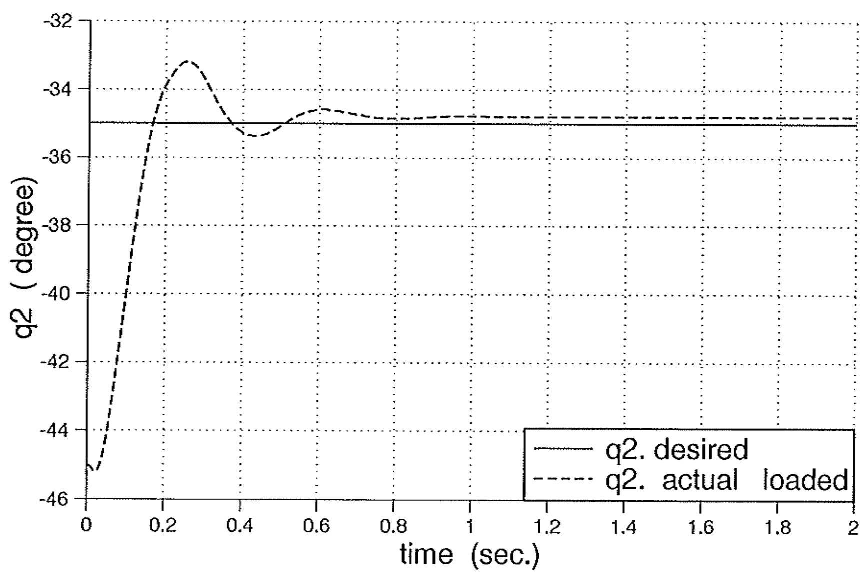

Figure 3.21: Step response; q_2 with non-interactive control (loaded three times inertia)

3.4 Load-insensitive Control

3.4.1 Construction of Load-insensitive System Control

In the joint motion control of an articulated robot arm, it is necessary to compensate for the changes of moment of inertia and gravity loading due to the joint angles and load condition. Also, for accurate control, the interaction among multiple link motions has to be reduced. All of the above-mentioned effects appear as a disturbance at the actuating force for the individual cylinder. Therefore, the degrading effects on performance can be reduced by applying the proper feedback of the actuating force.

From Equations (3.17) and (3.18) which represent the equation of motion and the actuating force of a single link mechanism, respectively, the original system is constructed as shown by solid lines in Figure 3.22-a.

$$q_i(s) = \frac{\hat{J}_i}{H_{ii}s^2 + \hat{J}_i^2 d_i s} F_{ai}(s) \tag{3.17}$$

$$F_{ai}(s) = \frac{1}{C_i s + K_{pi}}[K_{ui}U_i(A_{Ii} + A_{Oi}) - ({A_{Ii}}^2 + {A_{Oi}}^2)s\hat{J}_i q_i(s)] \tag{3.18}$$

A compensation circuit is introduced which is shown in Figure 3.22-a by broken lines, where r is an adjusting coefficient smaller than unity. The final block diagram with unity feedback is shown in Figure 3.22-b. From this construction, the load effect can be reduced and the resultant system approach the first order system when r approaches unity. This compensation is essentially based on the idea of load insensitive system construction. However, if the parameters $K_{ui}, K_{pi}, A_{Ii}, A_{Oi}$ and C_i are not exact (over estimated), the inner feedback loop might result in the equivalent effect of a positive feedback, which would make the system unstable. The adjusting parameter, r is employed to insure a local negative feedback effect.

Now, the control input becomes as follows:

$$\bar{U}_i = U_i^* + \frac{r(C_i s + K_{pi})}{K_{ui}(A_{Ii} + A_{Oi})} F_{ai} \tag{3.19}$$

where

$$U_i^* = U_i - \frac{K_{pfi}T_{fi}s}{1+T_{fi}s}F_{ai}$$

3.4.2 Simulation Results

In this experiment the robot was loaded (five times inertia load) and both joints were commanded to move at the same time from the reference position $q_1 = 90°$ to the desired position $q_1 = 99°$ and joint two, q_2, was commanded to move from the reference position $q_2 = -45°$ to the desired position $q_2 = -35°$.

Figures 3.23 and 3.24 represent the step responses for q_1 and q_2, respectively, without load-insensitive compensation (r=0). The effect of increasing the inertia load is a response with overshoots and increased settling time. Figures 3.25 and 3.26 represent the step responses for q_1 and q_2, respectively, with load-insensitive compensation (r=0.8). The responses are remarkably improved with load-insensitive system compensation. The system's degree of sensitivity was adjusted by varying the value of the coefficient r within a range of $(0 < r < 1)$. The more expected load, the higher value of r should be used in the force feedback gain to handle (compensate for) the effect of disturbance forces. Simulation results confirmed that this method (*load-insensitive system compensation*) is effective in all cases, even if system parameters are not exactly identified.

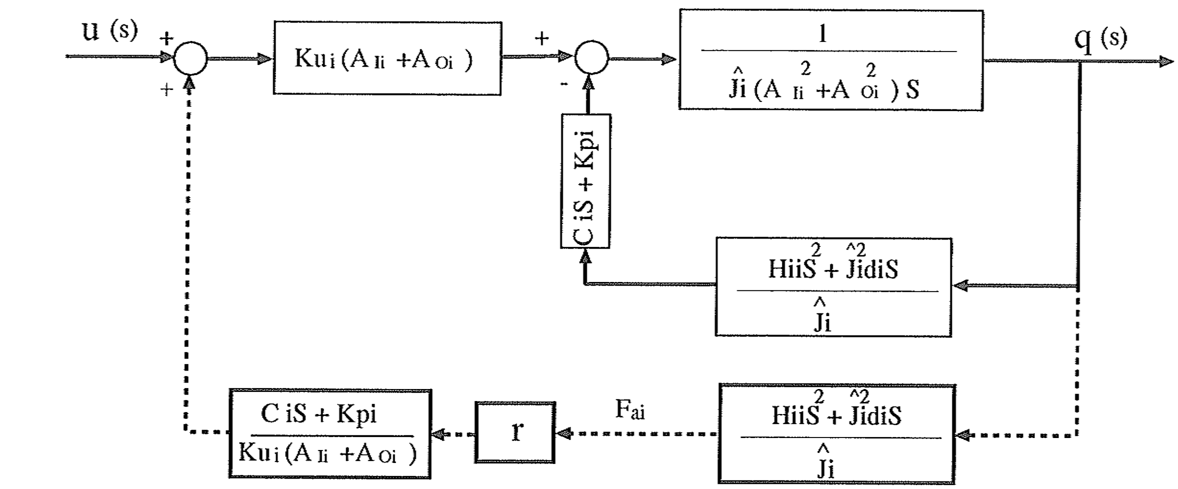

(a) Third-order sytem with positive actuating force feedback

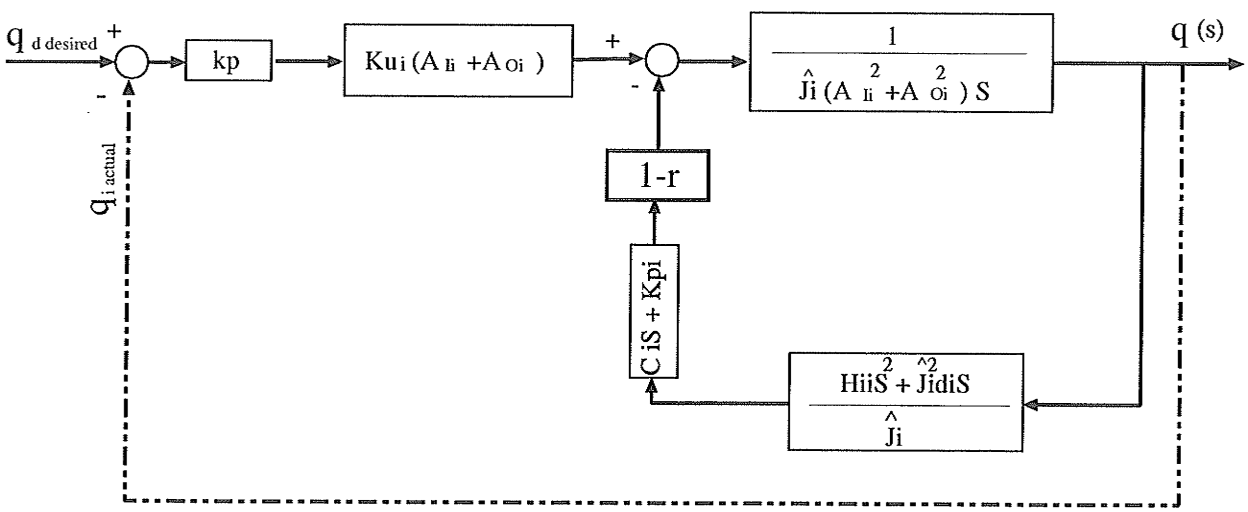

(b) Load -insensitive with proportional control

Figure 3.22: Construction of a load-insensitive system

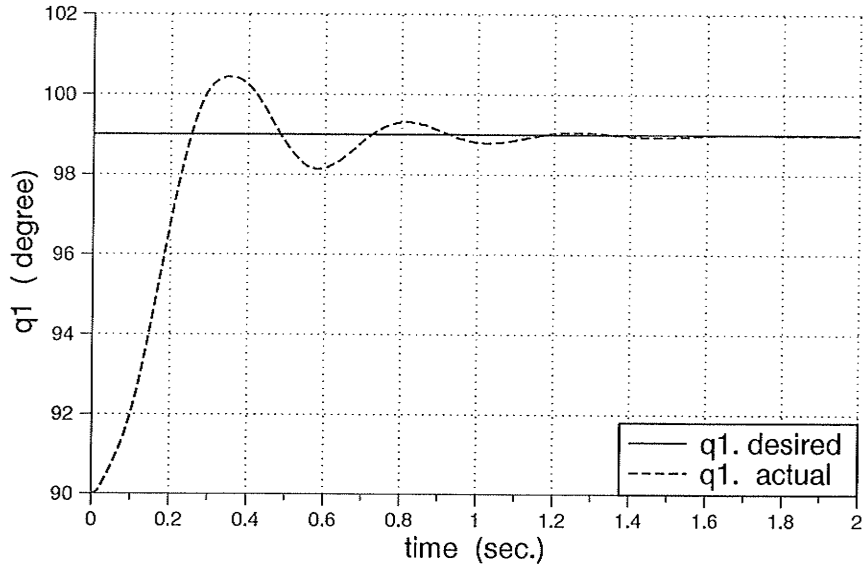

Figure 3.23: Step response; q_1 loaded (five times inertia) r=0

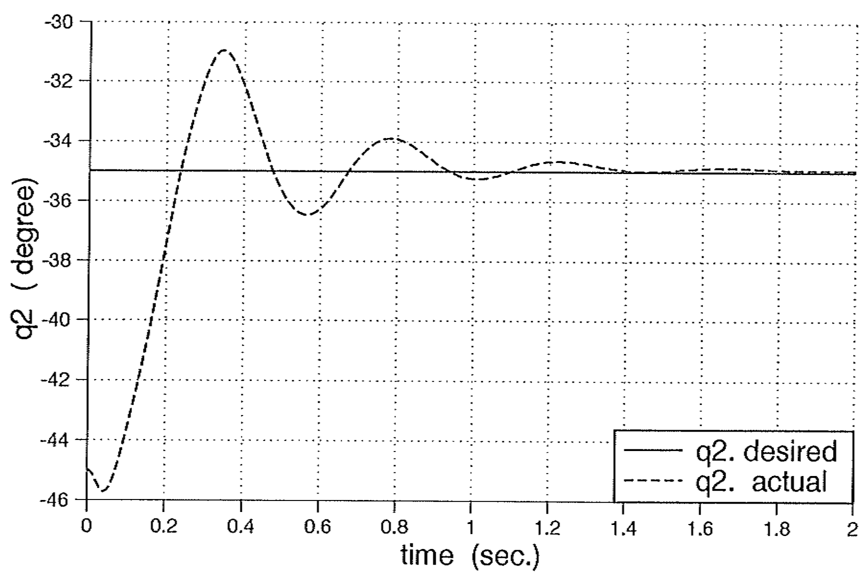

Figure 3.24: Step response; q_2 loaded (five times inertia) r=0

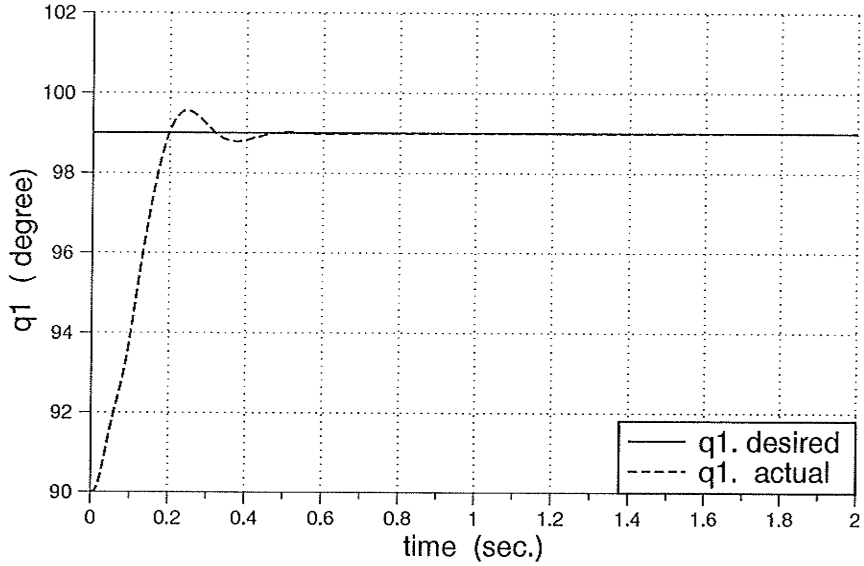

Figure 3.25: Step response; q_1 loaded (five times inertia) r=0.8

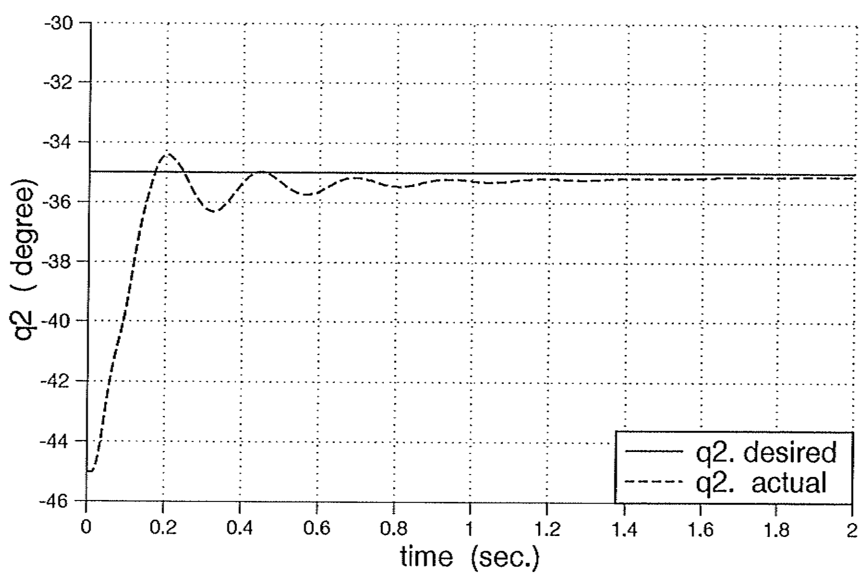

Figure 3.26: Step response; q_2 loaded (five times inertia) r=0.8

CHAPTER 4

HYDRAULIC ROBOT OPERATING FROM A CONSTANT FLOW

In the previous chapter we studied the performance of a typical robot operating from a constant pressure. In this chapter we extend our study to a different class of hydraulic manipulators that are operating from a constant flow pump system. This type of operating system is mainly used for outdoor heavy-duty machines such as excavators shown in Figure 2.2-a. The use of a constant flow pump system implies that a new type of valve (open-center valve) must be used. The necessity of using this type of valve is incurred by the need to maintain reasonable fluid temperature and continuous flow when the valve is at null position for extended periods of time. As was mentioned earlier, the performance of such model is described by a fourth-order system. In this study only the motion of boom and stick of an excavator are considered. The parameters are given in Appendix B. The actual system has a dead-band in the servo-valves input (either from the torque motor or a zener diode) that makes the system unresponsive within a range ($0 \rightarrow 0.3$) volt. There are also dead-bands on the orifices (over-lapped conditions) of the servo-valves.

In this chapter we analyze the effect of velocity and acceleration feedback on the performance of fourth order systems. Delay in the spool displacement, dead-band on the servo-valve input and over-lapped conditions are examined with simple closed-loop control.

4.1 Feedback Compensation of Fourth-order Systems

We have seen for a third-order and first type system that the effect of the real pole, σ on the unit-step response reduces the maximum overshoot and increases the settling time. In the fourth order system, the situation is different because the original system (without compensation) has two real and two complex roots, see Figure 4.1. The effects of velocity and acceleration feedback are described as follows:
Velocity feedback *adds a zero* to the transfer function. Acceleration and velocity feedback *adds two zeros* to the transfer function which could be real or complex.

By adding zeros to the transfer function of the system, the contribution of some poles to the overall dynamic behavior of the system is limited (Ogata, 1990). The following factors must be considered:

1. if there is a pole close to zero, then the residue, at this pole, is small and the coefficient of the transient response term corresponding to this pole becomes small.

2. a pole and zero closely located will effectively cancel each other.

3. in the case where a pole is located far from the origin, the residue at this pole may be small. The transient response corresponding to such a pole is small and will last a short time.

4.1.1 Velocity Feedback Control

Velocity feedback action is represented by adding a zero to the transfer function of the system. The system type does not change (first type system) and there is no steady-state error due to the unit-step input. Error due to the unit-ramp input increases with velocity feedback. Referring to Figure 4.1-b, the steady-state error due to the

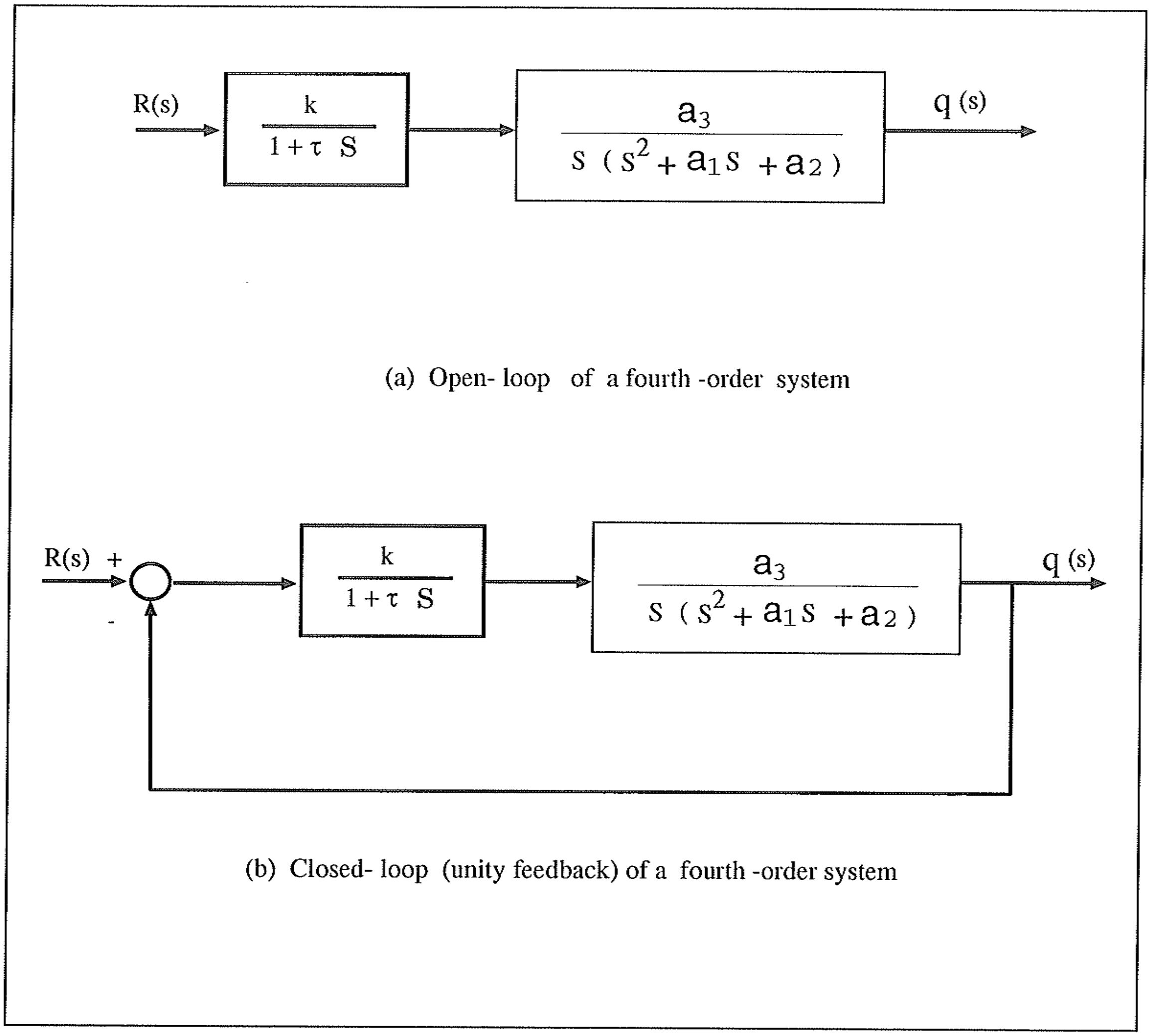

Figure 4.1: Open-loop and closed-loop (unity feedback) of fourth-order system

unit-ramp input is $e_{ss} = \frac{a_2}{ka_3}$. When velocity feedback is added as shown in Figure 4.2, the steady state error to unit-ramp input is $e_{ss} = \frac{a_2+a_3k_v}{ka_3}$.

Thus, the effect of adding a zero to the system increases the steady-state error and therefore, zero location must be selected carefully. The initial location of poles was found in Chapter 2 for the original system see Figure 2.6.

Referring to Figure 4.2, the open-loop transfer function of the system is

$$K\frac{Z(s)}{P(s)} = \frac{K(s+\frac{1}{k_v})}{s(s+\frac{1}{\tau})(s^2+a_1s+a2)}$$

where $K = \frac{a_3kk_v}{\tau}$ is the parameter of interest. There are one zero and four poles, two real and two complex located at

$$
\begin{aligned}
z_1 &= -\frac{1}{k_v} \\
s_{1,2} &= -\frac{a_1}{2} \pm j\sqrt{a_2 - \frac{a_1{}^2}{4}} = -\zeta\omega_n \pm j\omega_n\sqrt{1-\zeta^2} \\
s_3 &= 0 \\
s_4 &= -\frac{1}{\tau}
\end{aligned}
$$

where

$\omega_n = \sqrt{a_2}$

$\zeta = \frac{a_1}{2\sqrt{a_2}}$

The root locus plot is shown in Figure 4.3 for two different values of k_v $(k_v < \tau, k_v > \tau)$.

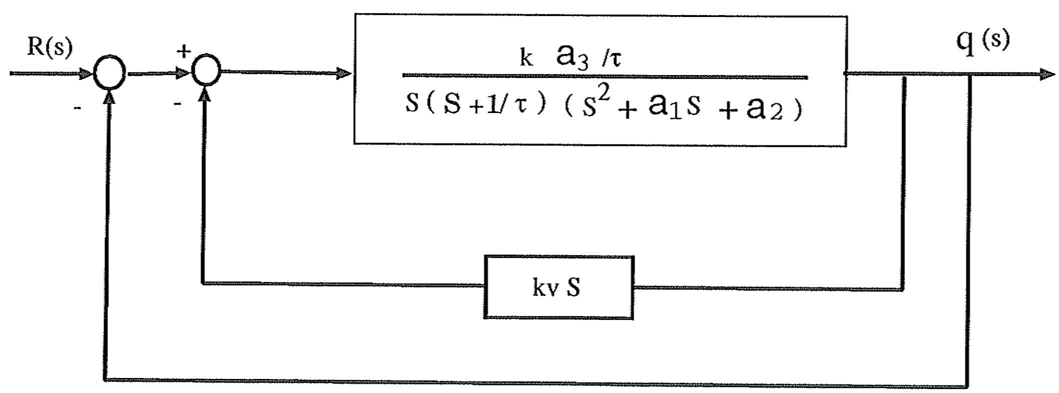

Closed- loop (velocity feedback) for fourth order system

Figure 4.2: Closed-loop system with velocity feedback compensation

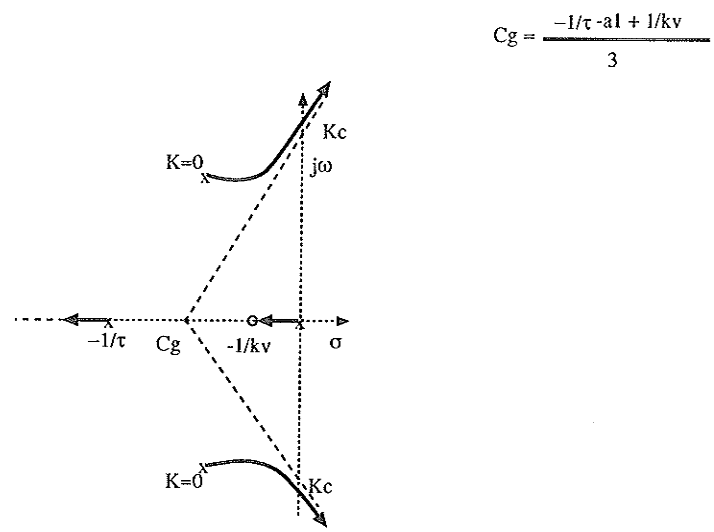

a- Root locus plot ; fourth-order system with velocity feedback (kv > τ)

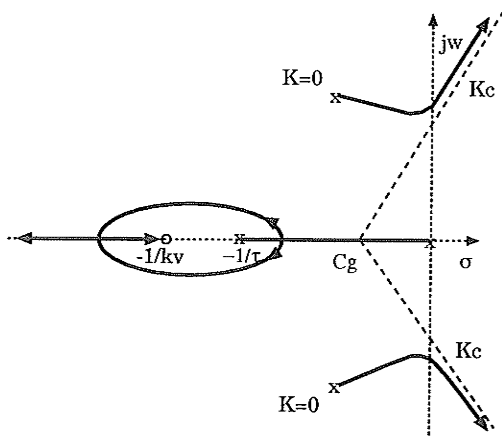

b- Root locus plot ; fourth-order system with velocity feedback (kv < τ)

Figure 4.3: Root locus for fourth-order system with velocity feedback

4.1.2 Velocity & Acceleration Feedback Control

Velocity and acceleration feedback action is represented by adding two zeros (that can be real or complex) to the transfer function of the system. The system type does not change (first type system) and there is no steady-state error due to the unit-step input. The nature of the two zeros due to velocity and acceleration feedback depends on the values of k_v and k_a, and it can be clarified as follows:

- *Two real zeros*

$$k_a s^2 + k_v s + 1 = k_a(s^2 + \frac{k_v}{k_a}s + \frac{1}{k_a})$$

If $k_v > 2\sqrt{k_a}$ we have two real zeros at

$$z_{1,2} = -\frac{k_v}{2k_a} \pm \sqrt{(\frac{k_v}{k_a})^2 - \frac{4}{k_a}}$$

- *Two complex zeros*

If $k_v < 2\sqrt{k_a}$ we have two complex zeros at

$$z_{1,2} = -\frac{k_v}{2k_a} \pm j\sqrt{(\frac{k_v}{k_a})^2 - \frac{4}{k_a}}$$

Referring to Figure 4.4, the open-loop transfer function of the system is

$$K\frac{Z(s)}{P(s)} = \frac{K(s^2 + \frac{k_v}{k_a}s + \frac{1}{k_a})}{s(s+\frac{1}{\tau})(s^2 + a_1 s + a2)}$$

where $K = \frac{a_3 k k_v k_a}{\tau}$ is the parameter of interest

There are two real zeros and four poles, two real and two complex poles, located as follows:

$$\begin{aligned} z_{1,2} &= -\frac{k_v}{2k_a} \pm \sqrt{(\frac{k_v}{k_a})^2 - \frac{4}{k_a}} \\ s_{1,2} &= -\frac{a_1}{2} \pm j\sqrt{a_2 - \frac{a_1{}^2}{4}} = -\zeta\omega_n \pm j\omega_n\sqrt{1-\zeta^2} \end{aligned}$$

$$s_3 = 0$$
$$s_4 = -\frac{1}{\tau}$$

where

$\omega_n = \sqrt{a_2}$

$\zeta = \frac{a_1}{2\sqrt{a_2}}$

Adding two zeros to the system, either reals or complex (with negative real parts) the system must be stable for all values of K. Root locus plot for the case of both zeros are reals is shown in Figure 4.5.

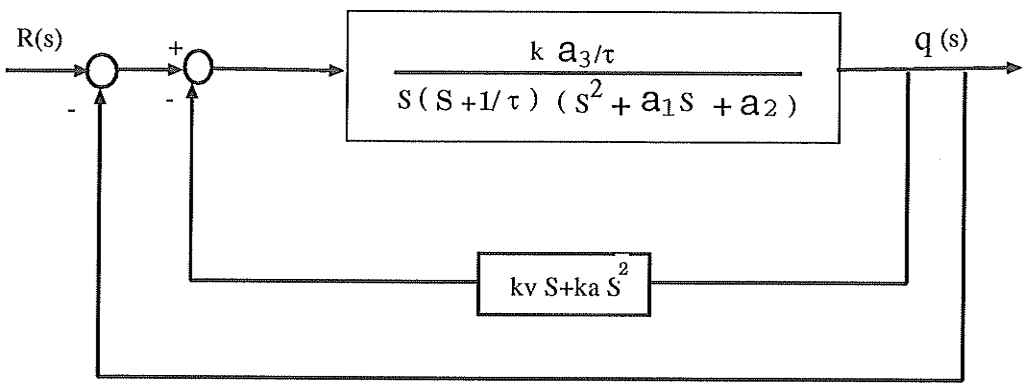

Closed- loop (velocity+ acceleration feedback) for fourth order system

Figure 4.4: Closed-loop system with velocity and acceleration feedback

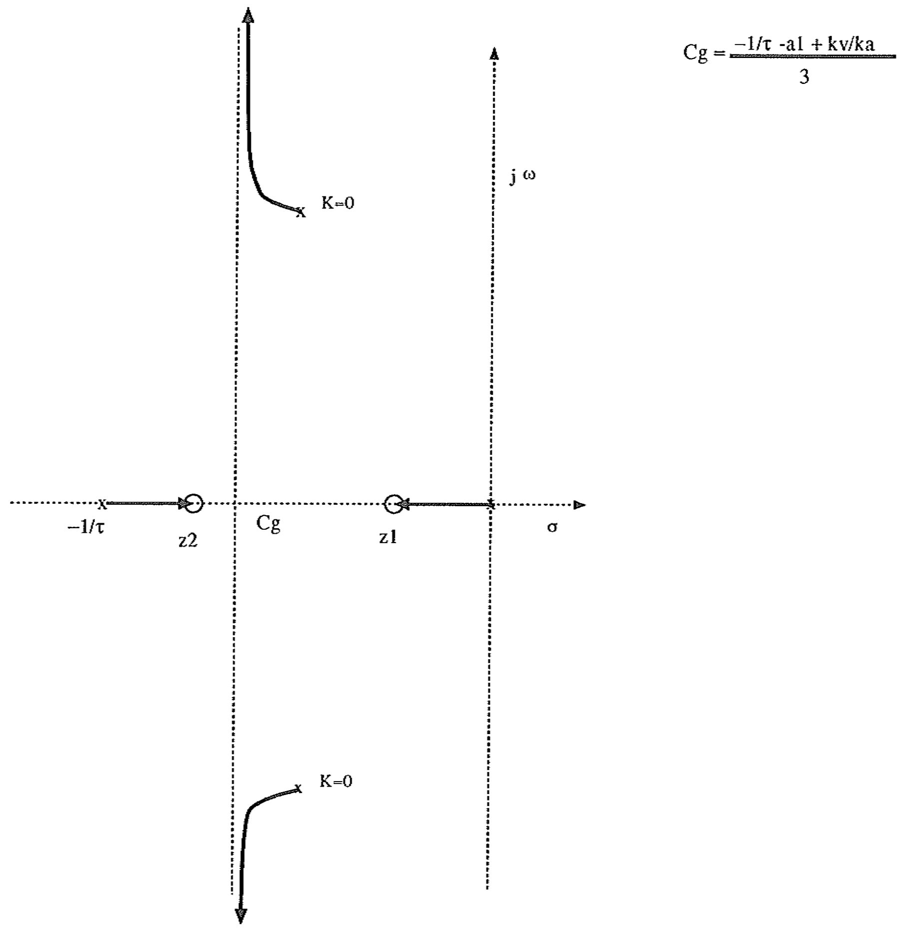

Root locus plot ; fourth-order hydraulic system with velocity and acceleration feedback compensation

Figure 4.5: Root locus plot; velocity and acceleration feedback

4.2 Case Studies

In the remaining chapter we study the performance of a two degree-of-freedom heavy-duty robot arm similar to the one shown in Figure 2.2. Four different models are studied:

- Model I: without delay in the spool displacement, without dead-band in the control input and zero-lapped valve.
- Model II: with delay in the spool displacement, without dead-band in the control input and zero-lapped valve.
- Model III: with delay in the spool displacement, with dead-band in the control input and zero-lapped valve.
- Model IV: with delay in the spool displacement, with dead-band in the control input and over-lapped valve.

The reasons for considering these models are; firstly, orifice dead-bands are part of the control design. Therefore, in order to observe the effects of using velocity feedback, the over-lapped condition must be removed. Secondly, there is a size relationship between dead-band in the servo-valve input (voltage) and the lap conditions. Results and discussion of each model will be shown separately. Previous study by Gulillon (1961) showed that the over-lapped valve is often used to improve the stability of the equipment that is connected to it, this improvement is made at the cost of accuracy.

4.2.1 Simulation Results of Model I

Model I is basically a third-order system controlled by a simple position feedback. Both links were commanded to move from a reference position to a desired position as shown on the plots. Figures 4.6 and 4.7 show the step responses of boom and stick at low gain $k_p = 5$, and Figures 4.8 and 4.9 show the responses of boom and stick at high gain $k_p = 10$. The variation of line pressures as well as the pump pressure is shown in Figures 4.10 and 4.11. The spool displacements for both valves are shown in Figures 4.12 and 4.13.

Referring to Figure 4.8, a steady state error is observed in the boom up-motion. This result is different from our finding in Chapter 3 (Figure 3.4) where the step response of a third-order system operating from a constant pressure exhibited a zero steady-state error. The steady-state error, in this case, is due to the utilization of different valving system (open-center valve). Referring to the schematic of the hydraulic driving unit with open-center valve, see Figure 2.2, this type of valving system allows the fluid flow to return to the tank (or to other coupled valves) when the spool is at a neutral position. When the spool is displaced to the right or to the left, the input/output orifices (a_i, a_o) start to open, while a_e starts to close, restricting the constant flow. This results in a rise in the pump pressure, which will produce motion of the corresponding link. As the boom approaches the desired position, a_i and a_o start to close and a_e starts to open. The main pressure decreases until it reaches a value less than the pressure in the input line, which stops the motion leaving steady-state error.

The interaction effect is shown in Figures 4.14 and 4.15 for both links boom and stick, respectively. Referring to Figures 4.8, 4.9, 4.10, and 4.11, one can conclude qualitatively that Model I is performing at low frequency and high damping ($\alpha > \beta$). This implies that velocity feedback can be used to improve the system's stability.

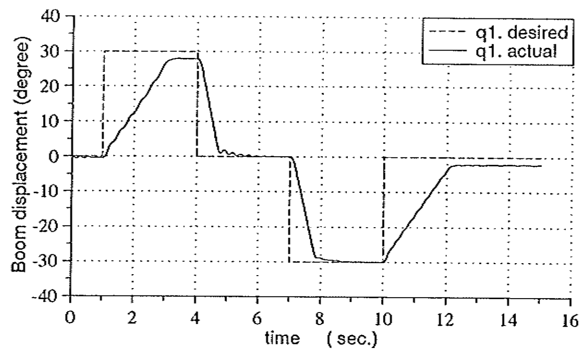

Figure 4.6: Step input response; boom

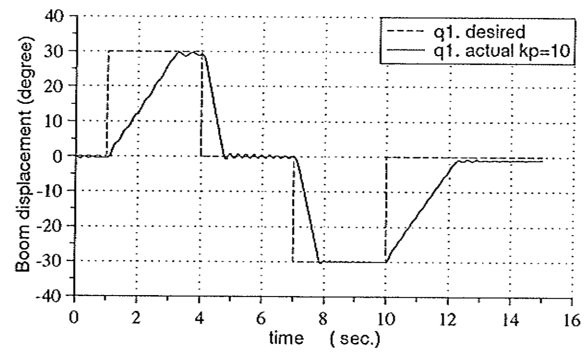

Figure 4.8: Step input response; boom

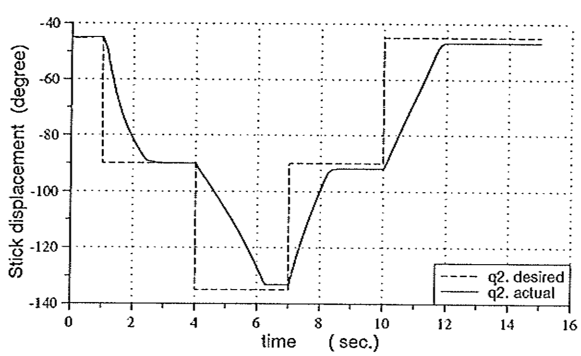

Figure 4.7: Step input response; stick

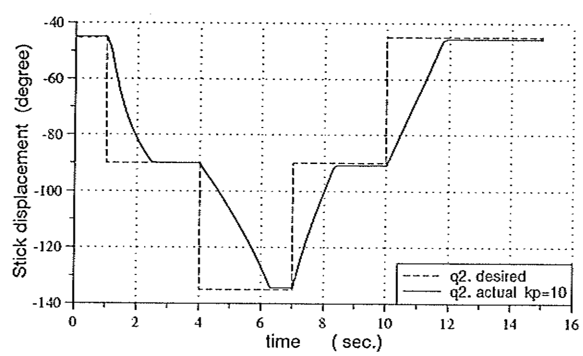

Figure 4.9: Step input response; stick

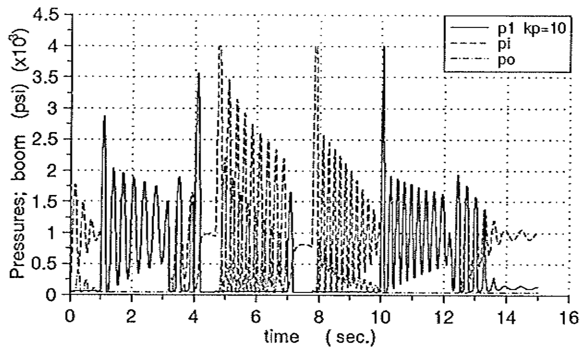

Figure 4.10: Pressures (p1,pi,po); boom

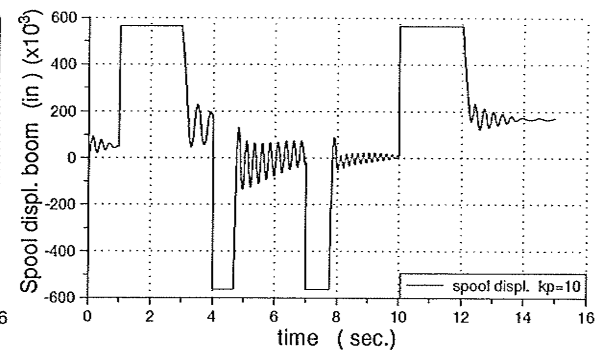

Figure 4.12: Spool displacement; boom

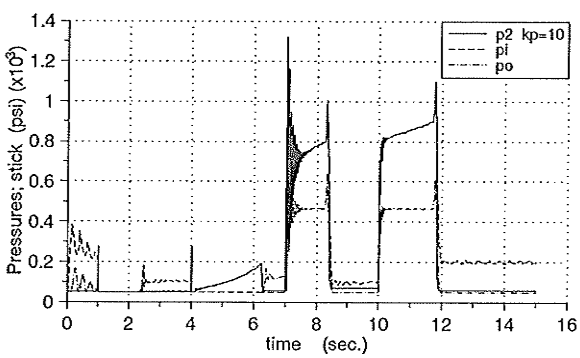

Figure 4.11: Pressures (p2,pi,po); stick

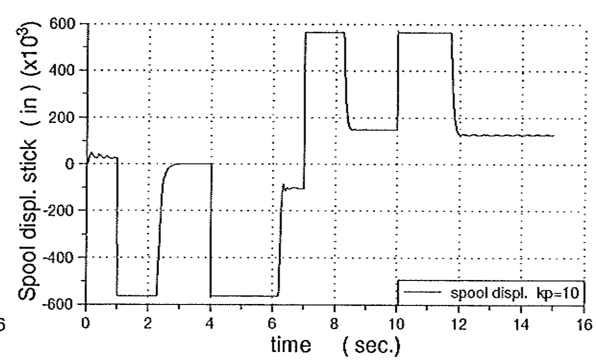

Figure 4.13: Spool displacement; stick

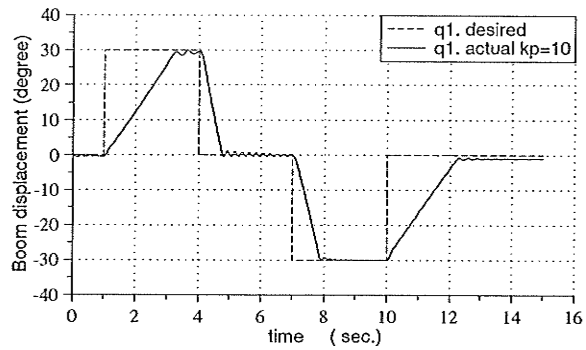

Figure 4.14: Step input response; boom

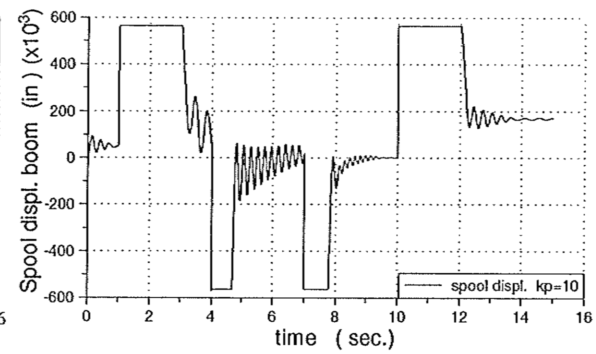

Figure 4.16: Spool displacement; boom

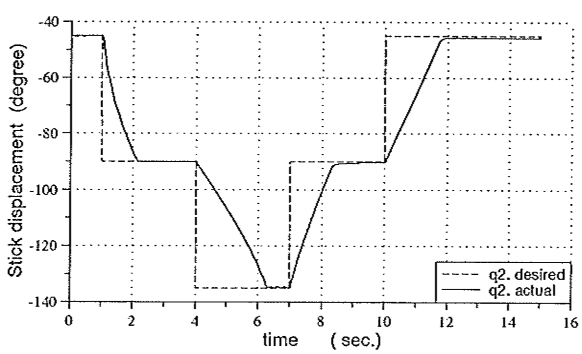

Figure 4.15: Step input response; stick

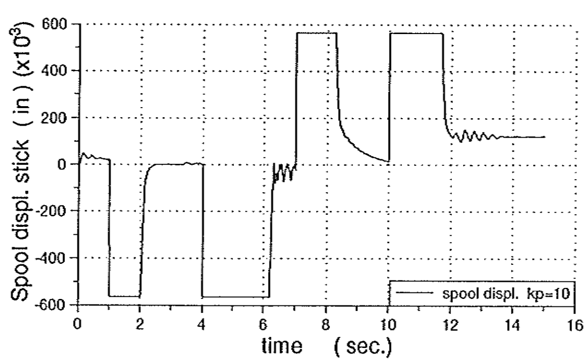

Figure 4.17: Spool displacement; stick

4.2.2 Simulation Results of Model II

Model II is basically a fourth-order system controlled by first, proportional control and second, proportional and velocity feedback compensation that are used in controlling the joint motion of boom and stick. Both links were commanded to move at the same time from a reference position to a desired position as shown on the plots. Unit-step input and unit-ramp input are used as test signals in the simulation program.

Results of only using proportional control are shown in Figures 4.18 and 4.19 for both joints. From these plots, the effect of the first-order lag time in the spool displacement resulted in a response with steady state error and overshoot. Results of adding velocity feedback, where $k_v = 2$ was chosen within a range of $k_v > \tau$ to keep the root locus of the real poles always on the real axis are shown in Figures 4.26 and 4.27 for both joints, respectively. Velocity feedback compensation is effective when $k_v > \tau$, because the contribution of the real poles was damping the system response. These results agreed with the root locus analysis. Ramp input responses indicate that, when the joints are driven at constant velocities they are affected differently by the gravity load and the interaction forces (the second link is more stable than the first link).

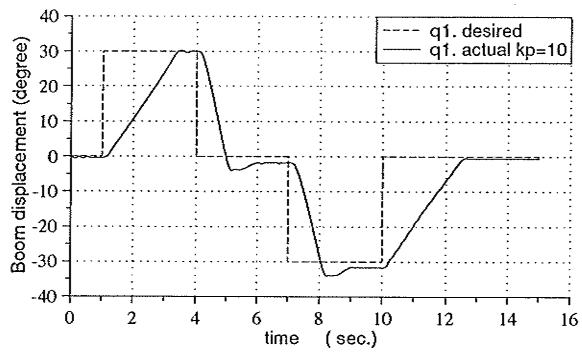

Figure 4.18: Step input response; boom

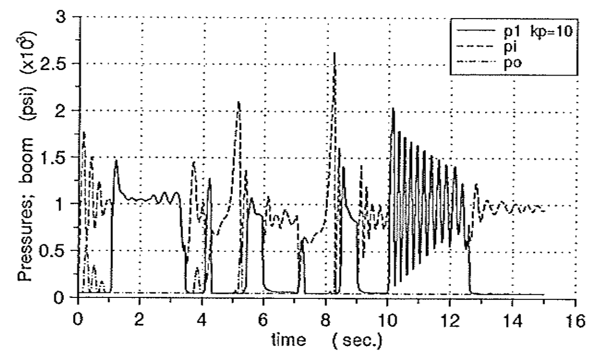

Figure 4.20: Pressures (p1,pi,po); boom

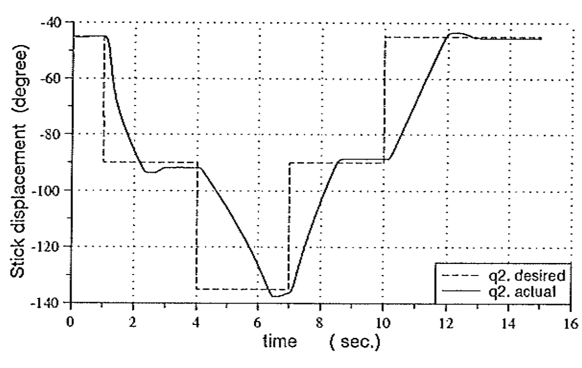

Figure 4.19: Step input response; stick

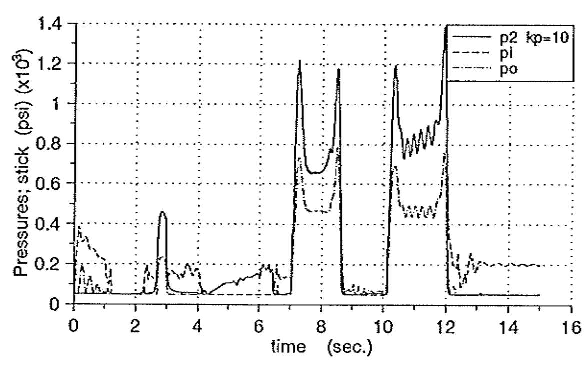

Figure 4.21: Pressures (p2,pi,po); stick

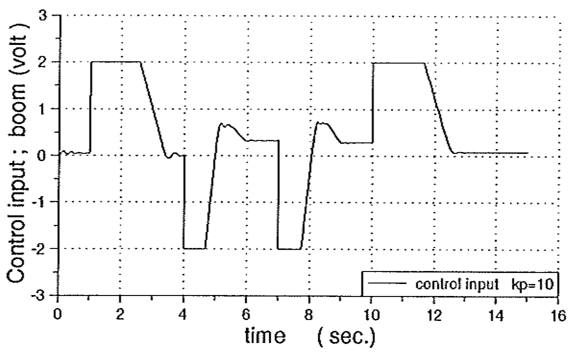

Figure 4.22: Control input; boom

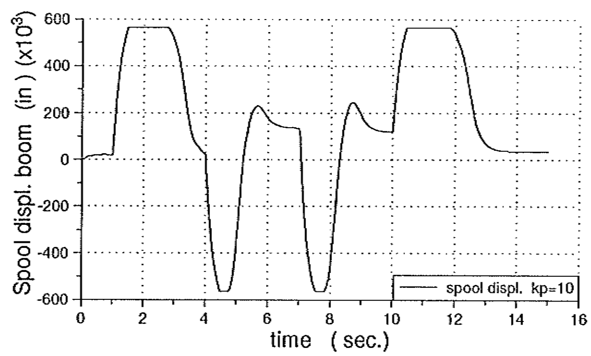

Figure 4.24: Spool displacement; boom

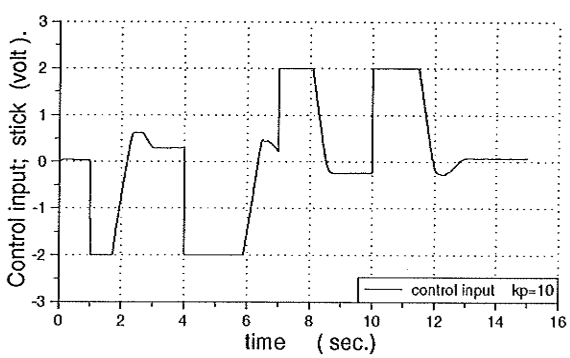

Figure 4.23: Control input; stick

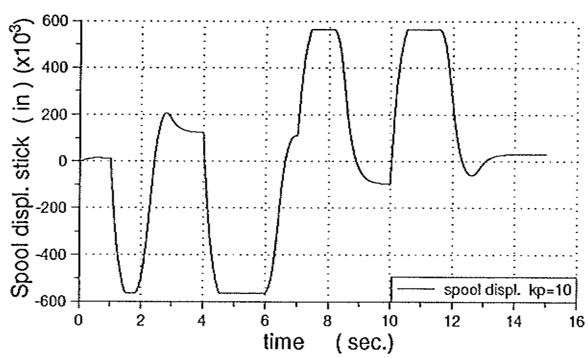

Figure 4.25: Spool displacement; stick

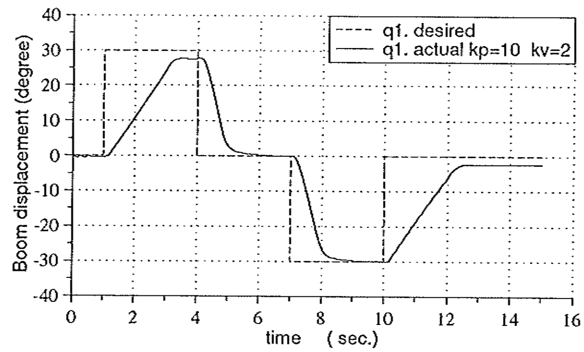

Figure 4.26: Step input response; boom

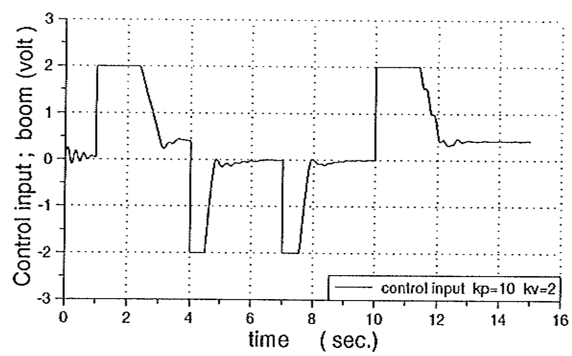

Figure 4.28: Control input; boom

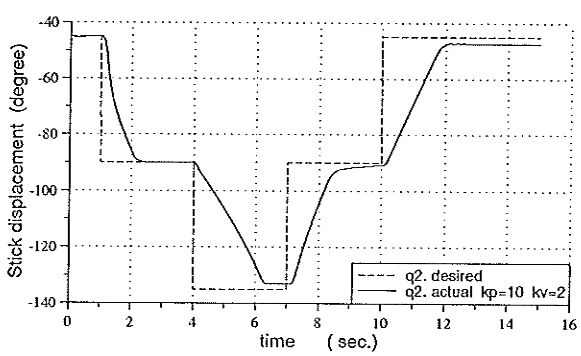

Figure 4.27: Step input response; stick

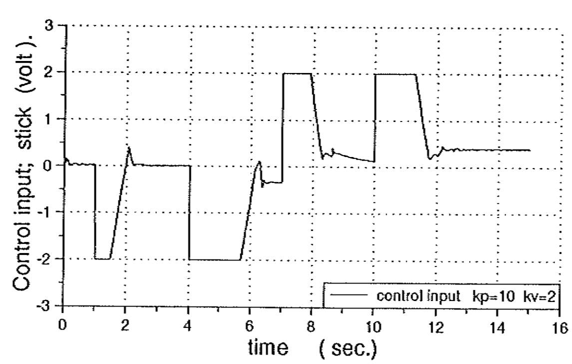

Figure 4.29: Control input; stick

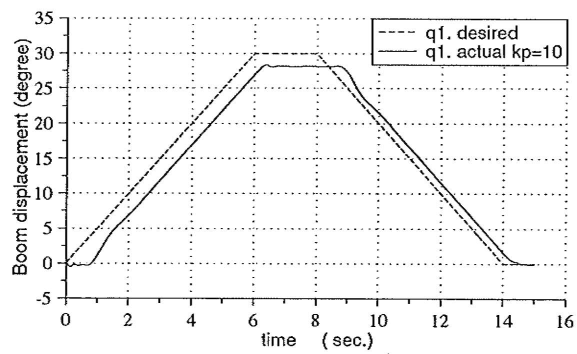

Figure 4.30: Ramp input response; boom

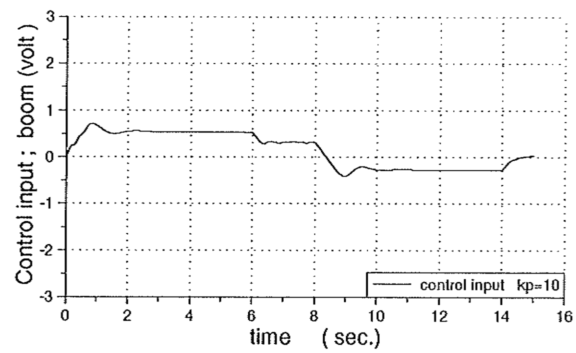

Figure 4.32: Control input; boom

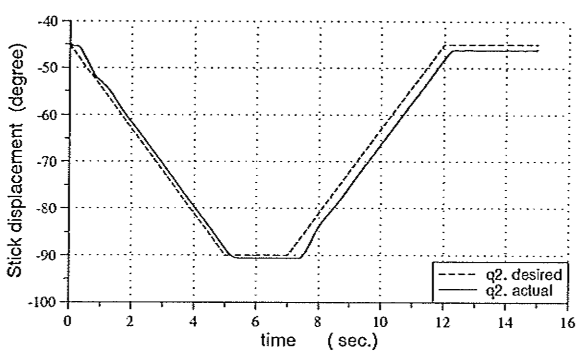

Figure 4.31: Ramp input response; stick

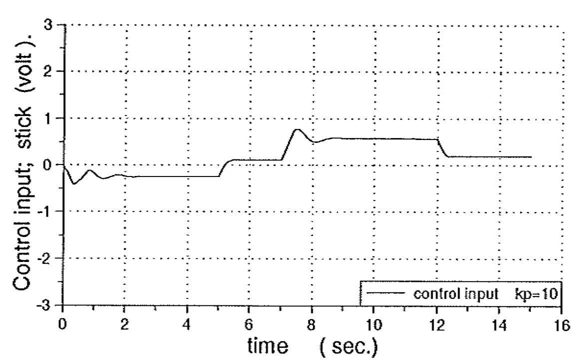

Figure 4.33: Control input; stick

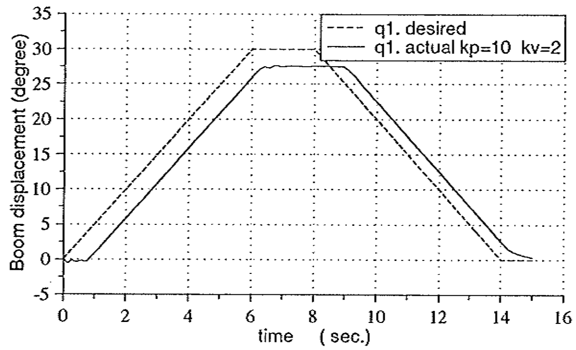

Figure 4.34: Ramp input response; boom

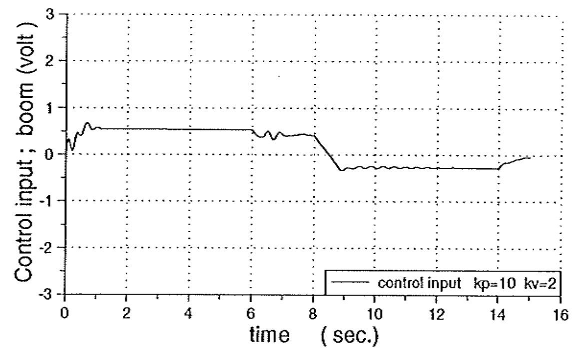

Figure 4.36: Control input; boom

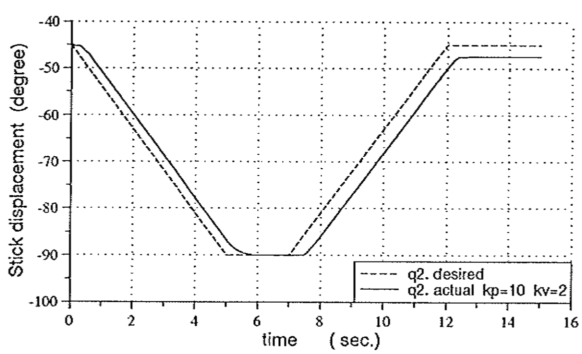

Figure 4.35: Ramp input response; stick

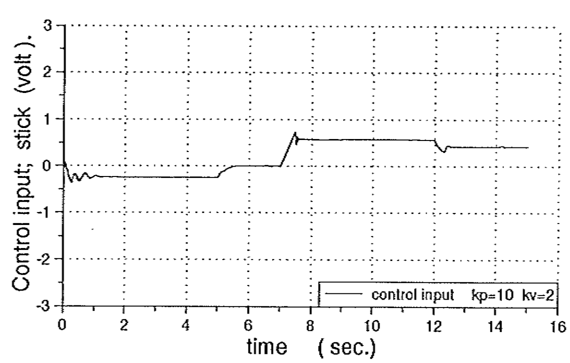

Figure 4.37: Control input; stick

4.2.3 Simulation Results of Model III

Model III is a fourth-order system that is different from model II, it has dead-bands in the servo-valves input (the system does not respond within a certain region). Proportional and velocity feedback compensation are used in controlling the joint motion of boom and stick. Both links were commanded to move at the same time from a reference position to a desired position as shown on the plots. Unit-step input was used as a test signal in the simulation program.

Results when only the proportional control is used are shown in Figures 4.38 and 4.39 for both joints. Results of adding velocity feedback, where $k_v = 2$ was chosen within a range of $k_v > \tau$ to keep the root locus of the real poles always on the real axis, shown in Figures 4.40 and 4.41 for both joints. The effect of dead-bands on the control input made the system unresponsive within a range of $(0 \rightarrow 0.3)$ volt shown in Figures 4.42 and 4.43 for both joints, respectively. Comparing these results with results of model II, it is observed that system with dead-bands in the control inputs required higher gain than the one without such dead-bands.

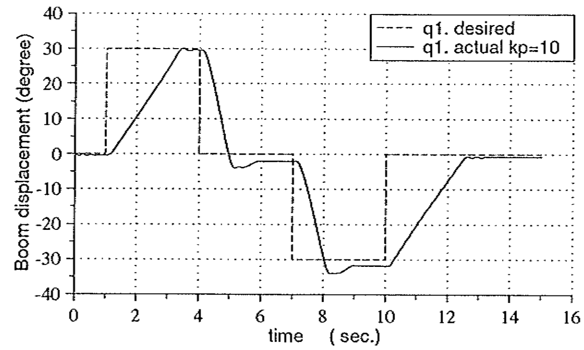

Figure 4.38: Step input response; boom

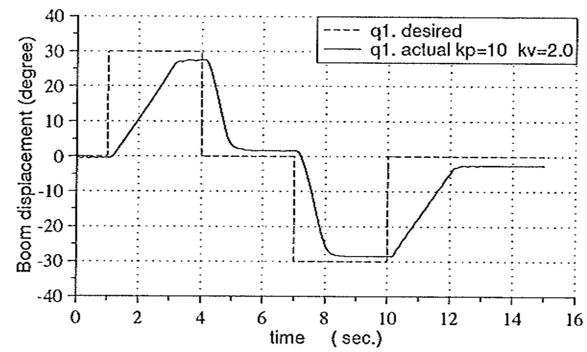

Figure 4.40: Step input response; boom

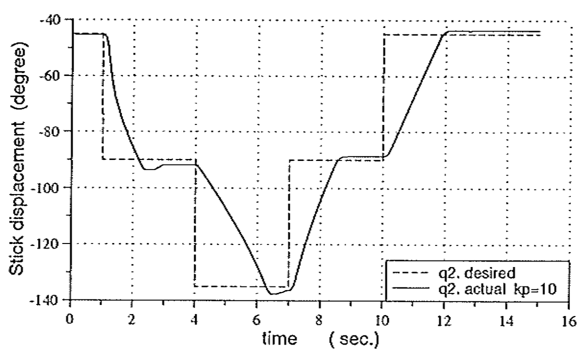

Figure 4.39: Step input response; stick

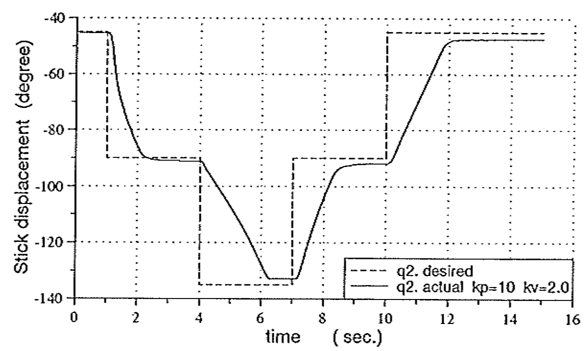

Figure 4.41: Step input response; stick

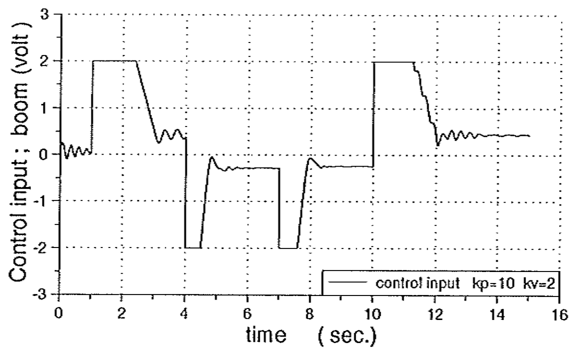

Figure 4.42: Control input; boom

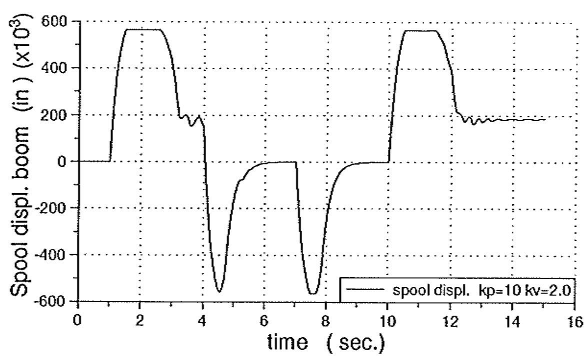

Figure 4.44: Spool displacement; boom

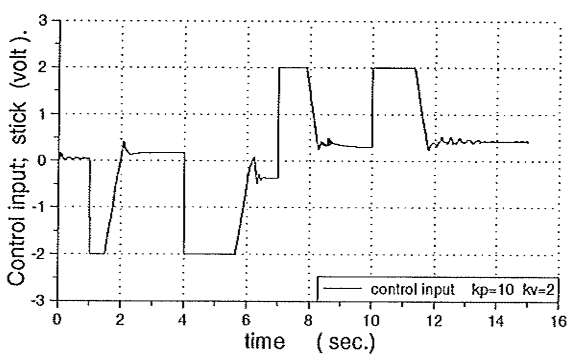

Figure 4.43: Control input; stick

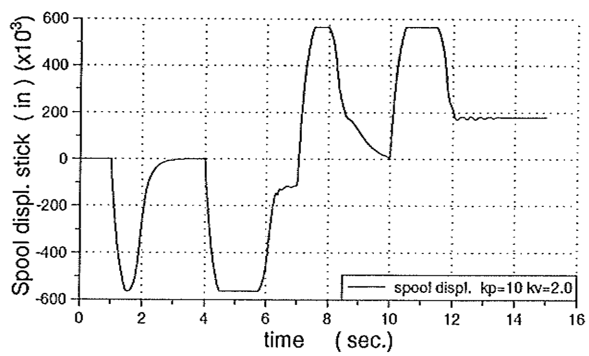

Figure 4.45: Spool displacement; stick

4.2.4 Simulation Results of Model IV

Model IV is a fourth-order system. This model is different from model III in that, it has dead-bands in the orifices due to the over-lapped valve. There is a 0.3 volt dead-band in the servo-valve input and 0.18 inches over-lapping in the orifices. Fundamentally, the function of orifice's dead-band is to close the fluid flow through the corresponding line in which more force can be held by the hydraulic actuator. This force may be used to compensate for error caused by dead-band of the servo valve input and to improve the stability of the joint motion (eliminate the oscillation caused by the interaction forces and load condition).

Proportional control is applied to control the join motion of the boom and stick. Both links were commanded to move at the same time from a reference position to a desired position as shown on the plots. Unit-step input and unit-ramp input are used as test signals in the simulation program. Results were obtained for the actual values of the dead-bands in the servo-valves input and orifices. From the results of this model, we may conclude that dead-bands in the control input (servo-valve input) have caused steady-state error. This error can be eliminated by using over-lapped conditions. Also, these results have shown that dead-band in the servo-valve input and the over-lap magnitude in the actual design should be designed carefully, see Figures 4.52 and 4.53 which show the spool displacement of both valves. In the case of over-sizing these values (volt dead-band and over-lap) they may lead to a tool damage.

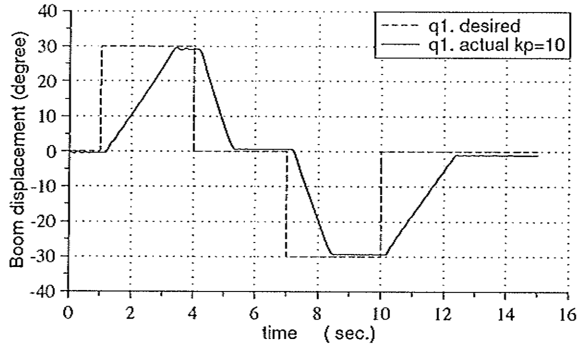

Figure 4.46: Step input response; boom

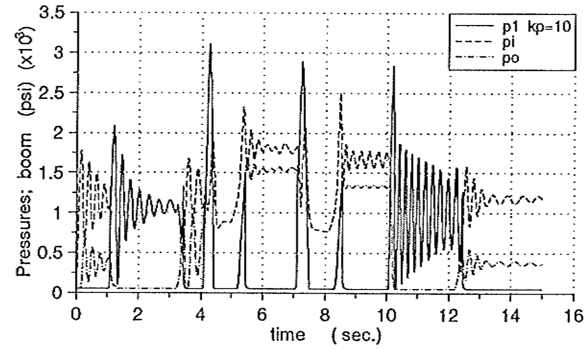

Figure 4.48: Pressures (p1,pi,po); boom

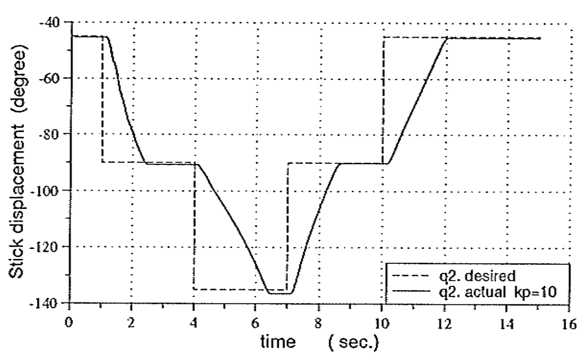

Figure 4.47: Step input response; stick

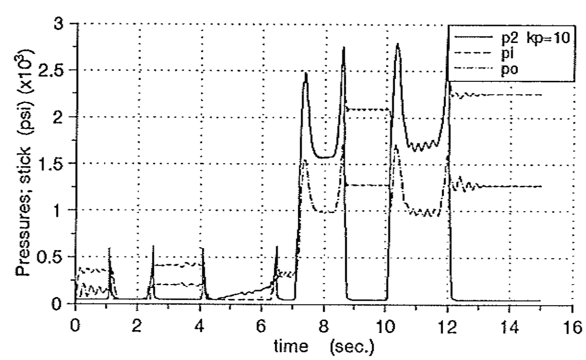

Figure 4.49: Pressures (p2,pi,po); stick

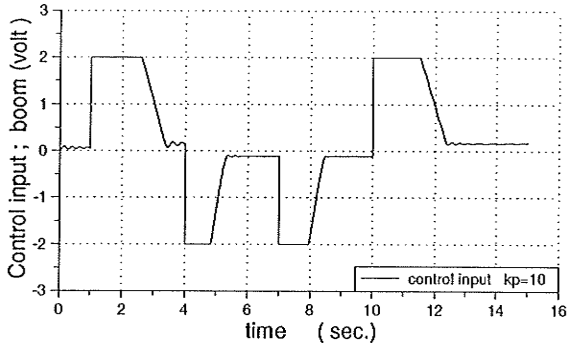

Figure 4.50: Control input; boom

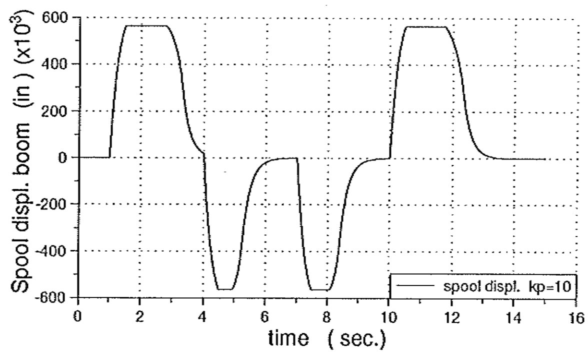

Figure 4.52: Spool displacement; boom

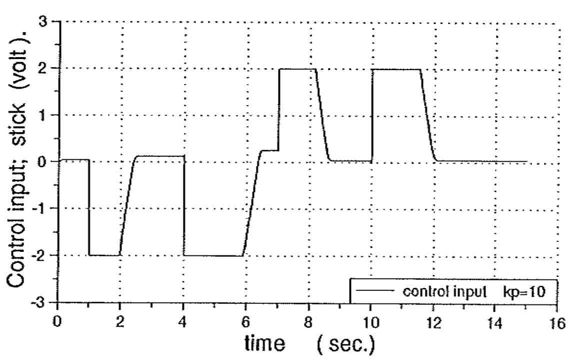

Figure 4.51: Control input; stick

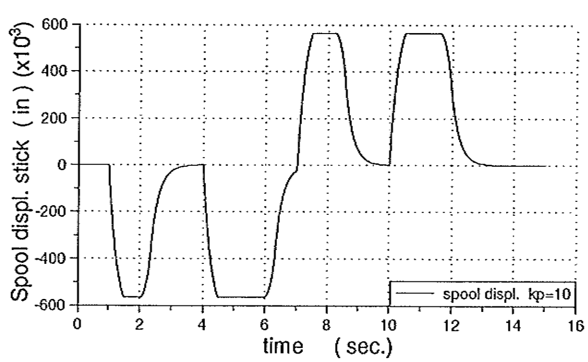

Figure 4.53: Spool displacement; stick

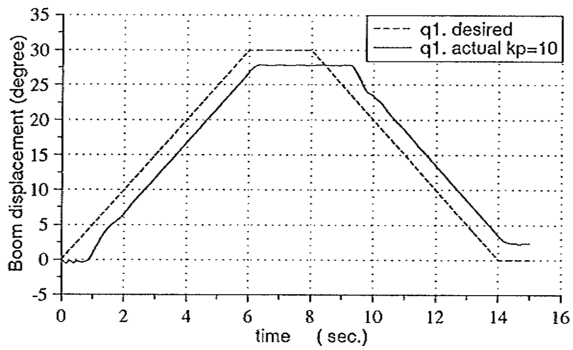

Figure 4.54: Ramp input response; boom

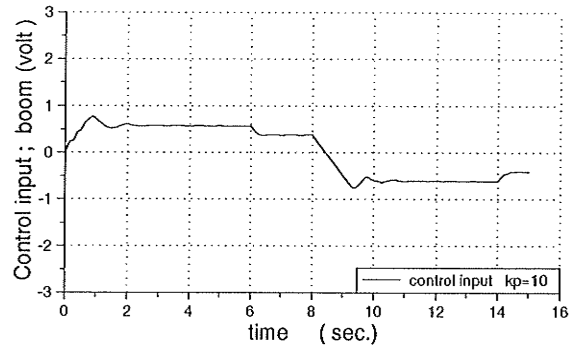

Figure 4.56: Control input; boom

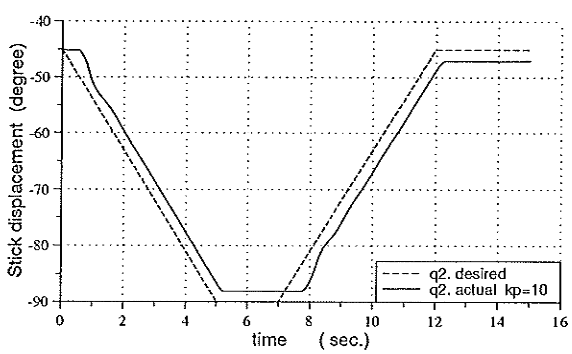

Figure 4.55: Ramp input response; stick

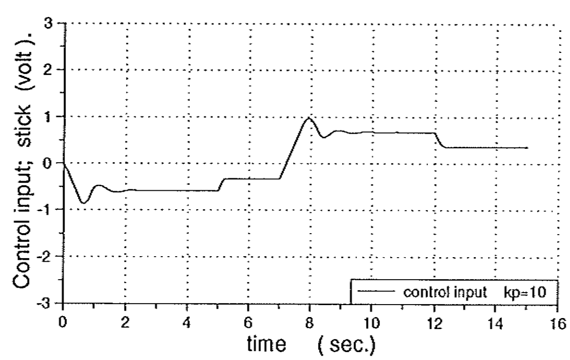

Figure 4.57: Control input; stick

CHAPTER 5

EXPERIMENT WITH UNIMATE ROBOT

In this chapter some experimental results are shown. The experiments were performed on a Unimate MK II hydraulic robot which is shown in Figure 5.1. The Unimate robot is a five degree-of-freedom manipulator. The main axes are powered by electrohydraulic servo-valves and pneumatic for the end-effector. The original boards of the control system have been removed from the machine. The aim is to establish a platform for testing modern data acquisition and control techniques on an existing industrial manipulator.

The robot operates from a constant pressure pump system. The experimental test station consists of servo-valves to control the joint motion, encoders to feedback the actual joint angles and a computer that determines the control action. The servo-valves regulate fluid flow to and from hydraulic cylinders proportionally to the control input (current). The digital-to-analog (D-to-A) card allows the computer to output a value of current proportional to the voltage.

Experimental results obtained for the main axes (swing , up/down and in/out), using only proportional control with different gains are plotted. The objective was to compare these results with those found through simulations and to validate the simulation models developed in this study.

Figures 5.2, 5.4 and 5.6 show the step responses of the swing joint, the up/down joint and the in/out joint, respectively. These figures show that a steady state error was observed. This error is due to dead-bands in the orifices (over-lapped valve). Also, increases in the proportional gain reduces the response time. These results are similar to our simulation results in Figure 3.4. From Figure 5.4, it can be seen by considering the responses with high and low inertia for the same gain ($k_p = 8.5$), that high inertia produces higher oscillations. This result agreed with the trend shown in Figure 3.8. Figures 5.3, 5.5 and 5.7 show the control input to the servo-valves which controlled the above mentioned joints.

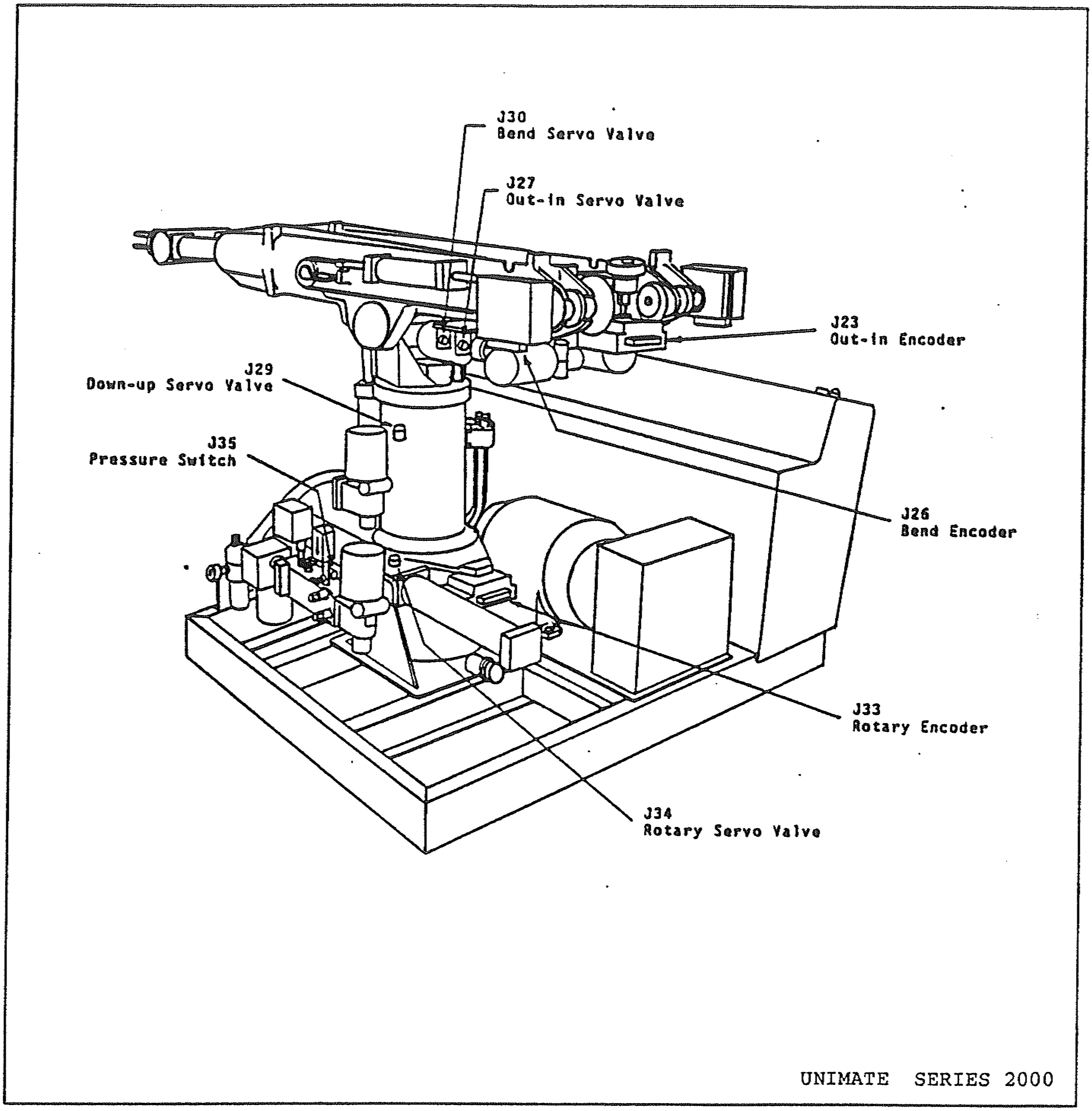

Figure 5.1: Schematic of Unimate MK II hydraulic robot

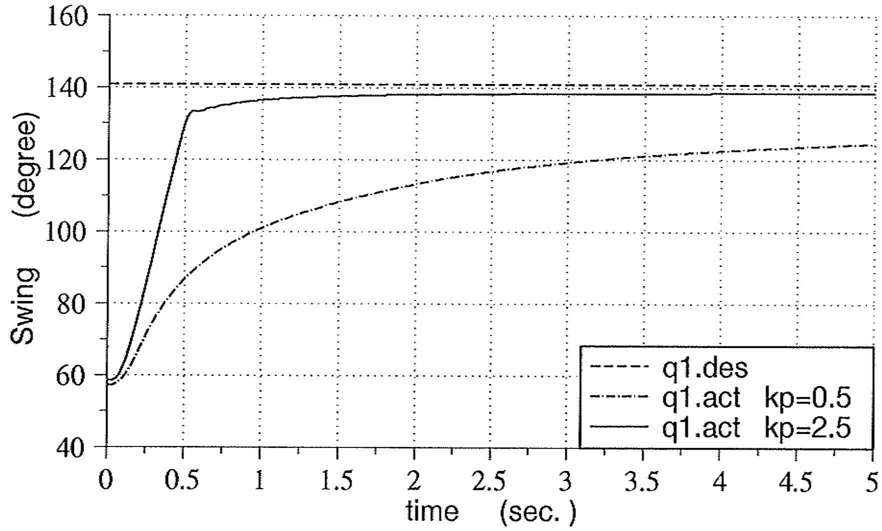

Figure 5.2: Step input response; q1

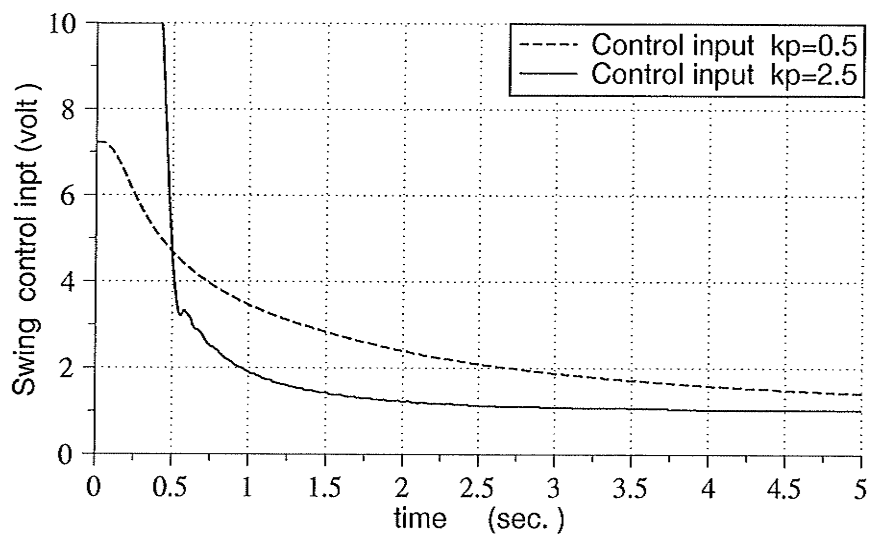

Figure 5.3: Control input; q1

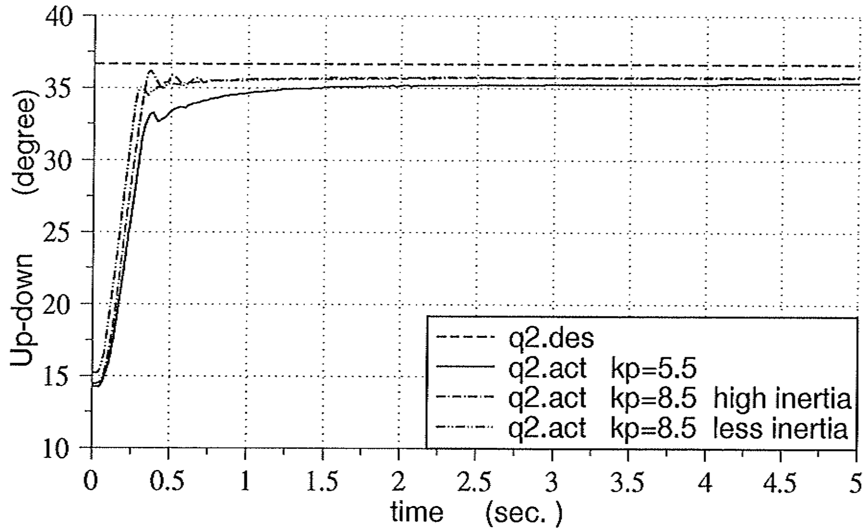

Figure 5.4: Step input response; q2

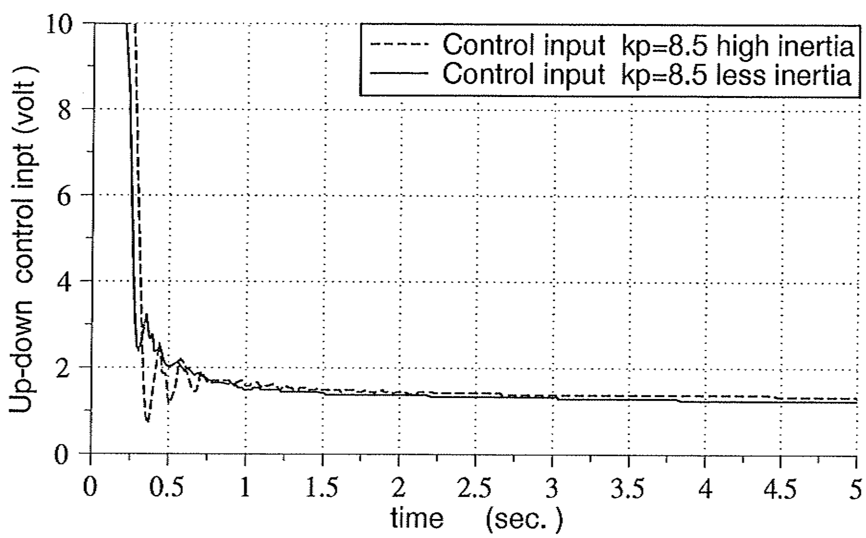

Figure 5.5: Control input; q2

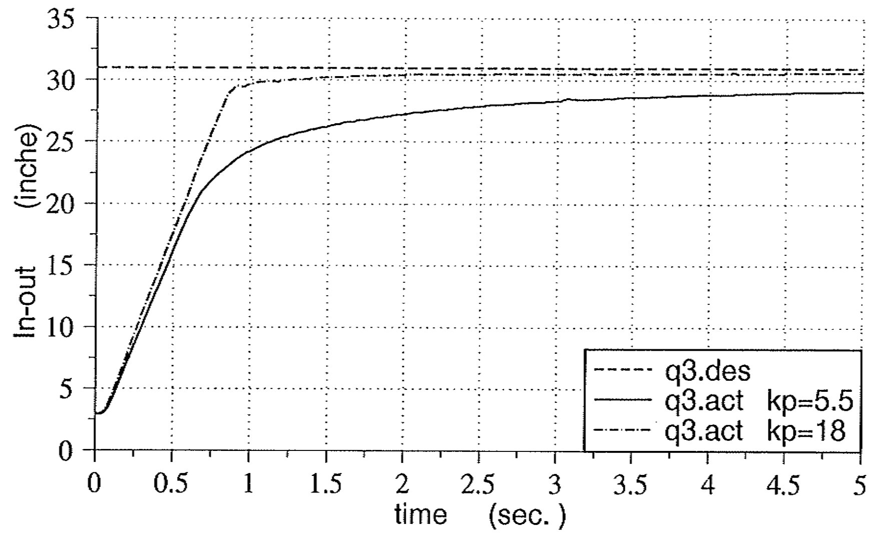

Figure 5.6: Step input response; q3

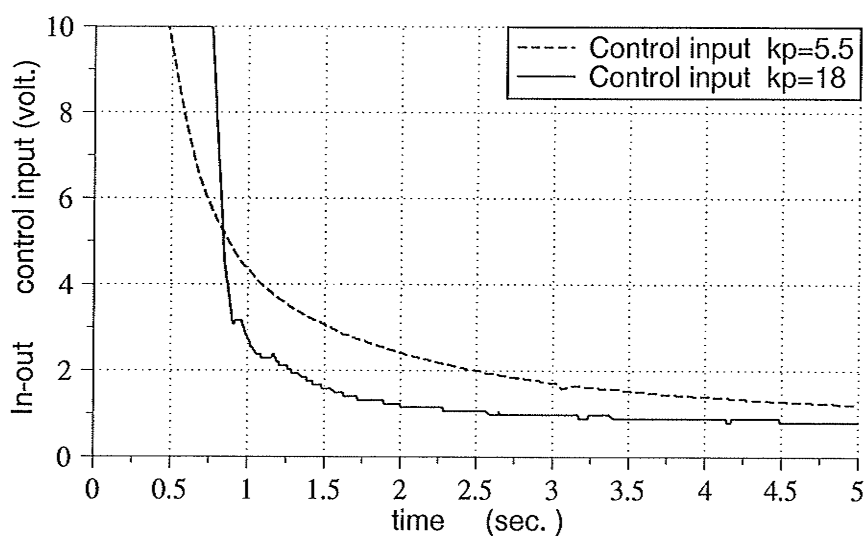

Figure 5.7: Control input; q3

CHAPTER 6

CONCLUSIONS

6.1 Achievements

In this thesis, some aspects of position control in two classes of hydraulically-actuated manipulators were studied. The first class of manipulators operate from a constant pressure pump system and are controlled by fast response electro-hydraulic servo-valves (closed-center valves). The second class of manipulators operate from a constant flow pump system and are controlled by slow response open-center valves. Mathematical models were derived and simulation programs were written using the C programming language. Parameters of the models such as supply pressure, actuators sizes and valves conditions were carefully determined to match the available data. The accuracy of the simulation models were qualitatively verified with the experimental data obtained from a hydraulically-actuated robot test station as well as other available literature. Once the confidence on the simulation models was established, they were used to study and compare different control strategies.

For the first class of manipulators, it was found that the actuation force feedback compensation is a suitable method for controlling the joint motion of a single-link servomechanism. Non-interactive compensation was found to be a suitable method for controlling the joint motion of multi-link servomechanisms. This method was more effective in reducing the interaction forces when system parameters were known exactly. However, the controller did not perform well in the case of excessive loading. The load-insensitive control method was found to be the most promising method for controlling the joint motions. The effect of both interaction and loading were handled within a very simple algorithm. The load-insensitive method did not require knowledge of the linkage parameters.

For the second class of manipulators, four different models were derived to simulate the joint motion of a two-degree-of-freedom heavy-duty robot arm operating from a constant flow using open-center five-way valves. Dead-band in the servo-valve input and the lap conditions were examined and it was found that the joint motions, with or without dead-band in the servo-valves input and zero-lapped valves, can be controlled effectively by using proportional and velocity feedback compensation. In systems with dead-band in the servo-valve input and over-lapped valves, the joint motion was controlled using simple proportional control.

6.2 Future Development

This work could be extended to study the aspects of position control of manipulators with additional degrees of freedom end to account for swing motion for each manipulator. The addition of more degrees of freedom to the manipulator could allow the end effector to operate in 3-D work envelopes.

The effects of over-lapped conditions of the valves for the first class of manipulators (operating from constant pressure), should be studied. For the second class of manipulators (operating from constant flow), The non-interactive and load-insensitive control strategies should be studied through simulations to decide on the effectiveness of these algorithms. Further developments will depends on the outcome of these studies.

REFERENCES

Davis, B. L., and Ihnatowicz, E., 1981, "Hydraulic Power for Industrial Robot Manipulators", *Proceedings, 6^{th} International Fluid Power Symposium*, England, pp. 361–372.

Excavator Hydraulic System, "System Operation Testing and Adjusting", Service Manual: 215B Excavator, Caterpillar Inc, Form No. SENR2 170.

Funakubo, H., 1991, *Actuators For Control*, Gordon & Breach Science, New-york.

Gulillon, M., 1961, *Hydraulic Servo Systems Analysis and Deign*, Butterworth and Co, New-york.

Hanafusa, H., Asada, H., and Mikoshi, T., 1980, " Design Of Electrohydraulic Servo System For Articulated Robot Arm Control", *Proceedings of The IFAC Symposium* , Warsaw, Poland, pp. 223–228.

Hanafusa, H., and Wang, Z., 1983, "Pressure Feedback Compensation For Hydraulic Servomechanism Which Drive Articulated Robots", *Proceedings of The ISA Symposium* , Paper No. 0-87664-741-7/83/0909-8, pp. 909–915.

Halme, A., Vaha, P., and Soininen, J., 1985, " Application of a Multivariable Adaptive Technique to Digital Control of Hydraulic Manipulators", *Proceedings, 7th IFAC/IFORS Symposium* , H.A. Barker and P.C. Young, ed., Pergamon Press, Oxford, England, Vol. 2, pp. 1285–1291

Hall, F.J., 1988, *Introduction To Control system Analysis and Design*, Prentice Hall, New-Jersey.

Johnson, J.E., 1973, *Electrohydraulic Servo Systems*, Butterworth & Co, New-York.

Karkkainen, P., and Manninen M., 1983, "Real-Time Control Method of Large-Scale Manipulators in Robotics 1983", *(B. Rooks ed.), Anchor Press Ltd.*, Colchester, England, pp. 227–230.

Merritt, H., 1967, *Hydraulic Control Systems*, John Wiley & Son, Toronto.

Ogata, K., 1990, *Modern Control Engineering*, Prentice Hall, New-Jersey.

Rivin, E.I., 1985, "Effective Rigidity of Robot Structure: Analysis and Enhancement", *Proceedings, American Control Conference*, Boston, Ma, pp. 381–382.

Schilling, R.J., 1990, *Fundamentals of Robotics Analysis and Control*, Prentice Hall, New-Jersey.

Sepehri, N., and Lawrence, P. D., 1992, "Sensor-Based Velocity Control of Teleoperated Heavy-duty Hydraulic Machines", *Proceedings, IEEE Int. Conference on Intelligent Robotics and Systems*, Raleigh, North Carolina, pp. 859–864.

Sepehri, N., Dumont, G.A.M., Lawrence, P.D., and Sassani, F., 1990, " Cascade Control of Hydraulically Actuated Manipulators", *Robotica*, Vol. 8, pp. 207–216.

Sepehri, N., 1990, *Dynamic Simulation and Control of Teleoperated Heavy-Duty Hydraulic Manipulator*, Ph.D. Thesis, Department of Mechanical Engineering, University of British Columbia.

Siljak, D.D., 1969, *Nonlinear Systems The Parameter Analysis and Design.* John Wiley and Sons, Inc., New-york.

Watton, J., 1987, "The Dynamic Performance of an Electro-Hydraulic Servovalve/Motor System with Transmission Line Effects", *ASME J. Dynamic Systems, Measurements and Control*, Vol. 190, pp. 14–18.

Welch, T.R., 1962, " The use of Derivative Pressure Feedback in High Performance Hydraulic Servomechanisms", *Trans. ASME. Ser. B 84 USA*, pp. 8–14.

APPENDICES

APPENDIX A

Linearization for the Equation of Motion

Equation (2.1) is a nonlinear equation and is linearized using Taylor's series about an operating point and neglecting the higher order terms. The operating points are $(\hat{q}_1, \hat{\dot{q}}_1, \hat{\ddot{q}}_1)$ and $(\hat{q}_2, \hat{\dot{q}}_2, \hat{\ddot{q}}_2)$ for links 1 and 2, respectively. By substituting

$$
\begin{aligned}
q_1 &= \hat{q}_1 + \Delta q_1, \\
q_2 &= \hat{q}_2 + \Delta q_2, \\
T_1 &= \hat{T}_1 + \Delta T_1, \\
T_2 &= \hat{T}_2 + \Delta T_2.
\end{aligned}
$$

$$
\begin{aligned}
T_1 &= [a_1 + 2a_3 cos q_2]\ddot{q}_1 + [a_2 + a_3 cos q_2]\ddot{q}_2 - a_3(2\dot{q}_1 + \dot{q}_2)\dot{q}_2 sin q_2 + a_4 cos q_1 \\
&\quad + a_5 cos q_1 + a_6 cos(q_1 + q_2). \\
T_1 &= \hat{T}_1 + \frac{\partial T_1}{\partial q_1}\Delta q_1 + \frac{\partial T_1}{\partial q_2}\Delta q_2 + \frac{\partial T_1}{\partial \dot{q}_1}\Delta \dot{q}_1 + \frac{\partial T_1}{\partial \dot{q}_2}\Delta \dot{q}_2 + \frac{\partial T_1}{\partial \ddot{q}_1}\Delta \ddot{q}_1 + \frac{\partial T_1}{\partial \ddot{q}_2}\Delta \ddot{q}_2 \\
\hat{T}_1 &= [a_1 + 2a_3 cos \hat{q}_2]\hat{\ddot{q}}_1 + [a_2 + a_3 cos \hat{q}_2]\hat{\ddot{q}}_2 - a_3(2\hat{\dot{q}}_1 + \hat{\dot{q}}_2)\hat{\dot{q}}_2 sin \hat{q}_2 + a_4 cos \hat{q}_1 \\
&\quad + a_5 cos \hat{q}_1 + a_6 cos(\hat{q}_1 + \hat{q}_2). \\
\frac{\partial T_1}{\partial q_1}\Delta q_1 &= -[(a_4 + a_5) sin \hat{q}_1 + a_6 sin(\hat{q}_1 + \hat{q}_2)]\Delta q_1. \\
\frac{\partial T_1}{\partial q_2}\Delta q_2 &= -[2a_3\hat{\ddot{q}}_1 sin \hat{q}_2 + a_3\hat{\ddot{q}}_2 sin \hat{q}_2 + a_3(2\hat{\dot{q}}_1 + \hat{\dot{q}}_2)\hat{\dot{q}}_2 cos \hat{q}_2 + a_6 sin(\hat{q}_1 + \hat{q}_2)]\Delta q_2. \\
\frac{\partial T_1}{\partial \dot{q}_1}\Delta \dot{q}_1 &= -[2a_3\hat{\dot{q}}_2 sin \hat{q}_2]\Delta \dot{q}_2. \\
\frac{\partial T_1}{\partial \dot{q}_2}\Delta \dot{q}_2 &= -[a_3(2\hat{\dot{q}}_1 + 2\hat{\dot{q}}_2) sin \hat{q}_2]\Delta \dot{q}_2. \\
\frac{\partial T_1}{\partial \ddot{q}_1}\Delta \ddot{q}_1 &= [a_1 + 2a_3 cos \hat{q}_2]\Delta \ddot{q}_1.
\end{aligned}
$$

$$\frac{\partial T_1}{\partial \ddot{q}_2}\Delta\ddot{q}_2 = [a_2 + a_3 cos\hat{q}_2]\Delta\ddot{q}_2.$$

For small variation about the corresponding reference point and neglecting small terms the final linearized model becomes:

$$\Delta T_1 = T_1 - \hat{T}_1 = [a_1 + 2a_3 cos\hat{q}_2]\Delta\ddot{q}_1 + [a_2 + a_3 cos\hat{q}_2]\Delta\ddot{q}_2.$$

Similarly for T_2:

$$\begin{aligned}
T_2 &= [a_2 + a_3 cosq_2]\ddot{q}_1 + [a_2]\ddot{q}_2 + a_3\dot{q}_1{}^2 sinq_2 + a_6 cos(q_1 + q_2). \\
T_2 &= \hat{T}_2 + \frac{\partial T_2}{\partial q_1}\Delta q_1 + \frac{\partial T_2}{\partial q_2}\Delta q_2 + \frac{\partial T_2}{\partial \dot{q}_1}\Delta\dot{q}_1 + \frac{\partial T_2}{\partial \dot{q}_2}\Delta\dot{q}_2 + \frac{\partial T_2}{\partial \ddot{q}_1}\Delta\ddot{q}_1 + \frac{\partial T_2}{\partial \ddot{q}_2}\Delta\ddot{q}_2 \\
\hat{T}_2 &= [a_2 + a_3 cos\hat{q}_2]\hat{\ddot{q}}_1 + [a_2]\hat{\ddot{q}}_2 + a_3\hat{\dot{q}}_1{}^2 sin\hat{q}_2 + a_6 cos(\hat{q}_1 + \hat{q}_2). \\
\frac{\partial T_2}{\partial q_1}\Delta q_1 &= [-a_6 sin(\hat{q}_1 + \hat{q}_2)]\Delta q_1. \\
\frac{\partial T_2}{\partial q_2}\Delta q_2 &= [-a_3\hat{\ddot{q}}_1 sin\hat{q}_2 + a_3\hat{\dot{q}}_1{}^2 cos\hat{q}_2 - a_6 sin(\hat{q}_1 + \hat{q}_2)]\Delta q_2. \\
\frac{\partial T_2}{\partial \dot{q}_1}\Delta\dot{q}_1 &= [2a_3\hat{\dot{q}}_1 sin\hat{q}_2]\Delta\dot{q}_1. \\
\frac{\partial T_2}{\partial \dot{q}_2}\Delta\dot{q}_2 &= 0.0, \\
\frac{\partial T_2}{\partial \ddot{q}_1}\Delta\ddot{q}_1 &= [a_2 + a_3 cos\hat{q}_2]\Delta\ddot{q}_1. \\
\frac{\partial T_2}{\partial \ddot{q}_2}\Delta\ddot{q}_2 &= [a_2]\Delta\ddot{q}_2.
\end{aligned}$$

For small variation about the corresponding reference point and neglecting small terms the linearized model of T_2 becomes:

$$\Delta T_2 = T_2 - \hat{T}_2 = [a_2 + a_3 cos\hat{q}_2]\Delta\ddot{q}_1 + [a_2]\Delta\ddot{q}_2.$$

Writing the linearized equations in matrix form:

$$\Delta T_i = H_{i1}\Delta\ddot{q}_1 + H_{i2}\Delta\ddot{q}_2$$

$$\begin{vmatrix} \Delta T_1 \\ \Delta T_2 \end{vmatrix} = \begin{vmatrix} H_{11} & H_{12} \\ H_{21} & H_{22} \end{vmatrix} \begin{vmatrix} \Delta\ddot{q}_1 \\ \Delta\ddot{q}_2 \end{vmatrix} \tag{A.1}$$

where

$$
\begin{aligned}
H_{11} &= a_1 + 2a_3cos\hat{q_2}, \\
H_{12} &= a_2 + a_3cos\hat{q_2}, \\
H_{21} &= a_2 + a_3cos\hat{q_2}, \\
H_{22} &= a_2.
\end{aligned}
$$

APPENDIX B

Design Consideration and Physical Parameters

B.1 Design Consideration

In the design of a control system, the design must begin with a statement of specifications. The determination of the control elements is not an easy task, experience and past history, for a particular kind of control system would make this task less easier. In the hydraulic control system there are some consideration in the selection of the hydraulic circuit components.

- Supply Pressure Selection

  Usually, the selection of supply pressure is the first step in the hydraulic control system operating from a constant pressure supply. Many considerations favor a large supply pressure beyond 4000 psi. As supply pressure is increased, less flow is required to achieve a given horsepower. Smaller pump, lines, valves and oil supply, are then possible. Because of smaller oil volume and higher bulk modulus, fast response can be achieved. The major considerations due to higher pressure supply are, leakage increases, higher oil temperature, decreases in components life. Therefore, tolerances must be tightened and result system cost increased. In general, lower supply pressure (500 - 2000 psi) are always desirable because they are more conductive to long component and system life, produce lower leakage, need less maintenance. And the final choice of supply pressure must be made in conjunction with the hydraulic actuator sizing to accommodate expected load.

- Hydraulic Actuator Selection

  In the selection of the hydraulic actuator, there are two basic considerations govern the size of the hydraulic actuator (*i.e.*, piston area or motor displacement), the size should be large enough to handle the loads expected during a duty cycle to obtain horsepower and force or torque load requirements. Also large enough to permit acceptable servo response, so that the associated hydraulic natural frequency is adequate.

- Servovalve Selection

  In the selection of electrohydraulic servovalve there are some factors need to be considered such as

- The pressure-flow curve for maximum stroke should encompass all load flow and load pressure points such that $P_L = \frac{2}{3}\ P_s$ maximum expected load. This assure that adequate flow and horsepower is delivered to the hydraulic actuator.
- Flow gain should be reasonably linear. The designer must know why, when and how to introduce a deadband, saturation etc.
- The pressure sensitivity should be large.

  Leakage flow should be limited to a reasonable percentage of rated flow to prevent unnecessary power loss.
- Null shifts with temperature should be minimum.
- Other factors such as weight, reliability, and cost may contribute to the final selection.

B.2 Physical Parameters

- Parameters for the system operating from a constant pressure

  $m_1 = 20\ kg$ mass of link one

  $L_1 = 1.0\ m$ length of link one

  $A_{i1} = 3.12 \times 10^{-3}\ m^2$ effective areas of piston one

$A_{o1} = 2.12 \times 10^{-3}\ m^2$ effective areas of piston one

$m_2 = 20\ kg$ mass of link two

$L_2 = 1.0\ m$ length of link two

$A_{i2} = 1.19 \times 10^{-3}\ m^2$ effective areas of piston two

$A_{o2} = 1.4 \times 10^{-3}\ m^2$ effective areas of piston two

$C_i = 2.2 \times 10^{-12}\ m^5/N$ compliance of the hydraulic system

$P_r = 0.0\ psi$ tank pressure

$P_s = 900\ psi$ $(900 \times 6.89\ kN/m^2)$ supply pressure (constant)

$w1 = 0.01\ m$ area gradient of valve one

$w2 = 0.01\ m$ area gradient of valve one

$-3\ mm < X_i < 3\ mm$ range of the spool displacement

$30° < q_1 < 150°$ range of joint one

$-150° < q_2 < -30°$ range of joint two

$l_1p = 0.22L_1\ m$

$l_1r = 0.80L_1\ m$

$l_2p = 0.75L_2\ m$

$l_2r = 0.2L_2\ m$

$d_1 = 8000.0\ Ns/rad$ coefficient of viscus damping (joint one)

$d_2 = 8000.0\ Ns/rad$ coefficinet of viscus damping (joint two)

- Parameters for the system operating from a constant flow

$m_1 = 1830\ kg$ mass of boom

$L_1 = 5.2\ m$ length of boom

$A_{i1} = 31.8\ in^2$ effective areas of piston one

$A_{o1} = 23.75\ in^2$ effective areas of piston one

$m_2 = 680\ kg$ mass of stick

$L_2 = 1.8\ m$ length of stick

$A_{i2} = 14.13\ in^2$ effective areas of piston two

$A_{o2} = 19.92\ in^2$ effective areas of piston two

$Q1 = 45.5\ GPM$ constant flow of pump one

$Q2 = 45.5\ GPM$ constant flow of pump two

$P_s = 4000\ psi$ $(4000 \times 6.89\ kN/m^2)$ maximum pump pressure

$P_e = 50\ psi$ tank pressure